Journal of Medicinal Chemistry

Article

pubs.acs.org/jmc

Synthesis and Biological Evaluation of *N*-((1-(4-(Sulfonyl)piperazin-1-yl)cycloalkyl)methyl)benzamide Inhibitors of Glycine Transporter-1

Christopher L. Cioffi,*[,†,⊥] Shuang Liu,*[,†,#] Mark A. Wolf,[†] Peter R. Guzzo,[†,#] Kashinath Sadalapure,[‡,▽] Visweswaran Parthasarathy,[‡] David T. J. Loong,[‡,○] Jun-Ho Maeng,[‡] Edmund Carulli,[‡] Xiao Fang,[‡] Kalesh Karunakaran,[‡] Lakshman Matta,[‡] Sok Hui Choo,[‡] Shailijia Panduga,[‡] Ronald N. Buckle,[†] Randall N. Davis,[†] Samuel A. Sakwa,[†] Priya Gupta,[‡] Bruce J. Sargent,[†] Nicholas A. Moore,[†,◆] Michele M. Luche,[∥] Grant J. Carr,[∥] Yuri L. Khmelnitsky,[§] Jiffry Ismail,[§] Mark Chung,[‡] Mei Bai,[‡] Wei Yee Leong,[‡] Nidhi Sachdev,[‡] Srividya Swaminathan,[‡] and Andrew J. Mhyre[∥,¶]

[†]Department of Medicinal Chemistry, AMRI, East Campus, 3 University Place, Rensselaer, New York 12144, United States

[‡]Discovery Research and Development Chemistry, Singapore Research Center, AMRI, 61 Science Park Road, Science Park III, 117525, Singapore

[§]Drug Metabolism and Pharmacokinetics, AMRI, East Campus, 17 University Place, Rensselaer, New York 12144, United States

[∥]Bothell Research Center, AMRI, 22215 26th Ave SE, Bothell, Washington 98021-4425, United States

Supporting Information

ABSTRACT: We previously disclosed the discovery of rationally designed *N*-((1-(4-(propylsulfonyl)piperazin-1-yl)-cycloalkyl)methyl)benzamide inhibitors of glycine transporter-1 (GlyT-1), represented by analogues **10** and **11**. We describe herein further structure−activity relationship exploration of this series via an optimization strategy that primarily focused on the sulfonamide and benzamide appendages of the scaffold. These efforts led to the identification of advanced leads possessing a desirable balance of excellent *in vitro* GlyT-1 potency and selectivity, favorable ADME and *in vitro* pharmacological profiles, and suitable pharmacokinetic and safety characteristics. Representative analogue (+)-**67** exhibited robust *in vivo* activity in the cerebral spinal fluid glycine biomarker model in both rodents and nonhuman primates. Furthermore, rodent microdialysis experiments also demonstrated that oral administration of (+)-**67** significantly elevated extracellular glycine levels within the medial prefrontal cortex (mPFC).

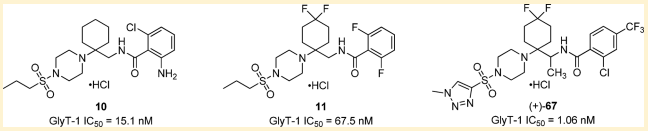

INTRODUCTION

The neurotransmitter glycine (**1**) (Figure 1) plays a key role in both inhibitory and excitatory neurotransmission within the central nervous system (CNS). Glycine acts as an endogenous agonist at the strychnine-sensitive glycine-A binding site of ionotropic glycine receptors (GlyRs), which induce inhibitory post synaptic potentials (IPSPs) via Cl^- influx and membrane hyperpolarization.[1,2] GlyRs are largely expressed within the hindbrain and spinal cord where their respective interneurons facilitate sensory motor learning, process sensory stimuli such as pain, relay reflex responses, and modulate respiratory rates and rhythm patterns.[3]

Glycine, along with D-serine, also serves as an obligatory coagonist that binds to the strychnine-insensitive glycine-B site located on the GluN1 subunit of *N*-methyl-D-aspartate (NMDA) receptors.[4] NMDA receptors are ligand and voltage-gated calcium permeable ionotropic glutamate receptors (iGluRs) involved in excitatory neurotransmission and CNS processes that underlie executive function, including long-term potentiation (LTP), long-term depression (LTD), and synaptic plasticity.[5] Activation of NMDA receptors relies on simultaneous binding of L-glutamate at the GluN2 subunit and obligatory coagonist glycine or D-serine at the GluN1 subunit followed by expulsion of a magnesium block from the channel pore via membrane depolarization.[4]

Homeostatic glycine levels within the CNS are maintained via two high affinity transporters; GlyT-1 and glycine transporter-2 (GlyT-2).[6] Both transporters are of the Na^+/Cl^- solute carrier family 6 (SLC6), share an approximate 50% sequence homology, and present overlapping expression patterns within caudal areas of the CNS (e.g., cerebellum, brainstem, and spinal cord). In addition, GlyT-1 is also expressed within the forebrain (e.g., hippocampus, striatum, and prefrontal cortex (PFC))[7] and on amacrine, ganglion, and Muller cells within mammalian and nonmammalian retinae.[8]

Within the GlyR-rich hindbrain, GlyT-1 is primarily expressed on glial astrocytes and is colocalized with GlyT-2, where it serves to modulate inhibitory neurotransmission by clearing glycine from the synaptic space surrounding the GlyRs. Thus, inhibition of GlyT-1 may lead to increased extracellular glycine levels with concomitant enhanced GlyR activity and inhibitory neurotransmission.[9] At excitatory glutamatergic synapses, GlyT-1 is highly colocalized with NMDA receptors

Received: June 17, 2016

DOI: 10.1021/acs.jmedchem.6b00914
J. Med. Chem. XXXX, XXX, XXX−XXX

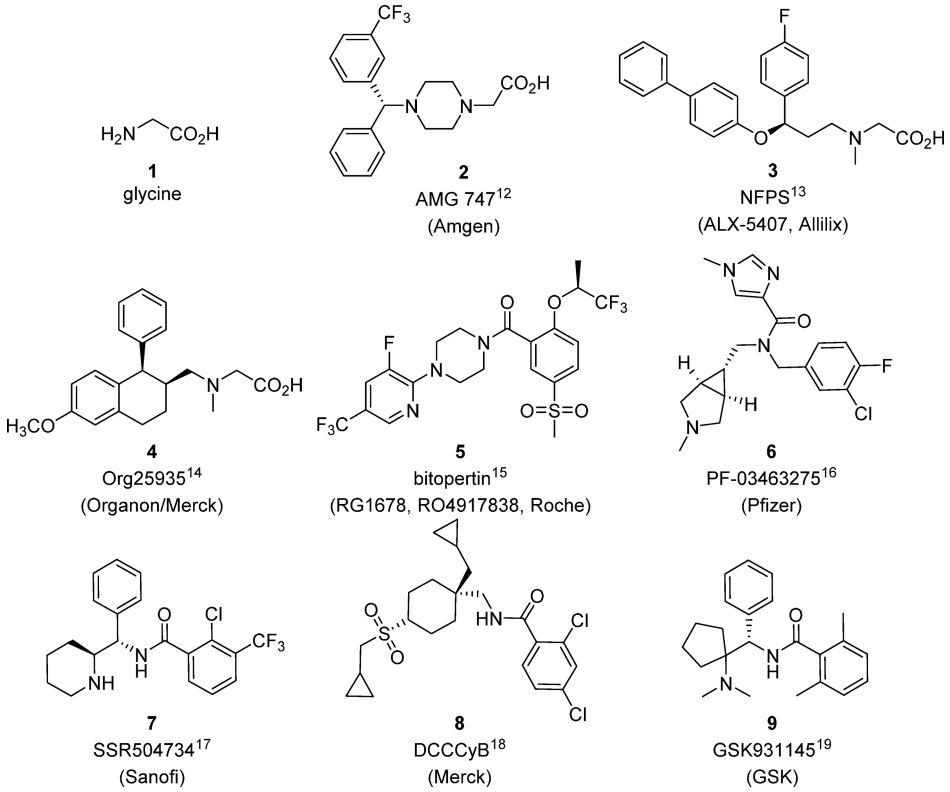

Figure 1. Representative GlyT-1 inhibitors.

on both glial and neuronal cells where it tightly maintains synaptic glycine concentrations at subsaturation levels.[10] Inhibition of GlyT-1 in these areas may lead to increased synaptic glycine levels and glycine-B site occupancy resulting in a potentiation of NMDA receptor function.[11] Thus, GlyT-1 inhibition can potentially lead to enhanced GlyR and/or NMDA receptor activity, and the approach has been under investigation to treat various CNS disorders that may be ameliorated by modulation of either inhibitory glycinergic or excitatory glutamatergic neurotransmission.

Numerous structurally diverse GlyT-1 inhibitors have been disclosed, and representatives of this class (e.g., **2**,[12] **3**,[13] **4**,[14] **5**,[15] **6**,[16] **7**,[17] **8**,[18] **9**[19]) are highlighted in Figure 1. Due to the emergence of the NMDA receptor hypofunction hypothesis for schizophrenia (i.e., the glutamate hypothesis),[20] selective inhibition of GlyT-1 became an attractive approach to enhance NMDA receptor activity by increasing local synaptic concentrations of glycine. Indeed, many of these agents were reported to be efficacious in several *in vivo* models predictive of antipsychotic and pro-cognitive activity.[21] Several GlyT-1 inhibitors entered clinical trials for the treatment of schizophrenia, and the approach enjoyed proof-of-concept in a series of Phase II trials;[22] however, a GlyT-1 inhibitor has yet to emerge as a novel antipsychotic available to treat patients.[21,23]

GlyT-1 inhibition has been studied in proof-of-concept clinical trials for other CNS disorders including depression,[24] obsessive compulsive disorder (OCD),[25] and addiction.[26,27] Furthermore, GlyT-1 inhibitors have demonstrated efficacy in animal models of neuropathic pain,[26,28] anxiety,[29] and epilepsy.[30] In addition, preclinical studies have shown that the approach may also promote neuroprotection,[31] provide a therapeutic strategy for autism spectrum disorders (ASDs),[32] and potentially present utility as an adjuvant treatment for symptomology associated Parkinson's disease.[33] Lastly, recent preclinical studies suggest that GlyT-1 inhibition may prevent hypoxia-induced neuronal degeneration of the retina[34] as well as provide a novel approach for the treatment of hematological disorders such as sickle cell anemia.[35]

We previously disclosed a novel series of *N*-((1-(4-(propylsulfonyl)piperazin-1-yl)cycloalkyl)methyl)benzamide GlyT-1 inhibitors derived from rationally designed hit **10** (Figure 2).[36]

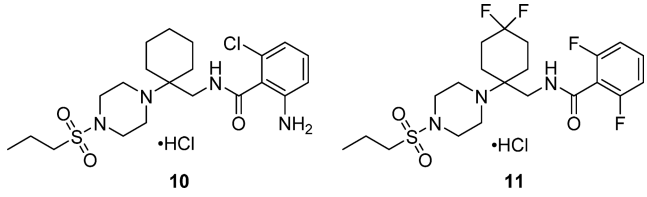

Figure 2. Previously reported *N*-((1-(4-(propylsulfonyl)piperazin-1-yl)-cycloalkyl)methyl)benzamide GlyT-1 inhibitors **10** and **11**.

Subsequent SAR campaigns led to the identification of compound **11**, which possesses a favorable balance of *in vitro* GlyT-1 potency and selectivity, ADME and *in vitro* pharmacological properties, and pharmacokinetic (PK) characteristics in rat. Inhibitor **11** also provided *in vivo* proof-of-concept for the series by producing a dose-dependent increase in rat cerebral spinal fluid (CSF) glycine levels upon oral administration.[36] We report herein further refinement to our series whereby optimization efforts focused on the sulfonamide and benzamide regions of the scaffold. This strategy led to the identification of advanced lead compounds that exhibited exquisite *in vitro* GlyT-1 potency, favorable ADME profiles, desirable binding characteristics, and robust *in vivo* glycine elevation activity within the CNS of both rodents and nonhuman primates.

DOI: 10.1021/acs.jmedchem.6b00914
J. Med. Chem. XXXX, XXX, XXX−XXX

Scheme 1[a]

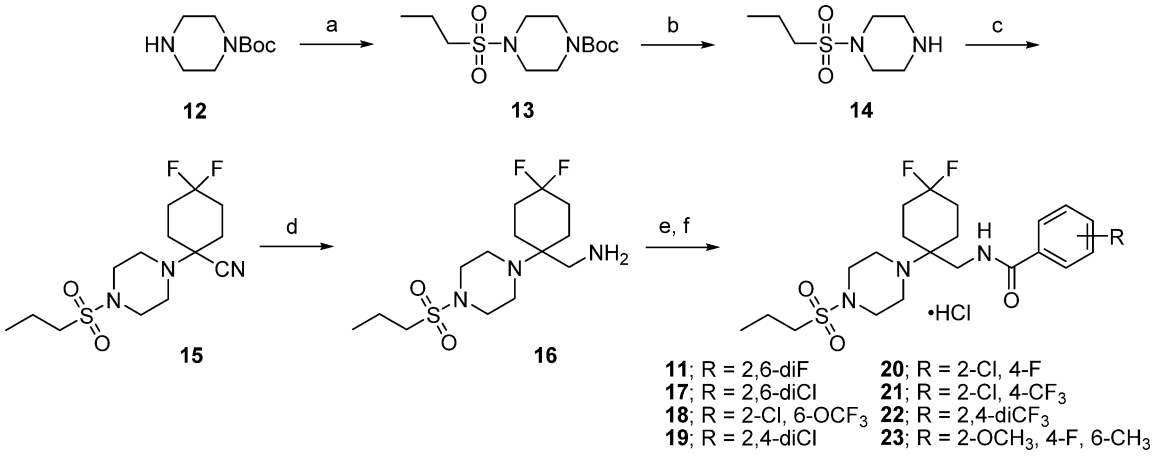

[a]Reagents and conditions: (a) 1-propanesulfonyl chloride, Et_3N, CH_2Cl_2, 0 °C to rt, 3 h; (b) TFA, CH_2Cl_2, 0 °C to rt, 16 h; (c) 4,4-difluorocyclohexanone, Et_2AlCN, Ti(*i*-PrO)$_4$, toluene, 0 °C to rt for 16 h; (d) $LiAlH_4$, Et_2O, 0 °C to rt, 12 h; (e) substituted benzoyl chloride, Et_3N, CH_2Cl_2, 0 °C to rt, 4 h; or substituted benzoic acid, EDCI·HCl, HOBt, Et_3N, DMF, rt, 16 h; (f) 1.0 M HCl in H_2O, CH_3CN, 0 °C to rt, 30 min.

Scheme 2[a]

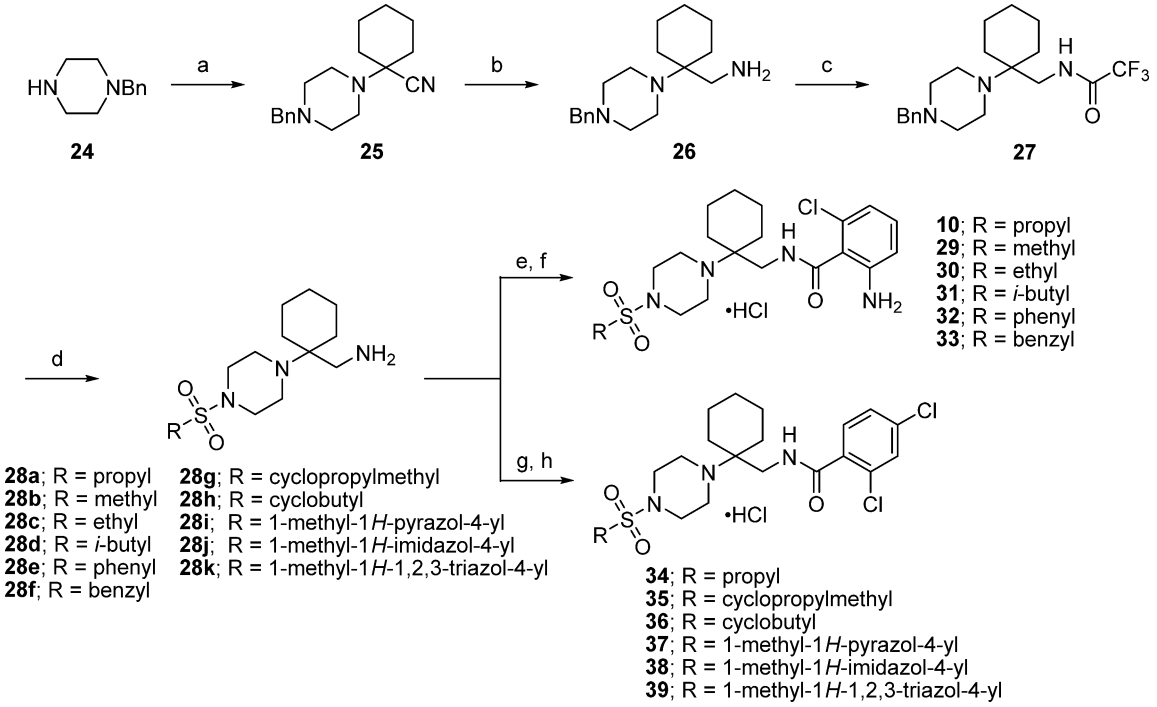

[a]Reagents and conditions: (a) cyclohexanone, PTSA, KCN, H_2O, rt, 16 h; (b), $LiAlH_4$, Et_2O, 0 °C to rt, 12 h; (c) trifluoroacetic anhydride, Et_3N, CH_2Cl_2, 0 °C to rt, 16 h; (d) (i) 10% Pd/C, NH_4HCO_2, CH_3OH, 65 °C, 3 h; (ii) substituted sulfonyl chloride, Et_3N, CH_2Cl_2, 0 °C to rt, 1 h; (iii) K_2CO_3, H_2O, CH_3OH, reflux, 16 h; (e) 2-amino-6-chlorobenzoic acid, HBTU, Et_3N, DMF, rt, 16 h; (f) 1.0 M HCl in Et_2O, CH_2Cl_2, 0 °C to rt, 30 min; (g) 2,4-dichlorobenzoyl chloride, Et_3N, CH_2Cl_2, 0 °C to rt, 16 h; (h) 10% HCl in H_2O, CH_3CN, 0 °C to rt, 30 min; or 1.0 M HCl in Et_2O, Et_2O, 0 °C to rt, 30 min.

CHEMISTRY

The synthesis of *n*-propyl sulfonamide analogues **11** and **17**−**23** presented in Scheme 1 began with the sulfonylation of *tert*-butyl piperazine-1-carboxylate (**12**) followed by Boc-deprotection to afford *n*-propyl sulfonamide **14** in good yield.[36,37] Strecker condensation between piperazine **14** and 4,4-difluorocyclohexanone in the presence of Et_2AlCN and Ti(*i*-PrO)$_4$ furnished quaternary amino nitrile **15**, which was subsequently reduced with $LiAlH_4$ to provide aminomethyl intermediate **16**. The desired final compounds were readily manufactured via acylation of **16** with either the corresponding benzoyl chloride or benzoic acid, followed by treatment with aqueous HCl to give the corresponding hydrochloride salts.[37] The synthesis of 4-fluoro-2-methoxy-6-methylbenzoic acid, which was used to manufacture analogue **23**, was achieved following the route reported by Coulton and co-workers.[38]

Scheme 2 highlights the synthetic routes used to access analogues **10** and **29**−**39**. A PTSA-mediated Strecker reaction between 1-benzylpiperazine (**24**) and cyclohexanone in the

DOI: 10.1021/acs.jmedchem.6b00914
J. Med. Chem. XXXX, XXX, XXX−XXX

Scheme 3[a]

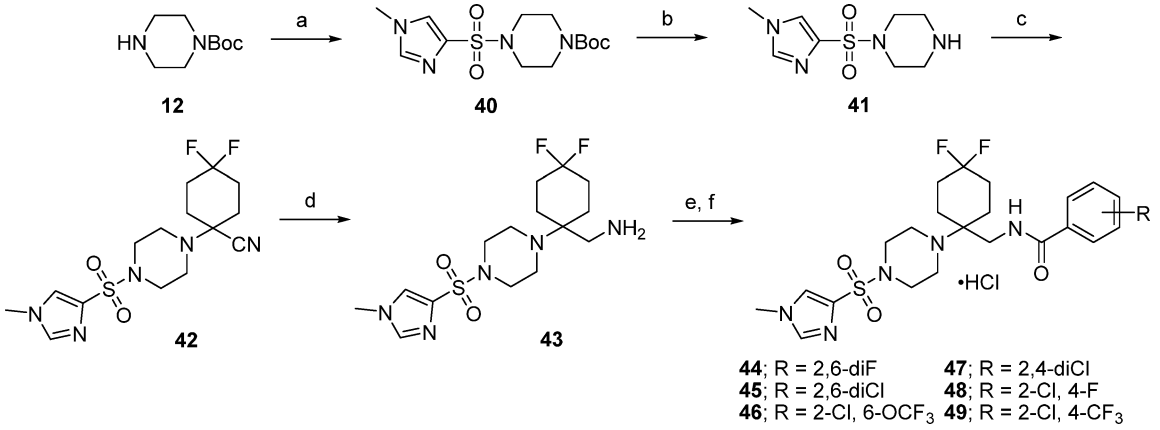

[a]Reagents and conditions: (a) 1-methyl-1*H*-imidazole-4-sulfonyl chloride, Et_3N, CH_2Cl_2, 0 °C to rt, 5 h; (b), 12 N HCl, 1,4-dioxane, 0 °C to rt, 2 h; (c) 4,4-difluorocyclohexanone, TMSCN, ZnI_2, toluene, CH_3OH, 0 °C then reflux for 4 h followed by rt for 16 h; (d) $LiAlH_4$, THF, 0 °C to rt, 5 h; (e) substituted benzoyl chloride, Et_3N, CH_2Cl_2, 0 °C to rt, 4 h; or substituted benzoic acid, EDCI·HCl, HOBt, Et_3N, DMF, rt, 16 h; (f) 1.0 M HCl in H_2O, CH_3CN, 0 °C to rt, 30 min.

Scheme 4[a]

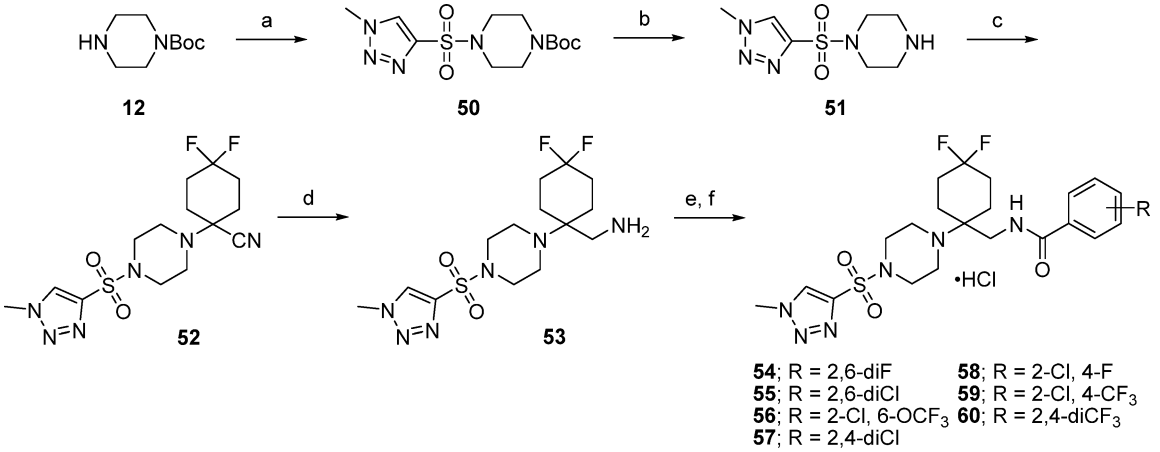

[a]Reagents and conditions: (a) 1-methyl-1*H*-1,2,3-triazole-4-sulfonyl chloride, Et_3N, CH_2Cl_2, 0 °C to rt, 5 h; (b), TFA, CH_2Cl_2, 0 °C to rt, 16 h; (c) 4,4-difluorocyclohexanone, TMSCN, ZnI_2, toluene, CH_3OH, 0 °C then reflux for 4 h followed by rt for 16 h; (d) $LiAlH_4$, THF, 0 °C to rt, 5 h; (e) substituted benzoyl chloride, Et_3N, CH_2Cl_2, 0 °C to rt, 4 h; or substituted benzoic acid, EDCI·HCl, HOBt, Et_3N, DMF, rt, 16 h; (f) 1.0 M HCl in H_2O, CH_3CN, 0 °C to rt, 30 min.

presence of KCN afforded amino nitrile **25** in good yield, which underwent smooth reduction with $LiAlH_4$ to provide aminomethyl intermediate **26**. Treatment of **26** with trifluoroactetic anhydride gave the trifluoroacetamide **27**. Advanced aminomethyl intermediates **28a−28k** were obtained via a three-step process that involved initial hydrogenolysis of **27** followed by sulfonylation of the resulting debenzylated piperazine with the corresponding sulfonyl chlorides and subsequent hydrolysis of the trifluoroacetamide with K_2CO_3 and H_2O in refluxing CH_3OH. Analogues **10** and **29−33** were then synthesized via an HBTU-mediated peptide coupling between precursor intermediates **28a−28f** and 2-amino-6-chlorobenzoic acid, followed by conversion to the hydrochloride salts in the presence of HCl. Compounds **34−39** were prepared via acylation of **28g−28k** with 2,4-dichlorobenzoyl chloride, followed by treatment with HCl to give the corresponding hydrochloride salts.[37]

The synthesis of *N*-((4,4-difluoro-1-(4-((1-methyl-1*H*-imidazol-4-yl)sulfonyl)piperazin-1-yl)cyclohexyl)methyl)benzamide analogues **44−49** is depicted in Scheme 3. Sulfonylation of **12** with 1-methyl-1*H*-imidazole-4-sulfonyl chloride followed by Boc-deprotection afforded sulfonamide **41**, which provided amino nitrile **42** using the aforementioned Strecker conditions. $LiAlH_4$ reduction of **42** afforded aminomethyl intermediate **43**, which was used to manufacture **44−49** via acylation with the corresponding benzoyl chloride or benzoic acid using standard peptide coupling conditions followed by treatment with HCl to give the corresponding hydrochloride salts.[37]

Construction of *N*-((4,4-difluoro-1-(4-((1-methyl-1*H*-1,2,3-triazol-4-yl)sulfonyl)piperazin-1-yl)cyclohexyl)methyl)benzamide analogues **54−60** was readily achieved following the route presented in Scheme 4. Sulfonylation of **12** with 1-methyl-1*H*-1,2,3-triazole-4-sulfonyl chloride[37] followed by subsequent Boc-deprotection and Strecker condensation with 4,4-difluorocyclohexanone in the presence of TMSCN and ZnI_2 provided amino nitrile **52**. Reduction of **52** with $LiAlH_4$ provided aminomethyl intermediate **53**, which was used to manufacture **54−60** via acylation with the corresponding benzoyl chloride or

DOI: 10.1021/acs.jmedchem.6b00914
J. Med. Chem. XXXX, XXX, XXX−XXX

Scheme 5[a]

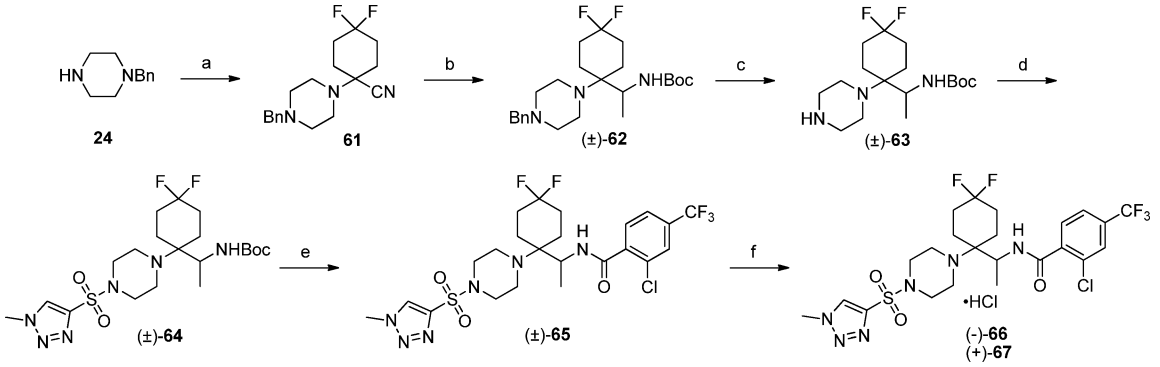

[a]Reagents and conditions: (a) 4,4-difluorocyclohexanone, TMSCN, ZnI_2, Et_2O, CH_3OH, toluene, rt for 4 h then reflux for 12 h; (b) (i) CH_3Li (3.0 M in DME), reflux, 6 h; (ii) $NaBH_4$, CH_3OH, rt, 2 h; (iii) Boc_2O, Et_3N, CH_2Cl_2, rt, 5 h; (c) 10% Pd/C, NH_4HCO_2, CH_3OH, reflux, 4 h; (d) 1-methyl-1*H*-1,2,3-triazole-4-sulfonyl chloride, Et_3N, CH_2Cl_2, 0 °C to rt, 2 h; (e) (i) 12 N HCl, CH_3OH, 0 °C to rt, 5 h; (ii) 2-chloro-4-(trifluoromethyl)benzoic acid, HOBt, EDCI·HCl, Et_3N, DMF, rt, 16 h; (f) (i) resolution of the enantiomers via preparative chiral HPLC (Daicel 5 cm I.D. × 50 cm L, eluting with an isocratic mobile phase of 70% heptanes and 30% *i*-PrOH); (ii) 1.0 M HCl in H_2O, CH_3CN, 0 °C to rt, 30 min.

benzoic acid followed by treatment with HCl to give the corresponding hydrochloride salts.[37]

We also explored the potential impact that substitution at the methylene alpha to the benzamide NH would have on GlyT-1 potency and ADME properties for the series. The preparation of the methyl-substituted enantiomers (−)-**66** and (+)-**67** is shown in Scheme 5. Strecker condensation between **24** and 4,4-difluorocyclohexanone in the presence of Et_2AlCN and $Ti(i\text{-}PrO)_4$ afforded amino nitrile **61** in good yield. Nitrile **61** was subsequently treated with CH_3Li followed by $NaBH_4$ reduction, and the resulting racemic amine was Boc-protected to give carbamate (±)-**62**.[37] Hydrogenolysis of (±)-**62** provided debenzylated piperazine (±)-**63**, which was sulfonylated with 1-methyl-1*H*-1,2,3-triazole-4-sulfonyl chloride to afford sulfonamide (±)-**64** in good yield. HCl-promoted Boc-deprotection of (±)-**64** followed by HOBt-mediated peptide coupling of the resulting amine with 2-chloro-4-(trifluoromethyl)benzoic acid afforded racemic benzamide (±)-**65**. Racemic (±)-**65** was resolved via chiral preparatory HPLC to give the corresponding enantiomers (−)-**66** and (+)-**67**.[37]

RESULTS AND DISCUSSION

We previously conducted a rational design effort with the objective of identifying novel chemical matter that incorporated benzamide and sulfonamide functionality positioned within a pharmacophoric proximity relative to several reported GlyT-1 inhibitors. These efforts led to the discovery of 2-amino-6-chloro-*N*-((1-(4-(propylsulfonyl)piperazin-1-yl)cyclohexyl)-methyl)benzamide **10**, which exhibited good *in vitro* potency (GlyT-1 IC_{50} = 15.1 nM) and excellent selectivity versus GlyT-2 (GlyT-2 IC_{50} > 75 μM).[36] Initial exploration of the benzamide SAR from hit **10** revealed that (1) the benzamide NH was critical for potency (methylation of the benzamide nitrogen significantly diminished potency), (2) at least two substituents were required on the benzamide phenyl ring for appreciable potency, (3) optimal GlyT-1 potency required at least one substituent to be positioned *ortho* to the benzamide carbonyl, and (4) monosubstitution at the *meta* position was highly disfavored. These efforts led to the discovery of highly potent GlyT-1 inhibitors, yet this initial series containing diverse benzamide analogues suffered from poor metabolic stability in the presence of human liver microsomes (HLM). Subsequent modifications to the central cyclohexyl ring suggested that this region of the scaffold provided potential metabolic soft-spots for CYP-mediated oxidation. Thus, installation of a 4,4-*gem*-difuoro moiety onto the central cyclohexyl ring led to the discovery *N*-((4,4-difluoro-1-(4-(propylsulfonyl)piperazin-1-yl)cyclohexyl)methyl)-2,6-difluorobenzamide **11**, which exhibited a favorable balance of potency (GlyT-1 IC_{50} = 67.5 nM), selectivity (GlyT-2 IC_{50} > 75 μM), and significantly improved HLM stability.[36] Compound **11** also provided *in vivo* proof-of-concept for the series by inducing a dose-dependent increase in rat CSF glycine levels upon acute oral administration of 20.8, 62.5, and 156.4 μmol/kg (10, 30, and 75 mg/kg).[36] The work reported herein describes follow-up optimization efforts on the sulfonamide and benzamide regions of analogues **10** and **11**, respectively. Key findings from both SAR campaigns converged to provide optimized lead compounds, which were further assessed for *in vivo* activity in rodents and nonhuman primates.

Structure−Activity Relationships. Guided by our previously reported SAR trends for the original *N*-((1-(4-(propylsulfonyl)piperazin-1-yl)cycloalkyl)methyl)benzamide series,[36] we sought to enhance the potency of analogue **11** while maintaining or improving its favorable HLM metabolic stability by initially varying the benzamide component of the scaffold and keeping the propyl sulfonamide in place. GlyT-1 potency and *in vitro* human and rat microsomal intrinsic clearance data (CL_{int}) for representatives of this series are shown in Table 1. The SAR for this series revealed that potency trends mirrored that of the previously reported *N*-((1-(4-(propylsulfonyl)-piperazin-1-yl)cycloalkyl)methyl)benzamide series; the most potent analogues featured two substituents on the benzamide phenyl ring with at least one substituent positioned *ortho* to the benzamide carbonyl, and there was no potency differentiation between substituents possessing electron-donating (**23**) or electron-withdrawing (**11**, **17**−**22**) character. Furthermore, this sample set (and the series as a whole) continued to demonstrate excellent selectivity for GlyT-1 versus GlyT-2 (GlyT-2 IC_{50} > 75 μM). This campaign led to the discovery of key analogues **21** and **22**, which exhibited significantly improved GlyT-1 potency with comparable CL_{int} values relative to **11**.

Concurrent with our benzamide SAR efforts, we explored alternative sulfonamide appendages starting from benchmark analogues 2-amino-6-chloro-*N*-((1-(4-(propylsulfonyl)piperazin-1-yl)cyclohexyl)methyl)benzamide (**10**, GlyT-1 IC_{50} = 15.1 nM) and 2,4-dichloro-*N*-((1-(4-(propylsulfonyl)piperazin-1-yl)

DOI: 10.1021/acs.jmedchem.6b00914
J. Med. Chem. XXXX, XXX, XXX−XXX

Table 1. SAR of Representative *N*-((4,4-Difluoro-1-(4-(propylsulfonyl)piperazin-1-yl)cyclohexyl)methyl)benzamide Analogues[a]

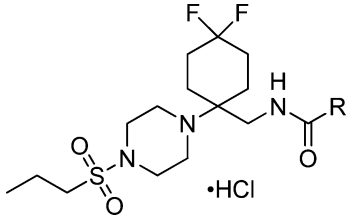

Compound	R	GlyT-1 IC_{50} (nM)[b]	Human CL_{int}[c] (μL/min/mg)	Rat CL_{int}[c] (μL/min/mg)
11		67.5 ± 5.4	13	5.5
17		42.4 ± 4.1	3.8	4.3
18		29.0	ND[d]	ND
19		36.4	37	27
20		38.4	ND	ND
21		12.6 ± 5.3	16	11
22		8.4 ± 1.5	19	4.9
23		28.5	ND	ND

[a]*In vitro* inhibitory GlyT-1 activity was determined using a whole-cell scintillation proximity assay (SPA).[37] The potency of each compound was assessed in inhibiting the uptake of radiolabeled glycine ([^{14}C]glycine) using the human choriocarcinoma cell line, JAR cells (ATCC#HTB-144), which endogenously express human GlyT-1 (*h*GlyT-1b). [b]For those compounds that were only tested twice (n = 2), the IC_{50} data is shown as the mean of two independent experiments. For compounds tested more than two times (n > 2), the IC_{50} data is represented as the mean ± standard deviation (SD). [c]Microsomes were incubated at 37 °C with the necessary cofactor regeneration system and individual test compounds at 3 μM. Reactions were terminated at 0, 5, 15, 30, 45, and 60 min time intervals in duplicate, and the amount of test compound remaining in the system was determined using LCMS quantitation. The residual compound remaining (%*R*) was determined by comparison to a zero time-point and the ln(%*R*) plotted vs time. The slope was normalized to the protein content in the incubation reaction to determine the intrinsic clearance (CL_{int}) value. Testosterone incubated at 10 μM was used as a standard. [d]ND = not determined.

cyclohexyl)methyl)benzamide (**34**, GlyT-1 IC_{50} = 22.7 nM). The results from this campaign revealed very narrow SAR for this region of the scaffold, which is highlighted in Table 2. Truncating the sulfonamide *n*-propyl chain to ethyl (**30**) led to a 5-fold decrease in potency relative to **10**, whereas further truncation to methyl (**29**) led to a more significant diminishment in potency. Introduction of bulkier *iso*-butyl (**31**), phenyl (**32**), or benzyl (**33**) sulfonamides was not well tolerated and also led to significant losses of potency relative to parent **10**. Interestingly, incorporation of a cyclopropylmethyl sulfonamide (**35**) resulted in a modest 2-fold loss in potency relative to *n*-propyl comparator **34**, whereas cyclobutyl (**36**) induced a >10-fold loss in potency. Acknowledging previously disclosed GlyT-1 inhibitors,[39] we also explored five-membered

Table 2. Sulfonamide SAR for Representative *N*-((1-(4-(Sulfonyl)piperazin-1-yl)cyclohexyl)methyl)benzamide Analogues[a]

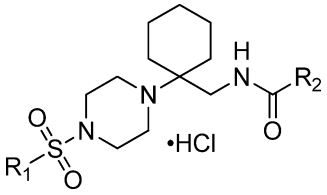

Compound	R_1	R_2	GlyT-1 IC_{50} (nM)[b]
10			15.1 ± 5.1
29	CH_3		339 ± 171
30	CH_2CH_3		73.8 ± 1.9
31			952
32			2294
33			9363
34			22.7 ± 9.1
35			56.6 ± 15.6
36			319 ± 114
37			146
38			2.14
39			1.54

[a]*In vitro* inhibitory GlyT-1 activity was determined using a whole-cell scintillation proximity assay (SPA).[37] The potency of each compound was assessed in inhibiting the uptake of radiolabeled glycine ([^{14}C]glycine) using the human choriocarcinoma cell line, JAR cells (ATCC#HTB-144), which endogenously express human GlyT-1 (*h*GlyT-1b). [b]For those compounds that were only tested twice (n = 2), the IC_{50} data is shown as the mean of two independent experiments. For compounds tested more than two times (n > 2), the IC_{50} data is represented as the mean ± standard deviation (SD).

heteroaromatic systems as potential sulfonamide appendages within our series. Installation of 1-methyl-1*H*-pyrazole sulfonamide (**37**) led to ∼6-fold loss in potency relative to **34**; however, incorporation of 1-methyl-1*H*-imidazole (**38**) or 1-methyl-1*H*-1,2,3-triazole (**39**) led to an approximate 10- to 20-fold improvement in GlyT-1 potency values, respectively. Interestingly, 2,6-difluororobenzamide analogues containing a regioisomeric 2-methyl-2*H*-1,2,3-triazole- or a des-methyl 1*H*-1,2,3-triazole-4-sulfonamide appendage exhibited a significant loss of potency relative to 1-methyl-1*H*-1,2,3-triazole **39** (GlyT-1 IC_{50} = 906.9 nM and 21.96 μM, respectively; structures not shown). The encouraging GlyT-1 potency results obtained for **38** and **39** were tempered by very poor *in vitro* HLM stability (5% remaining at 60 min and 0% remaining at 15 min, respectively). Thus, we explored a series of 1-methyl-1*H*-imidazole and 1-methyl-1*H*-1,2,3-triazole sulfonamide analogues that incorporated a central 4,4-*gem*-difluoro cyclohexyl ring while varying the benzamide region of the scaffold.

DOI: 10.1021/acs.jmedchem.6b00914
J. Med. Chem. XXXX, XXX, XXX−XXX

Table 3. SAR of Representative 1-Methyl-1*H*-imidazole and 1-Methyl-1*H*-1,2,3-triazole Sulfonamide GlyT-1 Inhibitors

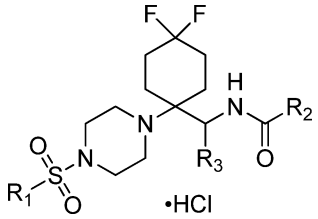

Compound	R_1	R_2	R_3	GlyT-1[b] IC_{50} (nM)	% Remaining[c] HLM[d], RLM[e]
44			H	18.3 ± 5.7	72, 92
45			H	5.56	22, 94
46			H	1.49	9.2, 91
47			H	5.29	30, 88
48			H	5.09 ± 0.94	85, 100
49		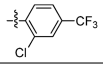	H	2.35	60, 90
54			H	5.10 ± 1.0	64, 95
55		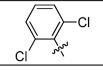	H	1.27 ± 0.05	33, 91
56		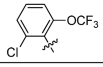	H	0.726	24, 87
57			H	1.24	46, 80
58			H	1.14 ± 0.19	69, 100
59		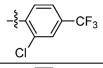	H	0.671 ± 0.19	60, 85
60		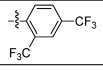	H	0.733 ± 0.16	64, 95
(±)-**65**		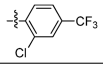	CH_3	1.03	54, 66
(-)-**66**		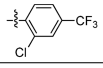	CH_3	33.1	51 (HLM)
(+)-**67**		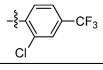	CH_3	1.06 ± 0.38	74, 76

[a] *In vitro* inhibitory GlyT-1 activity was determined using a whole-cell scintillation proximity assay (SPA).[37] The potency of each compound was assessed in inhibiting the uptake of radiolabeled glycine ([^{14}C]glycine) using the human choriocarcinoma cell line, JAR cells (ATCC#HTB-144), which endogenously express human GlyT-1 (*h*GlyT-1b). [b] For those compounds that were only tested twice (n = 2), the IC_{50} data is shown as the mean of two independent experiments. For compounds tested more than two times (n > 2), the IC_{50} data is represented as the mean ± standard deviation (SD). [c] Compound concentration was 3 μM, and incubation time with the liver microsomes was 15 min. [d] HLM = human liver microsomes. [e] RLM = rat liver microsomes.

Table 3 captures GlyT-1 potency, HLM, and rat liver microsomal (RLM) metabolic stability data for a series of 1-methyl-1*H*-imidazole and 1-methyl-1*H*-1,2,3-triazole sulfonamide analogues that feature a central 4,4-*gem*-difluoro cyclohexyl ring and varying benzamides. Strategic benzamide SAR for these series incorporated substituents and substitution patterns that provided the most potent analogues within the aforementioned *N*-((4,4-difluoro-1-(4-(propylsulfonyl)piperazin-1-yl)cyclohexyl)-methyl)benzamide series. Nearly all of these analogues displayed excellent GlyT-1 potency, selectivity over GlyT-2 (IC_{50} > 75 μM) and improved HLM metabolic stability relative to parent compounds **38** and **39**. Analogues **45**−**60** exhibited low single digit nanomolar to subnanomolar potency, with the 1-methyl-1*H*-1,2,3-triazole sulfonamides **54**−**59** exhibiting an approximate 2-fold improvement in potency values relative to their 1-methyl-1*H*-imidazole sulfonamide congeners **44**−**49**. In addition, introduction of a methyl group alpha to the benzamide nitrogen was well tolerated, with racemic (±)-**65** exhibiting a GlyT-1 IC_{50}

DOI: 10.1021/acs.jmedchem.6b00914
J. Med. Chem. XXXX, XXX, XXX−XXX

Table 4. *In Vitro* ADMET Profile for GlyT-1 Inhibitor (+)-67

	CL_{int} (μL/mL/min)[b]					%PPB[d]			Caco-2 permeability (P_{app} ($\times 10^{-6}$ cm/s))			
solubility[a]	H	R	cyno	CYP inhibition (IC_{50}) 3A4, 2C9, 2D6, 2C19	hERG[c] (IC_{50})	H	R	monkey	A-B	B-A	tPSA[e]	cLogP[e]
22.2 μM	4	6	12	all > 7.2 μM	20.2 μM	88	87	81	23.9	47.4	94.03	3.40

[a]Thermodynamic (shake flask) solubility measured in PBS (pH = 7.4). [b]Intrinsic clearance. [c]Patch-Xpress' patch-clamp assay; compounds were tested (n = 3) in a five-point concentration−response on HE293 cells stably expressing the hERG channel. [d]%PPB = plasma protein binding. [e]tPSA and cLogP values were determined by ChemDraw Ultra 12; H = human, R = rat, cyno = cynomolgus monkey.

Table 5. Rat and Cynomolgus Monkey PK Parameters of (+)-67[a]

species	dose	CL[b]	C_{max}[c] (ng/mL)	t_{max}[d] (h)	$t_{1/2}$[e] (h)	V_{ss}[f]	AUC_{last}[g] (h·ng/mL)	%F[h]
rat[i]	3.1 μmol/kg (IV) 15.7 μmol/kg (PO)	23.3 ± 2.83 (mL/min/kg)	352 ± 113	2.67 ± 2.89	4.33	1.75 ± 0.08 (L/kg)	1955 ± 611	27.2 ± 8.5
cyno[j]	1.5 μmol/kg (IV) 7.8 μmol/kg (PO)	1494 ± 219 (mL/h/kg)	105.0 ± 43.9	1.67 ± 0.58	6.27 ± 4.19	1929 ± 592 (mL/kg)	690.0 ± 395.1	31.0 ± 21.1

[a]Dosing groups consisted of three drug naïve adult male Sprague−Dawley rats or three female cynomolgus monkeys. Data represented as mean ± SD. [b]Total body clearance. [c]Maximum observed concentration of compound in plasma. [d]Time of maximum observed concentration of compound in plasma. [e]Apparent half-life of the terminal phase of elimination of compound from plasma. [f]Volume of distribution at steady state. [g]Area under the plasma concentration versus time curve from 0 to the last time point compound was quantifiable in plasma. [h]Bioavailability; $F = (AUC_{INFpo} \times Dose_{iv})/(AUC_{INFiv} \times Dose_{po})$. [i]IV formulation = 5% DMSO and 10% Solutol in saline; IV dosing volume = 5 mL/kg; PO formulation = 5% Solutol and 10% Captisol in 25 mM phosphate buffered saline (PBS; composition = 137 mM NaCl, 2.7 mM KCl, 4.3 mM Na_2HPO_4, 1.47 mM KH_2PO_4), pH adjusted to 2 with HCl. [j]IV formulation = 5% DMSO and 10% Solutol in saline, pH = 6.5; IV dosing volume = 2 mL/kg. PO formulation = 5% Solutol in 20% Captisol, 25 mM PBS, pH = 2; PO dosing volume = 5 mL/kg.

Table 6. Glycine Elevation in CSF and (+)-67 Concentrations in CSF, Brain, and Plasma 2 h Post Oral Dosing in Rat[a]

			concentration of (+)-67 (nM)		
dose (μmol/kg)	CSF glycine (ng/mL)	% vehicle control CSF glycine[b]	CSF	brain	plasma
0.4	470 ± 38.9	100.4 ± 8.3	bql[d]	3.2 ± 0.8	3.2 ± 0.5
1.5	558 ± 33.7	119.3 ± 7.2	0.1 ± 0.002	3.6 ± 0.4	11.4 ± 2.2
4.7	751 ± 44.0	160.5 ± 9.4[c]	0.5 ± 0.1	12.5 ± 4	52.2 ± 7.4
15.7	1528 ± 168.9	326.4 ± 36.1[c]	1.7 ± 0.3	32.2 ± 1.9	317.9 ± 49

[a]Dosing groups consisting of drug naïve adult male Sprague−Dawley rats (n = 4−5/group). [b]CSF glycine is summarized by treatment group mean % vehicle control CSF glycine ± standard error of the mean (SEM); $p < 0.05$ vs vehicle control. The CSF glycine level taken as 100% = 468.2 ± 27.3 ng/mL, which was obtained 30 min post vehicle dosing. Data were analyzed by 2-way ANOVA followed by Tukey's posthoc test using JMP v.6.0 statistical software. [c]*Statistical significance; $p < 0.05$ versus vehicle control. Test article vehicle = 5% Solutol and 10% Captisol in 25 mM phosphate buffered saline (PBS; composition = 137 mM NaCl, 2.7 mM KCl, 4.3 mM Na_2HPO_4, 1.47 mM KH_2PO_4), pH adjusted to 2 with HCl. [d]bql = below quantitation limit (1.0 ng/mL).

value = 1.03 nM. Interestingly, an enantiopreference was observed as chiral analogue (+)-**67** (GlyT-1 IC_{50} = 1.06 nM) was approximately 30-fold more potent than its corresponding enantiomer (−)-**66** (GlyT-1 IC_{50} = 33.1 nM).

Due to its exquisite potency and favorable microsomal stability, emerging analogue (+)-**67** was chosen for further evaluation, and the respective ADME and *in vitro* pharmacological profile is captured in Table 4. Compound (+)-**67** exhibited moderate thermodynamic (shake flask) solubility, favorable CL_{int} values (human, rat, and cynomolgus monkey), and no significant off-target activity at the hERG channel, CYPs, or within a standard panel of 69 GPCRs, ion channels, enzymes, and transporters (data not shown). Lastly, (+)-**67** exhibited favorable lipophilicity (cLogP = 3.40), and the compound was classified as highly permeable in a standard Caco-2 permeability assay (efflux ratio = 2).

***In Vivo* Properties: PK Characteristics in Rat and Cynomolgus Monkeys.** The overall favorable *in vitro* attributes of (+)-**67** prompted us to further investigate its PK profile in rat and cynomolgus monkey (*Macaca fascicularis*) (Table 5). Single dose PK studies were conducted with Sprague−Dawley rats at 3.1 μmol/kg (2 mg/kg) IV and 15.7 μmol/kg (10 mg/kg) PO and with cynomolgus monkeys at 1.5 μmol/kg (1 mg/kg) IV and 7.8 μmol/kg (5 mg/kg) PO. Compound (+)-**67** exhibited moderate CL and V_{ss} values with good half-lives ($t_{1/2}$) for both species. Maximal plasma concentrations (C_{max}) of 352 ng/mL for rat and 105 ng/mL for cynomolgus monkey were achieved at 2.67 and 1.67 h post oral dose, respectively. The observed plasma exposures (AUC_{last}) were good for both species, ranging between 1955 h·ng/mL for rat and 690 h·ng/mL for cynomolgus monkey, with resulting oral bioavailabilities (%F) of 27.2 and 31.0%, respectively.

***In Vivo* Activity: Rat CSF Glycine Biomarker Model.** Inhibition of GlyT-1 leads to elevated levels of extracellular glycine throughout the CNS, which spills over and pools within the CSF where it can be readily measured. The rat CSF glycine biomarker model allows for facile assessment of both *in vivo* GlyT-1 engagement and potential exposure−response relationships by providing both CSF glycine concentrations as well as drug exposure levels in plasma, brain, and CSF from a single study.[40] Encouraged by the suitable PK characteristics observed for (+)-**67**, we initially studied the compound's effect on CSF glycine levels in an acute dose−response study with rats. Drug naïve Sprague−Dawley rats were orally administered vehicle or

DOI: 10.1021/acs.jmedchem.6b00914
J. Med. Chem. XXXX, XXX, XXX−XXX

(+)-**67** at four different doses (0.4, 1.5, 4.7, and 15.7 μmol/kg; 0.3, 1, 3, and 10 mg/kg), and CSF glycine levels were subsequently measured 2 h post-dose. The rats were euthanized by CO_2 asphyxiation and a hypodermic needle was inserted into the cisterna magna to withdraw 50−100 μL of CSF. The CSF was diluted with deuterated-glycine as an internal standard, and glycine levels were quantified by LC−MS/MS. As shown in Table 6, oral administration of (+)-**67** produced increases in rat CSF glycine levels relative to vehicle that were statistically significant at the 4.7 and 15.7 μmol/kg doses, suggesting that the compound is engaging GlyT-1 *in vivo*. In addition, concentrations of (+)-**67** in plasma, brain, and CSF increased in a dose-dependent manner. Noteworthy, compound (+)-**67** exhibited statistically significant pharmacodynamic (PD) activity in this assay by inducing CSF glycine increases at the 4.7 and 15.7 μmol/kg dose levels despite relatively low total brain-to-plasma (B/P) (0.2−0.1) and CSF-to-unbound plasma concentration ($C_{CSF}/C_{u,p}$) (>0.1) ratios. The observed low CNS exposure of (+)-**67** may be attributed to a combination of relatively high topological polar surface area (tPSA = 94.03) and molecular weight (MW = 599.01 g/mol), which could be hindering passive permeability (P_{app}) across the blood−brain barrier (BBB). However, due to the high potency of the compound, the projected free drug concentrations in the CNS ($C_{u,b}$ and C_{CSF}) at the 4.7 and 15.7 μmol/kg doses appear to equal or slightly exceed that required to significantly inhibit GlyT-1 as measured by the whole cell SPA assay (GlyT-1 IC_{50} = 1.06 nM), leading to the observed CSF glycine level elevation trend.[41] Furthermore, the dissociative half-life (residence time) of (+)-**67** at GlyT-1 has not been established; thus, it is unclear to what extent this factor may also be contributing to the observed CSF glycine elevation trends.[42] Transporter occupancy data has also not yet been determined.

Analogous inhibitor **59**, which possesses an *in vitro* pharmacological and rodent *in vivo* CNS exposure profile similar to that of (+)-**67** (data not shown), was concurrently analyzed in the rat CSF glycine model in both an acute dose−response and subsequent 5-day subchronic oral dosing study in an effort to understand the potential effects of chronic exposure on PD. Figure 3 presents CSF glycine elevation (as % versus vehicle) and drug exposure levels of **59** (CSF, brain, and plasma) obtained from both studies. In the acute dose−response study, drug naïve Sprague−Dawley rats were administered oral dose of vehicle or **59** (0.4, 1.6, 4.8, 16.1, 48.2, and 160.9 μmol/kg; 0.3, 1, 3, 10, 30, and 100 mg/kg) and then sacrificed 2 h post dose. As shown in Figure 3A, **59** produced increases in CSF glycine levels that were statistically significant from vehicle control in the 1.6 to 160.9 μmol/kg dose range. The study demonstrated that, similar to (+)-**67**, analogue **59** also possesses excellent *in vivo* potency, as the effective oral dose required to double CSF glycine levels relative to vehicle (ED_{200}) lies between 1.6 and 4.8 μmol/kg. The CSF, brain, and plasma exposure levels of **59** also increased in the 0.4 to 16.1 μmol/kg dose group (Figure 3B). Drug exposure levels did not increase in a dose-dependent fashion from the 48.2 to 160.9 μmol/kg doses, which may be attributed to oral absorption limitations due to the moderate solubility of the compound (shake flask solubility = 9.9 μM). In a subsequent subchronic dosing study, drug naïve Sprague−Dawley rats were administered vehicle or an oral dose of **59** (1.6, 4.8, or 16.1 μmol/kg) once daily (QD) over a 5-day period. The animals were then sacrificed 2 or 48 h post last-dose. The observed CSF glycine elevations for the cohorts sacrificed 2 h post last-dose were comparable to those observed for the same dose levels in the acute dose−response study (1.6, 4.8, and 16.1 μmol/kg), indicating that no tolerance for **59** had occurred. In addition, drug exposure levels for the animals sacrificed 2 h post last-dose were within a 2-fold range of those observed for the same dose levels in the acute study, suggesting that there was no significant accumulation of **59** over the 5-day QD dosing period. CSF glycine levels returned to baseline 48 h post last-dose for

A

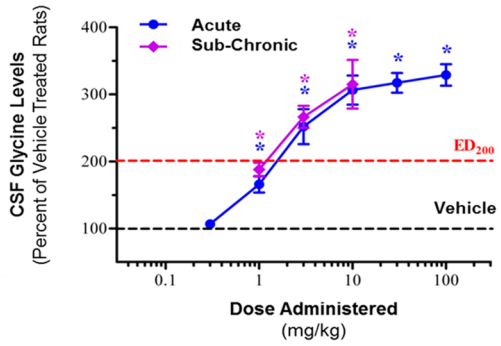

B

CSF Glycine Study	Dose (μmol/kg)	CSF Glycine (ng/mL)	% Vehicle Control CSF Glycine	Concentration of 59 (nM)		
				CSF	Brain	Plasma
Acute	0.4	432.8 ± 18.3	106.6 ± 4.0	2.7 ± 0.2	7.5 ± 2.3	18 ± 4.0
	1.6	673.8 ± 55.7	166.0 ± 12.3*	3.7 ± 0.3	13.1 ± 0.9	76.9 ± 17.7
	4.8	1022.4 ± 117.9	251.8 ± 26.0*	4.0 ± 0.4	39.2 ± 7.9	203.8 ± 55.6
	16.1	1244.0 ± 99.0	306.4 ± 21.8*	7.5 ± 0.8	64.9 ± 2.0	432.2 ± 60.4
	48.2	1288.0 ± 59.8	317.2 ± 14.7*	8.3 ± 1.1	66.8 ± 12.9	490 ± 103.3
	160.9	1336.0 ± 64.9	329.1 ± 16.0*	7.6 ± 0.6	46.3 ± 8.1	333.9 ± 71.9
Sub-Chronic (2 h post last dose)	1.6	980.0 ± 54.1	188.0 ± 10.4*	1.0 ± 0.1	21.0 ± 7.2	38.2 ± 4.7
	4.8	1388.0 ± 86.0	266.3 ± 16.5*	1.1± 0.1	44.8 ± 12.2	122.0 ± 21.2
	16.1	1642.0 ± 189.6	315.0 ± 36.4*	1.9 ± 0.3	69.4 ± 7.3	237.0 ± 28.2

Figure 3. (A) Effects of compound **59** on the % increase of CSF glycine from vehicle control for both acute (0.4, 1.6, 4.8, 16.1, 48.2, and 160.9 μmol/kg, PO; represented as blue) and subchronic dosing (1.6, 4.8, and 16.1 μmol/kg, PO, QD, 5 days; repesented as magenta). CSF glycine is summarized by treatment group mean % vehicle control CSF glycine ± SEM; $p < 0.05$ vs vehicle control. The CSF glycine level taken as 100% for the acute study = 406.0 ± 17.6 ng/mL, which was obtained 30 min post vehicle dosing. The CSF glycine level taken as 100% for the subchronic study = 521.2 ± 21.5 ng/mL, which was obtained 2 h post last-dose after QD dosing of vehicle over 5 days. All dose−response curves were plotted using the software program SigmaPlot, version 11.0. Data were analyzed by 2-way ANOVA followed by Tukey's posthoc test using JMP v.6.0 statistical software. Data are expressed as mean ± SEM; n = 5/group for each study. (B) Exposure levels of **59** in CSF, brain, and plasma for both acute and subchronic dosing (data acquired at the 2 h time-point post last-dose). Data are expressed as mean ± SEM; n = 5/group. *Statistical significance; $p < 0.05$ vs vehicle control. Vehicle preparation; 20 g of Captisol was added to 100 mL of 25 mM PBS. The pH was lowered to 2 via addition of HCl. The mixture was stirred for 30 min, or until dissolved and stored at 4 °C after use. Test article preparation; test compound was weighed and dissolved in Solutol (5% of total volume). Once dissolved, the solution is quickly stirred with 20% Captisol in 25 mM PBS, pH = 2 as stipulated above to the final compound concentration. The solution is then sonicated at room temperature for 20 min prior to dosing.

DOI: 10.1021/acs.jmedchem.6b00914
J. Med. Chem. XXXX, XXX, XXX−XXX

all three dose groups, demonstrating that the effect of **59** was reversible (data not shown). Lastly, no gross behavioral abnormalities with the animals were noted for either the acute dose−response study or throughout the duration of the subchronic dosing study.

***In Vivo* Activity: Cynomolgus Monkey CSF Glycine Biomarker Model.** Analogue (+)-**67** was subsequently studied in an acute dose−response CFS glycine study in cynomolgus monkeys. All of the animals used in the study were surgically prepared with indwelling cannulae inserted into the cisterna magna and connected to a subcutaneous port to permit cerebrospinal fluid sampling. CSF samples (approximately 0.30 mL) were obtained using a sterile Huber needle inserted into the subcutaneous ports at the following time-points in relation to dosing: predose (0), 0.5, 1, 2, 3, 4, 8, 12, and 24 h post dosing. Blood samples were also taken at these time points to assess drug exposure levels in the plasma.

Compound (+)-**67** was orally administered over a dose range of 0.4, 1.5, 4.7, and 15.7 μmol/kg, and statistically significant increases in CSF glycine levels were observed for the 4.7 and 15.7 μmol/kg doses (Figure 4A). Notably, the 15.7 μmol/kg dose produced a robust increase in glycine levels that exceeded 300% relative to vehicle control. Similar to rat, (+)-**67** exhibited highly potent PD activity in the cynomolgus monkey with a CSF glycine ED_{200} residing between 4.7 and 15.7 μmol/kg. The highest CSF glycine elevation levels occurred between the 2 and 4 h time-points, which were trending back to baseline over the remainder of the 24 h time-course. In addition, the time-points correlating with observed peak CSF glycine elevation track well with the (+)-**67** T_{max} obtained from the cynomolgus monkey PK study (1.67 h). Drug plasma exposure levels obtained in the CSF glycine study for the 4.7 and 15.7 μmol/kg doses also increased in a dose-dependent manner (Figure 4B), whereas drug levels for the 0.4 and 1.5 μmol/kg doses were below detection limits (<1.0 ng/mL). CSF drug exposure levels for the 15.7 μmol/kg dose group were also measurable; however, exposure levels for the 0.4, 1.5, and 4.7 μmol/kg dose groups were below detection limits. Similar to rat, a good correlation between (+)-**67** exposure levels (plasma and CSF) and CSF glycine elevation was observed for the 15.7 μmol/kg dose throughout the study time-course. Lastly, no gross behavioral abnormalities with the animals were observed throughout the duration of the study.

***In Vivo* Activity: Rat Medial Prefrontal Cortex Microdialysis Experiments.** We next examined if (+)-**67** could also elevate extracellular glycine levels within the rat medial prefrontal cortex (mPFC). Freely moving Sprague−Dawley rats were given an oral gavage of 1.5, 4.7, and 15.7 μmol/kg of (+)-**67**, and dialysate samples were taken from the mPFC over a 5 h time-course, which were analyzed by HPLC and tandem mass spectrometry. As shown in Figure 5, the mean normalized glycine levels within the rat mPFC were significantly increased compared to basal levels (t = −80 to 0 min) from time-points t = 80 to 300 min for the 4.7 and 15.7 μmol/kg dose groups ($p < 0.001$). Notably, the 4.7 and 15.7 μmol/kg doses increased the mean normalized glycine levels in a robust manner (>150% of vehicle control basal levels) and glycine elevation was sustained out to 5 h.

Mechanism of Binding. It has been suggested that competitive GlyT-1 inhibitors might offer potential therapeutic advantages over noncompetitive inhibitors as the degree of competitive inhibition could potentially depend on physiological glycine concentrations, whereas noncompetitive inhibition would not.[43]

A

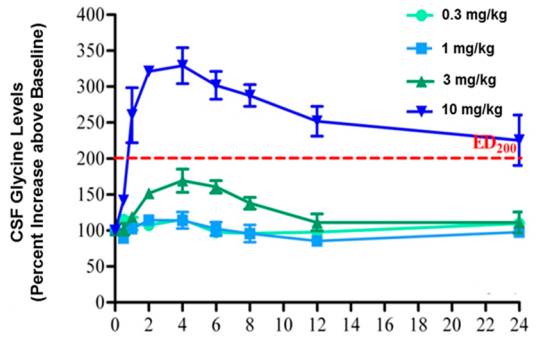

B

Time-point (h)	Plasma Exposure of (+)-67 (ng/mL)				CSF Exposure of (+)-67 (ng/mL)	
	4.7 μmol/kg dose	%CV	15.7 μmol/kg dose	%CV	15.7 μmol/kg dose	%CV
0.5	1.6 ± 0.6	34	67.9 ± 55.4	82	1.8	nc
1	3.6 ± 2.0	54	202.6 ± 170.5	84	5.9 ± 4.0	69
2	3.6 ± 2.3	63	221.7 ± 91.0	41	11.3 ± 6.0	53
3	5.7 ± 4.7	83	205.0 ± 117.0	57	11.3 ± 4.5	39
4	3.7 ± 2.4	66	224.3 ± 23.7	55	8.4 ± 2.3	43
8	2.0	nc[a]	156.3 ± 84.0	54	7.6 ± 1.6	30
12	bql[b]	nc	135.1 ± 53.4	40	5.0	32
24	bql	nc	10.3 ± 8.7	85	1.2	nc

Figure 4. (A) Effects of compound (+)-**67** at 0.4, 1.5, 4.7, and 15.7 μmol/kg on CSF glycince levels in cynomolgus monkeys. Data are expressed as mean ± SD; n = 3/group. (B) Corresponding plasma exposure levels of (+)-**67** for the 4.7 and 15.7 μmol/kg dosing groups and CSF exposure levels for the 15.7 μmol/kg dosing group. Plasma concentration data were analyzed with WinNonlin 5.2 software. [a]nc = noncalculable. [b]bql = below quantitation limit (1.0 ng/mL). %CV = Coefficient of Variation. Vehicle preparation; 20 g of Captisol was added to 100 mL of 25 mM PBS. The pH was lowered to 2 via addition of HCl. The mixture was stirred for 30 min or until dissolved and stored at 4 °C after use. Test article preparation; test compound was weighed and dissolved in Solutol (5% of total volume). Once dissolved, the solution is quickly stirred with 20% Captisol in 25 mM PBS, pH = 2 as stipulated above to the final compound concentration. The solution is then sonicated at room temperature for 20 min prior to dosing.

Thus, competitive inhibitors may provide more impactful inhibition in areas of the CNS where physiological glycine concentrations are lower (i.e., forebrain). In addition, competitive inhibition is potentially surmountable, which may circumvent potential mechanism-based adverse events due to excessive and prolonged glycine elevation.[43] Employing similar Michaelis−Menten saturation binding experiments reported by Mezler and co-workers,[43] we assessed the mechanism of binding for (+)-**67** at GlyT-1. A series of glycine transport experiments using a whole cell SPA assay with transfected HEK-293 cells expressing GlyT-1 were conducted whereby changes in B_{max} and K_d values were measured by increasing [^{3}H]-glycine concentrations in the presence of varying concentrations of (+)-**67** (Figure 6). Increasing concentrations of inhibitor (+)-**67** exhibited no effect on the B_{max} values for glycine whereas its K_d values increased, indicating that the compound was competing with glycine for the same binding site at GlyT-1. Several additional

DOI: 10.1021/acs.jmedchem.6b00914
J. Med. Chem. XXXX, XXX, XXX−XXX

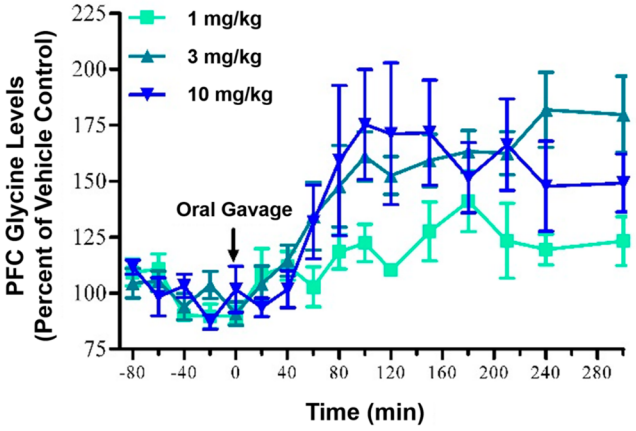

Figure 5. Effects of compound (+)-**67** on the extracellular levels of glycine in the mPFC of freely moving drug naïve adult male Sprague–Dawley rats (n = 5) administered by oral gavage of 1.5, 4.7, and 15.7 μmol/kg (1, 3, and 10 mg/kg) at time = 0. Data are expressed as mean ± SE; n = 5 or 6/group. The mean normalized glycine levels were significantly increased compared to basal levels (t = −80 to 0 min) from time points t = 80 to 300 min (p < 0.001), and glycine elevation was sustained over the 5 h time-course. Statistical analysis was performed using Sigmastat 3.2 for Windows (SPSS Corporation). Compound effects were compared, using two-way (time × dose) ANOVA for repeated measurements followed by Student–Newman–Keuls posthoc test. Vehicle preparation; 20 g of Captisol was added to 100 mL of 25 mM PBS. The pH was lowered to 2 via addition of HCl. The mixture was stirred for 30 min or until dissolved and stored at 4 °C after use. Test article preparation; test compound was weighed and dissolved in Solutol (5% of total volume). Once dissolved, the solution is quickly stirred with 20% Captisol in 25 mM PBS, pH = 2 as stipulated above to the final compound concentration. The solution is then sonicated at room temperature for 20 min prior to dosing.

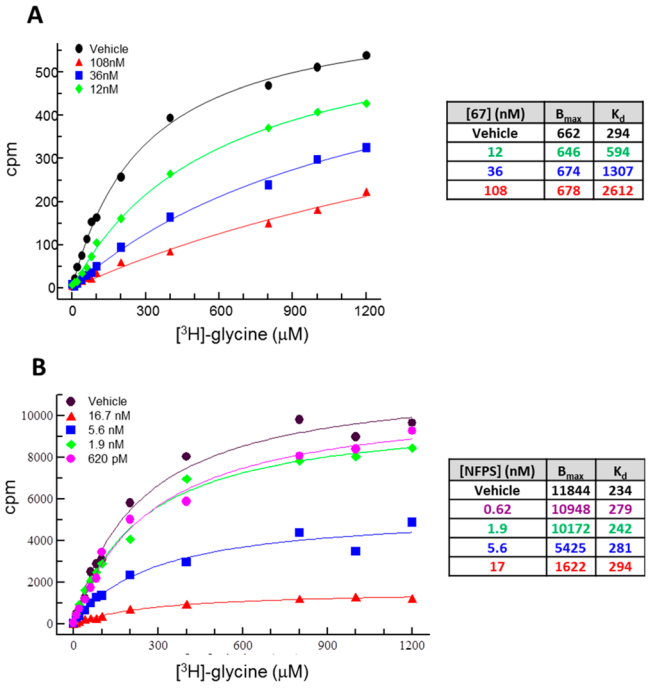

[67] (nM)	B_{max}	K_d
Vehicle	662	294
12	646	594
36	674	1307
108	678	2612

[NFPS] (nM)	B_{max}	K_d
Vehicle	11844	234
0.62	10948	279
1.9	10172	242
5.6	5425	281
17	1622	294

Figure 6. Determination of the mechanism of binding for compound (+)-**67**. (A) Glycine transport experiments conducted whereby B_{max} and K_d values were obtained by increasing concentration of [^{3}H]-glycine in the presence of varying concentrations of (+)-**67**. (B) Glycine transport experiments conducted whereby B_{max} and K_d values were obtained by increasing concentration of [^{3}H]-glycine in the presence of varying concentrations of **3**.

analogues within our series were also studied in these experiments, and all of them were confirmed to be competitive inhibitors of GlyT-1 (data not shown). In contrast, increasing concentrations of the known noncompetitive GlyT-1 inhibitor NFPS (ALX-5407) (**3**), which has been reported to induce mechanism-based toxicity,[44] led to changes in B_{max} values but did not alter the K_d values for glycine. These results confirm that **3** is not competing with glycine for binding at GlyT-1, and these findings were consistent with previously reported data.[44]

CONCLUSIONS

Lead optimization efforts for our GlyT-1 inhibitor series began with benzamide SAR exploration starting from previously reported *N*-((4,4-difluoro-1-(4-(propylsulfonyl)piperazin-1-yl)-cyclohexyl)methyl)benzamide **11**. These efforts led to the discovery of key inhibitors **21** and **22**, which were found to possess superior GlyT-1 potency and comparable *in vitro* microsomal metabolic stability relative to parent **11**. Concurrent with this campaign, sulfonamide SAR exploration of benchmark *N*-((1-(4-(propylsulfonyl)piperazin-1-yl)cyclohexyl)-methyl)benzamide inhibitors **10** and **34** was conducted, which lead to the discovery of key *N*-methyl imidazole and triazole sulfonamide analogues **38** and **39**. Our sulfonamide SAR findings were converged with the benzamide SAR campaign to provide standout analogues **59** and (+)-**67**.

Advanced lead (+)-**67** possesses a favorable balance of potency, ADME, and *in vitro* pharmacological profiles. The compound exhibited suitable rat and nonhuman primate PK characteristics and produced statistically significant elevations of CSF glycine levels for both species. In an acute dose–response rat CSF glycine study, analogues **59** and (+)-**67** induced dose-dependent and robust increases in glycine levels that correlated well with increasing plasma, brain, and CSF drug exposure levels. A subsequent 5-day subchronic dosing study with **59** revealed that CSF glycine elevation levels mirrored those observed in the acute dosing study at the same doses, suggesting that tolerance to the inhibitor had not occurred. In addition, exposures of **59** in the subchronic dosing study were also similar to those observed in the acute study for the same doses, providing evidence that there was no accumulation of the compound over the 5-day, QD dosing period. Furthermore, CSF glycine levels returned to baseline after a 48 h washout period for all dose groups, demonstrating that the effect of **59** was reversible.

The results obtained for the CSF glycine experiments prompted us to examine whether analogues from our series were also capable of elevating glycine levels in the mPFC, which is regarded as the putative site of action for neuropsychiatric disorders such as schizophrenia. Indeed, microdialysis experiments showed that inhibitor (+)-**67** produced robust increases in extracellular glycine levels within the mPFC of freely moving Sprague–Dawley rats, verifying that the compound is capable of engaging GlyT-1 in the forebrain.

Saturation binding experiments confirmed that compound (+)-**67** (in addition to several other analogues within our series) is competitive with glycine for binding at GlyT-1, demonstrating that the series possesses a differentiating and potentially preferable mechanism of binding relative to noncompetitive inhibitors such as NFPS (ALX-5407) (**3**). In conclusion, we believe that analogues from our series of

DOI: 10.1021/acs.jmedchem.6b00914
J. Med. Chem. XXXX, XXX, XXX–XXX

N-((4,4-difluoro-1-(4-(sulfonyl)piperazin-1-yl)cyclohexyl)-methyl)benzamide GlyT-1 inhibitors possess favorable *in vitro* and *in vivo* profiles that may prove beneficial for the treatment of the various neurological and neuropsychiatric disorders for which the field has been reported to show promise.

EXPERIMENTAL SECTION

General Chemistry. All reactions were performed under a dry atmosphere of nitrogen unless otherwise specified. Indicated reaction temperatures refer to the reaction bath, while room temperature (rt) is noted as 25 °C. Commercial grade reagents and anhydrous solvents were used as received from vendors, and no attempts were made to purify or dry these components further. Removal of solvents under reduced pressure was accomplished with a Buchi rotary evaporator at approximately 28 mmHg pressure using a Teflon-linked KNF vacuum pump. Thin layer chromatography was performed using 1″ × 3″ AnalTech No. 02521 silica gel plates with fluorescent indicator. Visualization of TLC plates was made by observation with either short wave UV light (254 nm lamp), 10% phosphomolybdic acid in ethanol, or in iodine vapors. Preparative thin layer chromatography was performed using Analtech, 20 × 20 cm, 1000 μm preparative TLC plates. Flash column chromatography was carried out using a Teledyne Isco CombiFlash Companion Unit with RediSepRf silica gel columns. If needed, products were purified by reverse phase chromatography, using a Teledyne Isco CombiFlash Companion Unit with RediSepGold C18 reverse phase column. Proton NMR spectra were obtained either on a 300, 400, or 500 MHz Bruker Nuclear Magnetic Resonance Spectrometer and chemical shifts (δ) are reported in parts per million (ppm), coupling constant (J) values given in Hz, and with the following spectral pattern designations: s, singlet; d, doublet; t, triplet, q, quartet; dd, doublet of doublets; m, multiplet; br, broad. Tetramethylsilane (TMS) was used as an internal reference. Melting points are uncorrected and were obtained using a MEL-TEMP Electrothermal melting point apparatus. Mass spectroscopic analyses were performed using the following: (1) ESI ionization on a Varian ProStar LCMS with a 1200L quadrapole mass spectrometer; (2) ESI, APCI, or DUIS ionization on a Shimadzu LCMS-2020 single quadrapole mass spectrometer. High pressure liquid chromatography (HPLC) purity analysis was performed using the following: (1) Varian Pro Star HPLC system with a binary solvent system A and B using a gradient elusion [A, H_2O with either 0.05% or 0.1% trifluoroacetic acid (TFA); B, CH_3CN with either 0.05% or 0.1% TFA] and flow rate = 1 mL/min, with UV detection at either 223 or 254 nm; (2) Shimadzu LC-20A HPLC system with a binary solvent system A and B using a gradient elusion [A, H_2O with either 0.05% TFA; B, CH_3CN with either 0.05% or 0.1% TFA] and flow rate = 1 mL/min, with UV detection at either 223 or 254 nm. All final compounds were purified to ≥95% purity, and these purity levels were measured by using the following HPLC methods:

(A) Varian Pro Star HPLC system; Phenomenex Luna C18(2) 5 μm column (4.6 × 150 mm), mobile phase, A = H_2O with 0.05% TFA and B = CH_3CN with 0.05% TFA; gradient 10−90% B (0.0−15.0 min), UV detection at 223 nm.

(B) Shimadzu LC-20A HPLC system; Phenomenex Luna C18(2) 5 μm column (4.6 × 250 mm), mobile phase, A = H_2O with 0.05% TFA and B = CH_3CN with 0.05% TFA; gradient 10−90% B (0.0−15.0 min), UV detection at 223 or 254 nm.

(C) Shimadzu LC-20A HPLC system; Xterra MS C18 5 μm column (4.6 × 150 mm); mobile phase, A = H_2O with 0.05% TFA and B = CH_3CN with 0.05% TFA; gradient 10−90% B (0.0−15.0 min), UV detection at 223 or 254 nm.

(D) Varian Pro Star HPLC system; Inertsil ODS C18 5 μm column (4.6 × 250 mm), mobile phase, A = H_2O with 0.1% TFA and B = CH_3CN with 0.1% TFA; gradient 10−90% B (0.0−15.0 min), UV detection at 254 nm.

Racemic (±)-**65** was resolved by preparative chiral HPLC using a Daicel 5 cm I.D. × 50 cm L chiral preparative column, eluting with an isocratic mobile phase of 70% heptanes and 30% *i*-PrOH, flow rate = 1 mL/min, to give enantiopure (−)-**66** and (+)-**67**.

Enantiopurity analysis for chiral compounds (−)-**66** and (+)-**67** was performed using a Shimadzu LC-20A HPLC system with a binary solvent system A and B using an isocratic elusion [30% A, *i*-PrOH; 70% B, heptanes] and flow rate = 1 mL/min, with UV detection at 254 nm (Method E). Optical rotation for (−)-**66** and (+)-**67** was measured using a PerkinElmer polarimeter model 341. Measurements were performed at 20 °C using a Na source lamp (589 nm) and CH_3OH as the solvent.

***In Vitro* GlyT-1 Inhibition Assessment.** *In vitro* inhibitory GlyT-1 activity was determined using a whole-cell scintillation proximity assay (SPA).[37] The potency of each compound was assessed in inhibiting the uptake of radiolabeled glycine ([^{14}C]glycine) using the human choriocarcinoma cell line, JAR cells (ATCC#HTB-144), which endogenously express human GlyT-1 (*h*GlyT-1b). In brief, 50,000 JARS cells were plated per well of tissue culture treated 96-well Cytostar-T plate (PerkinElmer) in RPMI media supplemented with 10% heat inactivated FBS and allowed to attach overnight at 37 °C and 5% CO_2. The compounds were then diluted into Uptake Buffer (10 mM Hepes, 120 mM NaCl, 2 mM KCl, 1 mM $CaCl_2$, 1 mM $MgCl_2$, and 5 mM alanine, pH 7.4) with a final DMSO concentration of 0.75% (v/v). Following the overnight incubation, the media was replaced with Uptake Buffer in the presence or absence of diluted compound and preincubated at room temperature for 10 min prior to the addition of [^{14}C]glycine at a final concentration of 5 mM. Following a 3 h incubation period at 37 °C and 5% CO_2, the plates were sealed and placed at room temperature in the dark for 15 min prior to quantification of incorporated radioactivity using a MicroBeta Trilux scintillation plate reader (PerkinElmer). Compounds were serially diluted 3-fold in DMSO generating a nine data point response curve for each compound. A minimum of two replicates were performed per determination. Data were plotted using XLfit software (IDBS) and fit into a four-parameter logistic model to determine the inhibitor concentration at half-maximal response (IC_{50}). Plate statistics tracked included average, standard deviation (SD), and CV of the positive (max) and negative control wells (min); signal ratio; z' of the plate; IC_{50} value of the positive control, its r^2 and hill slope. The following was tracked for each compound: IC_{50} values (in nM); % inhibition at maximum concentration; r^2 and hill slopes of the fitted response curves. Calculations were based on the following formulas: signal ratio = (positive control)/(negative control) z' = 1 − (((3 × SD negative control) + (3 × SD positive control))/(average of positive control − average of negative control)); % inhibition of sample = (100 − ((sample − average of negative control)/(average of positive control − average of negative control)) × 100. The assay window was established by control wells incubated with [^{14}C]glycine in the presence or absence of 10 mM nonlabeled glycine. A dose response curve for a synthesized reference standard was generated on every plate as a positive control.[37] Plate performances were assessed using a combination of assay window, z', and IC_{50} of positive control.

***In Vitro* GlyT-2 Inhibition Assessment.** Selectivity for GlyT-1 versus GlyT-2 was established using a GlyT-2 transfected cell model.[37] The cDNA for the human gene of GlyT-2 (SLC6A5, solute carrier family 6, member 5; Accession #NM_004211) was synthesized (Enzymax LLC) and subcloned into mammalian expression vector, pcDNA3.1 (Invitrogen Corp.) using standard molecular biology techniques. HEK293 cells (ATCC #CRL-1573) transfected with GlyT-2 modified pcDNA3.1 (Invitrogen Corp.) were selected for stable incorporation of the construct by resistance to the selective pressure of Geneticin (450 mg/mL; Invitrogen Corp.). A polyclonal HEK-GlyT2 cell population was used in the [^{14}C]glycine uptake assay previously described to evaluate the activity of the compounds of the invention with the following protocol modifications. The HEK-GlyT-2 cells were plated on poly-L-lysine coated Cytostar-T plates in DMEM media supplemented with 10% heat inactivated FBS. After an overnight incubation at 37 °C and 5% CO_2, the media was removed, and the assay was conducted as described above. Compounds of the invention were diluted in Uptake Buffer and tested against JAR or

DOI: 10.1021/acs.jmedchem.6b00914
J. Med. Chem. XXXX, XXX, XXX−XXX

HEK-GlyT-2 cells in parallel to evaluate relative potency and selectivity for GlyT-1 versus GlyT-2.[37]

Syntheses. *2-Amino-6-chloro-N-((1-(4-(propylsulfonyl)-piperazin-1-yl)cyclohexyl)methyl)benzamide Hydrochloride (**10**). Step A.* Cyclohexanone (5.0 g, 50.9 mmol) was added to a solution of 1-benzylpiperazine (**24**, 6.30 g, 34.0 mmol) and PTSA (7.76 g, 40.8 mmol) in H_2O (40 mL). The mixture stirred at rt for 30 min followed by addition of a solution of KCN (2.88 g, 44.2 mmol) in H_2O (20 mL). The mixture stirred at rt for 16 h and was filtered to afford 1-(4-benzylpiperazin-1-yl)cyclohexanecarbonitrile (**25**) as an off-white solid (9.05 g, 94%) ^{1}H NMR (300 MHz, $CDCl_3$) δ 7.32−7.24 (m, 5H), 3.50 (s, 2H), 2.79−2.60 (m, 4H), 2.60−2.38 (m, 4H), 2.14−2.09 (m, 2H), 1.79−1.72 (m, 2H), 1.59−1.51 (m, 5H), 1.31−1.24 (m, 1H).

Step B. A solution of 1-(4-benzylpiperazin-1-yl) cyclohexanecarbonitrile (**25**, 5.0 g, 17.6 mmol) in Et_2O (90 mL) was added dropwise over 30 min to a 0 °C cooled suspension of $LiAH_4$ (1.40 g, 35.2 mmol) in Et_2O (100 mL), and the resulting mixture stirred at rt for 12 h. The reaction was quenched by careful addition of H_2O (5 mL) and 1 N aq NaOH (2 mL). The mixture was filtered through a pad of Celite, and the filtrate was extracted with Et_2O (100 mL). The combined organic extracts were washed with H_2O (50 mL) and brine (50 mL). The organic layer was dried over Na_2SO_4, filtered, and concentrated under reduced pressure to afford the (1-(4-benzylpiperazin-1-yl)cyclohexyl)methanamine (**26**) as a colorless oil (5.0 g, quantitative): ^{1}H NMR (300 MHz, $CDCl_3$) δ 7.30−7.23 (m, 5H), 3.47 (s, 2H), 2.68 (s, 2H), 2.65−2.56 (m, 4H), 2.52−2.35 (m, 4H), 1.68 (s, 2H), 1.59−1.29 (m, 10H).

Step C. To a 0 °C solution of (1-(4-benzylpiperazin-1-yl)cyclohexyl)-methanamine (**26**, 5.0 g, 17.4 mmol) and Et_3N (7.3 mL, 52.3 mmol) in CH_2Cl_2 (80 mL) was added trifluoroacetic anhydride (3.0 mL, 21.2 mmol). The resulting mixture stirred at rt for 16 h and was then washed with saturated aqueous $NaHCO_3$ solution (50 mL), H_2O (50 mL) and brine (50 mL). The organic layer was dried over Na_2SO_4, filtered, and concentrated under reduced pressure, and the resulting residue was chromatographed over silica gel (0−50% EtOAc in hexanes) to give *N*-((1-(4-benzylpiperazin-1-yl)cyclohexyl)methyl)-2,2,2-trifluoroacetamide (**27**) as a colorless oil (4.74 g, 71%). ^{1}H NMR (300 MHz, $CDCl_3$) δ 7.34−7.21 (m, 5H), 3.48 (s, 2H), 2.40 (bs, 2H), 2.67−2.54 (m, 4H), 2.52−2.33 (m, 4H), 1.71−1.30 (m, 9H), 1.20−1.05 (m, 1H).

Step D. A mixture of *N*-((1-(4-benzylpiperazin-1-yl)cyclohexyl)-methyl)-2,2,2-trifluoroacetamide (**27**, 10.0 g, 26.1 mmol), Pd/C (10% w/w, 1.50 g), and NH_4HCO_2 (4.93 g, 78.3 mmol) in CH_3OH (200 mL) was heated at 65 °C for 3 h. The reaction was allowed to cool to rt and was filtered through a pad of Celite, which was rinsed with CH_3OH (100 mL). The filtrate was concentrated under reduced pressure, and the resulting residue was dissolved in CH_2Cl_2 (100 mL) and washed with saturated aqueous $NaHCO_3$ (3 × 100 mL) and brine (100 mL). The organic layer was dried over Na_2SO_4, filtered, and concentrated under reduced pressure to afford 2,2,2-trifluoro-*N*-((1-(piperazin-1-yl)cyclohexyl)methyl)acetamide as a clear oil (5.50 g, 72%). To a 0 °C solution of 2,2,2-trifluoro-*N*-((1-(piperazin-1-yl)cyclohexyl)methyl)acetamide (5.50 g, 18.8 mmol) and Et_3N (8.7 mL, 56.3 mmol) in CH_2Cl_2 (80 mL) was added a solution of propane-1-sulfonyl chloride (2.94 g, 20.6 mmol) in CH_2Cl_2 (30 mL) dropwise. The reaction mixture stirred at rt for 1 h and was then washed with H_2O (100 mL). The organic layer was dried over Na_2SO_4, filtered, and concentrated under reduced pressure. The resulting residue was dissolved in CH_3OH (5 mL) and H_2O (0.5 mL) to which K_2CO_3 (3.71 g, 26.8 mmol) was added. The reaction mixture stirred at reflux for 16 h and was then allowed to cool to rt and diluted with H_2O (30 mL). The aqueous mixture was extracted with CH_2Cl_2 (3 × 30 mL), and the organic extracts were dried over Na_2SO_4, filtered and concentrated under reduced pressure to afford the (1-(4-(propylsulfonyl)piperazin-1-yl)cyclohexyl)methanamine (**28a**) as a clear oil (0.39 g, 68%) ^{1}H NMR (500 MHz, DMSO-d_6) δ 10.03 (bs, 1H), 7.56 (d, J = 8.1 Hz, 1H), 7.38 (d, J = 7.1 Hz, 1H), 7.22 (m, 2H), 5.13 (dd, J = 14.3 Hz, 1.0 Hz, 2H), 4.71 (m, 1H), 3.83 (s, 3H), 3.73 (m, 1H), 3.48 (m, 1H), 3.31−3.19 (m, 3H), 2.42 (m, 1H), 2.18 (m 1H), 1.99−1.97 (m, 3H); ESI MS m/z 296 $[M + H]^+$.

Step E. A mixture of (1-(4-(propylsulfonyl)piperazin-1-yl)-cyclohexyl)methanamine (**28a**, 0.630 g, 2.07 mmol), 2-amino-6-chlorobenzoic acid (0.374 g, 2.17 mmol), Et_3N (0.86 mL, 6.21 mmol), and HBTU (1.17 g, 3.10 mmol) in DMF (20 mL) was stirred at rt for 16 h. The mixture was diluted with H_2O (100 mL) and extracted with EtOAc (3 × 80 mL). The combined organic extracts were washed with H_2O (3 × 80 mL) and brine (80 mL), dried over Na_2SO_4, filtered, and concentrated under reduced pressure. The resulting residue was chromatographed over silica gel (0−50% EtOAc in hexanes) to give 2-amino-6-chloro-*N*-((1-(4-(propylsulfonyl)piperazin-1-yl)-cyclohexyl)methyl)benzamide as a white foam (0.756 g, 80%) ^{1}H NMR (500 MHz, DMSO-d_6) δ 10.03 (bs, 1H), 7.56 (d, J = 8.1 Hz, 1H), 7.38 (d, J = 7.1 Hz, 1H), 7.22 (m, 2H), 5.13 (dd, J = 14.3 Hz, 1.0 Hz, 2H), 4.71 (m, 1H), 3.83 (s, 3H), 3.73 (m, 1H), 3.48 (m, 1H), 3.31−3.19 (m, 3H), 2.42 (m, 1H), 2.18 (m 1H), 1.99−1.97 (m, 3H); ESI MS m/z 296 $[M + H]^+$.

Step F. To a 0 °C solution of 2-amino-6-chloro-*N*-((1-(4-(propylsulfonyl)piperazin-1-yl)cyclohexyl)methyl)benzamide (0.750 g, 1.64 mmol) in CH_2Cl_2 (5 mL) was added a 1.0 M solution of HCl in Et_2O (4.92 mL, 4.92 mmol). The mixture was concentrated under reduced pressure to give 2-amino-6-chloro-*N*-((1-(4-(propylsulfonyl)-piperazin-1-yl)cyclohexyl)methyl)benzamide hydrochloride (**10**), which was lyophilized from CH_3CN and H_2O (0.790 g, quantitative): ^{1}H NMR (500 MHz, DMSO-d_6) δ 10.03 (bs, 1H), 7.15 (d, J = 8.1 Hz, 1H), 6.81−6.68 (m, 3H), 3.74 (m, 8H), 3.34 (m, 2H), 3.08 (m, 2H), 2.11−1.98 (m, 4H), 1.74−1.57 (m, 8H), 1.17 (m, 2H), 1.01 (t, J = 7.5 Hz, 3H); ESI MS m/z 296 $[M + H]^+$; HPLC > 99% (AUC) (Method A), t_R = 12.5 min.

*N-((4,4-Difluoro-1-(4-(propylsulfonyl)piperazin-1-yl)cyclohexyl)-methyl)-2,6-difluorobenzamide Hydrochloride (**11**). Step A.* To a 0 °C solution of *tert*-butyl piperazine-1-carboxylate (**12**, 10.0 g, 53.69 mmol) and Et_3N (22.4 mL, 161 mmol) in CH_2Cl_2 (200 mL) was slowly added 1-propanesulfonyl chloride (7.65 g, 53.6 mmol). The mixture stirred at rt for 3 h, then washed with 2 N aq NaOH (50 mL), 2 N aq HCl (50 mL), H_2O (50 mL), and brine (50 mL). The organic extracts were dried over Na_2SO_4, filtered, and concentrated under reduced pressure to afford *tert*-butyl 4-(propylsulfonyl)piperazine-1-carboxylate (**13**) as an off-white solid (15.7 g, quantitative): ^{1}H NMR (500 MHz, $CDCl_3$) δ 7.91 (d, J = 1.7 Hz, 1H), 7.48 (d, J = 1.6 Hz, 1H), 7.21 (m, 1H), 7.14 (s, 1H), 7.09 (s, 1H), 3.96 (s, 3H), 3.75 (s, 3H); ESI MS m/z 293 $[M + H]^+$.

Step B. To a 0 °C solution of *tert*-butyl 4-(propylsulfonyl)-piperazine-1-carboxylate (**13**, 15.7 g, 53.6 mmol) in CH_2Cl_2 (200 mL) was slowly added TFA (21.4 mL, 268 mmol). The mixture was stirred at rt for 16 h and washed with 2 N aq NaOH (3 × 50 mL), H_2O (50 mL), and brine (50 mL). The organic layer was dried over Na_2SO_4, filtered, and concentrated under reduced pressure to afford 1-(propylsulfonyl)piperazine (**14**) as a crystalline solid (10.3 g, quantitative): ^{1}H NMR (500 MHz, $CDCl_3$) δ 7.91 (d, J = 1.7 Hz, 1H), 7.48 (d, J = 1.6 Hz, 1H), 7.21 (m, 1H), 7.14 (s, 1H), 7.09 (s, 1H), 3.96 (s, 3H), 3.75 (s, 3H).

Step C. To a 0 °C solution of 4,4-difluorocyclohexanone (0.200 g, 1.49 mmol) in toluene (2 mL) was added a solution of piperazine-4-propyl sulfonamide (**14**, 0.287 g, 1.49 mmol) in toluene (2 mL), followed by dropwise addition of Ti(*i*-PrO)$_4$ (0.87 mL, 2.98 mmol). The reaction mixture stirred at rt for 2 h, then cooled back down to 0 °C. To this was added a 1.0 M solution of Et_2AlCN in toluene (2.98 mL, 2.98 mmol) dropwise. The mixture then stirred at rt for 16 h. H_2O (10 mL) was then carefully added, and the resulting precipitate was filtered. To the filtrate was added CH_2Cl_2 (20 mL) and H_2O (20 mL), and the aqueous layer was separated and extracted with CH_2Cl_2 (3 × 20 mL). The combined organic extracts were dried over Na_2SO_4, filtered, and concentrated under reduced pressure. The resulting residue was chromatographed over silica gel (0−30% EtOAc in hexanes) to give 4,4-difluoro-1-(4-(propylsulfonyl)piperazin-1-yl) cyclohexanecarbonitrile (**15**) as a white foam (0.233 g, 50%): ^{1}H NMR (300 MHz, $CDCl_3$) δ 3.38−3.34 (m, 4H), 2.93−2.90 (m, 2H), 2.75−2.72 (m, 4H), 2.18−2.02 (m, 8H), 1.90−1.83 (m, 2H), 1.07 (t, J = 4.9 Hz, 3H).

DOI: 10.1021/acs.jmedchem.6b00914
J. Med. Chem. XXXX, XXX, XXX−XXX

Step D. To a 0 °C solution of 4,4-difluoro-1-(4-(propylsulfonyl)-piperazin-1-yl) cyclohexanecarbonitrile (**15**, 2.95 g, 8.79 mmol) in Et_2O (60 mL) was added $LiAlH_4$ (0.67 g, 18 mmol). The mixture stirred at rt for 12 h, cooled back to 0 °C, then quenched by the sequential addition of H_2O (0.87 mL), 4 N aq NaOH (0.87 mL), and H_2O (4 mL). The resulting mixture was stirred at rt for 30 min, then filtered. The filtrate was concentrated under reduced pressure, and the resulting residue was chromatographed over silica gel (0−10% CH_3OH in CH_2Cl_2) to give (4,4-difluoro-1-(4-(propylsulfonyl)piperazin-1-yl)cyclohexyl)methanamine (**16**) as a colorless oil (2.2 g, 74%): ^{1}H NMR (300 MHz, $CDCl_3$) δ 3.23 (t, J = 4.8 Hz, 4H), 2.94−2.85 (m, 2H), 2.76 (t, J = 4.8 Hz, 4H), 2.72 (s, 2H), 2.15−1.75 (m, 10H), 1.70−1.45 (m, 2H), 1.07 (t, J = 7.5 Hz, 3H); ESI MS m/z 340 $[M + H]^+$.

Step E. To a 0 °C solution of (4,4-difluoro-1-(4-(propylsulfonyl)-piperazin-1-yl)cyclohexyl)methanamine (**16**, 0.15 g, 0.44 mmol) in CH_2Cl_2 (5 mL) was added Et_3N (0.12 mL, 0.88 mmol) and 2,6-difluorobenzoyl chloride (0.05 mL, 0.44 mmol). The resulting mixture stirred at rt for 4 h was diluted with CH_2Cl_2, then washed with saturated aqueous $NaHCO_3$ (10 mL). The organic layer was dried over Na_2SO_4, filtered, and concentrated under reduced pressure. The resulting residue was chromatographed over silica gel (0−50% EtOAc in hexanes) to give *N*-((4,4-difluoro-1-(4-(propylsulfinyl)piperazin-1-yl)cyclohexyl)methyl)-2,6-difluorobenzamide as a white solid (0.072 g, 46%): ^{1}H NMR (300 MHz, $CDCl_3$) δ 7.42−7.36 (m, 1H), 6.96 (t, J = 8.1 Hz, 2H), 6.13 (bs, 1H), 3.55 (d, J = 3.15 Hz, 2H), 3.34−3.27 (m, 4H), 2.91−2.85 (m, 2 H), 2.79−2.72 (m, 4 H), 2.02−1.82 (m, 8H), 1.71−1.56 (m, 2H), 1.06 (t, J = 4.9 Hz, 3H); ESI MS m/z 480 $[M + H]^+$.

Step F. To a 0 °C solution of *N*-((4,4-difluoro-1-(4-(propylsulfonyl)piperazin-1-yl)cyclohexyl)methyl)-2,6-difluorobenzamide (0.065 g, 0.135 mmol) in CH_3CN (1 mL) was added a 1.0 M solution of HCl in H_2O (1.5 mL). The mixture was stirred at rt for 30 min and lyophilized to give *N*-((4,4-difluoro-1-(4-(propylsulfonyl)piperazin-1-yl)cyclohexyl)methyl)-2,6-difluorobenzamide hydrochloride (**11**) as an amorphous white solid (0.068 g, quantitative): mp 165−169 °C; ^{1}H NMR (300 MHz, DMSO-d_6) δ 10.68 (bs, 1H), 9.32 (m, 0.4H), 8.78 (m, 0.6H), 7.62−7.42 (m, 1H), 7.30−7.13 (m, 2H), 4.00−3.68 (m, 7H), 3.56−2.94 (m, 6H), 2.79 (m, 2H), 2.30−1.54 (m, 7H), 0.99 (t, J = 4.8 Hz, 3H); APCI MS m/z 480 $[M + H]^+$; HPLC > 99% (AUC) (Method B), t_R = 22.3 min.

*2,6-Dichloro-N-((4,4-difluoro-1-(4-(propylsulfonyl)piperazin-1-yl)-cyclohexyl)methyl)benzamide Hydrochloride (**17**).* Compound **17** was prepared according to a similar procedure described for the synthesis of **11**. mp 220−223 °C; ^{1}H NMR (300 MHz, DMSO-d_6) δ 10.48 (bs, 1H), 9.12 (bs, 0.3H), 8.63 (bs, 0.7H), 7.68−7.38 (m, 3H), 3.92−2.99 (m, 9H), 2.80−2.68 (m, 3H), 2.30−1.58 (m, 10H), 0.99 (t, J = 7.5 Hz, 3H); APCI MS m/z 512 $[M + H]^+$; HPLC 95.7% (AUC) (Method B), t_R = 23.1 min.

*2-Chloro-N-((4,4-difluoro-1-(4-(propylsulfonyl)piperazin-1-yl)-cyclohexyl)methyl)-6-(trifluoromethoxy)benzamide Hydrochloride (**18**). Step A.* (4,4-Difluoro-1-(4-(propylsulfonyl)piperazin-1-yl)-cyclohexyl)methanamine (**16**, 0.15 g, 0.44 mmol), 2-chloro-6-(trifluoromethoxy)benzoic acid (0.105 g, 0.44 mmol), EDCI·HCl (0.09 g, 0.44 mmol), HOBt (0.07 g, 0.44 mmol), and Et_3N (0.3 mL, 1.91 mmol) in DMF (10 mL) stirred at rt for 16 h. The mixture was diluted with H_2O (20) mL and extracted with EtOAc (3 × 20 mL). The combined organic extracts were washed with H_2O (3 × 20 mL) and brine (20 mL). The organic layers were then dried over Na_2SO_4, filtered, and concentrated under reduced pressure. The resulting residue was chromatographed over silica gel (0−50% EtOAc in hexanes) to give 2-chloro-*N*-((4,4-difluoro-1-(4-(propylsulfonyl)-piperazin-1-yl)cyclohexyl)methyl)-6-(trifluoromethoxy)benzamide as a white solid (0.155 g, 63%): ESI MS m/z 562 $[M + H]^+$.

Step B. To a 0 °C solution of 2-chloro-*N*-((4,4-difluoro-1-(4-(propylsulfonyl)piperazin-1-yl)cyclohexyl)methyl)-6-(trifluoromethoxy)-benzamide (0.050 g, 0.08 mmol) in CH_3CN (5 mL) was added a 1.0 M solution of HCl in H_2O (1.0 mL, 1.0 mmol). The mixture stirred at rt for 30 min and was lyophilized to give 2-chloro-*N*-((4,4-difluoro-1-(4-(propylsulfonyl)piperazin-1-yl)cyclohexyl)methyl)-6-(trifluoromethoxy) benzamide hydrochloride (**18**) as a white solid (0.058 g, quantitative): mp 200−205 °C; ^{1}H NMR (300 MHz, DMSO-d_6) δ 10.55 (bs, 1H), 9.15 (m, 0.3H), 8.77 (m, 0.7H), 7.62−7.31 (m, 3H), 4.00−3.00 (m, 9H), 2.80−2.68 (m, 3H), 2.29−1.60 (m, 10H), 1.00 (t, J = 7.5 Hz, 3H); ESI MS m/z 562 $[M + H]^+$; HPLC > 99% (AUC) (Method C), t_R = 20.4 min.

*2,4-Dichloro-N-((4,4-difluoro-1-(4-(propylsulfonyl)piperazin-1-yl)-cyclohexyl)methyl)benzamide Hydrochloride (**19**).* Compound **19** was prepared according to a similar procedure described for the synthesis of **11**. mp 124−126 °C; ^{1}H NMR (300 MHz, DMSO-d_6) δ 10.66 (bs, 1H), 8.96 (bs, 0.5H), 8.47 (bs, 0.5H), 7.80−7.35 (m, 3H), 3.95−3.00 (m, 9H), 2.82 (m, 3H), 2.30−1.50 (m, 10H), 0.99 (t, J = 7.5 Hz, 3H); ESI MS m/z 512 $[M + H]^+$; HPLC 98.2% (AUC) (Method B), t_R = 23.5 min.

*2-Chloro-N-((4,4-difluoro-1-(4-(propylsulfonyl)piperazin-1-yl)-cyclohexyl)methyl)-4-fluorobenzamide Hydrochloride (**20**).* Compound **20** was prepared according to a similar procedure described for the synthesis of **18**. mp 220−225 °C; ^{1}H NMR (300 MHz, DMSO-d_6) δ 10.91 (s, 1H), 9.00 (m, 0.7H), 8.66 (m, 0.3H), 7.61−7.43 (m, 2H), 7.42−7.31 (m, 1H), 4.00 (m, 4H), 3.82−3.59 (m, 4H), 3.31−3.22 (m, 2H), 3.26−3.01 (m, 3H), 2.75 (bs, 1H), 2.30−1.99 (m, 6H), 1.75 (m, 2H), 0.98 (t, J = 7.5 Hz, 3H); ESI MS m/z 496 $[M + H]^+$; HPLC 98.2% (AUC) (Method C), t_R = 18.8 min.

*2-Chloro-N-((4,4-difluoro-1-(4-(propylsulfonyl)piperazin-1-yl)-cyclohexyl)methyl)-4-(trifluoromethyl)benzamide Hydrochloride (**21**).* Compound **21** was prepared according to a similar procedure described for the synthesis of **18**. mp 115−120 °C; ^{1}H NMR (400 MHz, DMSO-d_6) δ 11.20 (bs, 1H), 9.12 (bs, 1H), 8.00 (m, 1H), 7.62−7.59 (m, 2H), 3.90−3.61 (m, 6H), 3.30 (m, 2H), 3.21−3.00 (m, 3H), 2.76 (m, 1H), 2.31−1.72 (m, 10H), 1.05 (t, J = 7.3 Hz, 3H); ESI MS m/z 546 $[M + H]^+$; HPLC > 99% (AUC) (Method B), t_R = 29.6 min.

*N-((4,4-Difluoro-1-(4-(propylsulfonyl)piperazin-1-yl)cyclohexyl)-methyl)-2,4-bis(trifluoromethyl)benzamide Hydrochloride (**22**).* Compound **22** was prepared according to a similar procedure described for the synthesis of **18**. mp 124−131 °C; ^{1}H NMR (300 MHz, DMSO-d_6) δ 11.20 (bs, 1H), 9.14 (bs, 1H), 8.20−8.17 (m, 2H), 7.98−7.73 (m, 1H), 4.24−4.13 (m, 3H), 3.94−3.67 (m, 4H), 3.30−3.02 (m, 4H), 2.73−2.50 (m, 1H), 2.20−1.53 (m, 10H), 0.97 (t, J = 7.3 Hz, 3H). ESI MS m/z 580 $[M + H]^+$; HPLC > 99% (AUC) (Method C), t_R = 21.6 min.

*N-((4,4-Difluoro-1-(4-(propylsulfonyl)piperazin-1-yl)cyclohexyl)-methyl)-4-fluoro-2-methoxy-6-methylbenzamide (**23**).*[38] To a stirring suspension of 4-fluoro-2-hydroxybenzoic acid (10.0 g, 64.0 mmol) and K_2CO_3 (22.0 g, 160 mmol) in DMF (200 mL) was slowly added CH_3I (20.0 g, 140 mmol) at rt. The mixture was then heated at 90 °C for 16 h. After allowing to cool to rt, the mixture was concentrated under reduced pressure, and the resulting white solid rinsed over a plug of silica gel (CH_2Cl_2 eluent) to afford methyl 4-fluoro-2-methoxybenzoate as clear oil (10.0 g, 92%). The intermediate was taken into the next step without any further analysis.

To a solution of 4-fluoro-2-methoxybenzoate (10.0 g, 58.8 mmol) in CH_3OH (50 mL) was slowly added 6 N aq NaOH (30 mL) over a period of 15 min. The mixture was stirred at rt for 1 h and was acidified to pH = 2 with 6 N aq HCl. The resulting precipitate was collected via vacuum filtration to afford 4-fluoro-2-methyl benzoic acid (9.2 g, 85%). ^{1}H NMR (300 MHz, $CDCl_3$) δ 8.21 (dd, J = 9.0 Hz, 6.9 Hz, 1H), 6.82−6.88 (m, 1H), 6.79 (dd, J = 7.8 Hz, 2.1 Hz, 1H), 4.07 (s, 1H).

To a −78 °C cooled solution of TMEDA (1.95 mL, 19.2 mmol) in THF (8 mL) was slowly added *sec*-BuLi (1.4 M solution in cyclohexane, 18.5 mL, 25.8 mmol), followed by a solution of 4-fluoro-2-methyl-benzoic acid (1.0 g, 5.88 mmol) in THF (2 mL). The mixture stirred at −78 °C for 2 h before addition of a solution of CH_3I (1.46 mL, 23.5 mmol) in THF (2 mL). The mixture stirred at −78 °C for 1 h and was then allowed to warm to rt and quenched with H_2O (10 mL). The crude mixture was diluted with H_2O (10 mL) and extracted with EtOAc (50 mL). The aqueous layer was collected and acidified to pH = 2 with 2 N aq HCl then extracted with EtOAc (2 × 20 mL). The combined organic extracts were dried over Na_2SO_4, filtered, and concentrated under reduced pressure. The resulting

DOI: 10.1021/acs.jmedchem.6b00914
J. Med. Chem. XXXX, XXX, XXX−XXX

residue was chromatographed over silica gel (0−50% EtOAc in hexanes) to give 4-fluoro-2-methoxy-6-methyl benzoic acid as a white solid (0.18 g, 16%). ^{1}H NMR (300 MHz, $CDCl_3$) δ 6.53−6.62 (m, 2H), 3.90 (s, 1H), 2.48 (s, 1H); MS (ESI$^+$) m/z 185 (M + H).

Step E. To a 0 °C solution of 2-methoxy-6-methyl-4-fluorobenzoic acid (0.08 g, 0.44 mmol) in CH_2Cl_2 (4 mL) was added oxalyl chloride (0.08 mL, 0.88 mmol) followed by 2 drops of DMF, and the mixture was stirred at rt for 1.5 h to generate 2-methoxy-6-methyl-4-fluorobenzoyl chloride. This mixture was concentrated under reduced pressure and dissolved in CH_2Cl_2 (1 mL), which was then added to a 0 °C solution of (4,4-difluoro-1-(4-(propylsulfonyl)piperazin-1-yl)cyclohexyl)methanamine (**16**, 0.15 g, 0.44 mmol) and Et_3N (0.18 mL, 1.31 mmol) in CH_2Cl_2 (4 mL). The resulting mixture stirred at rt for 4 h and was then diluted with CH_2Cl_2 and washed with saturated aqueous $NaHCO_3$ solution (5 mL). The organic layer was dried over Na_2SO_4, filtered, and concentrated under reduced pressure, and the resulting residue was chromatographed over silica gel (0−50% EtOAc in hexanes) to give *N*-((4,4-difluoro-1-(4-(propylsulfonyl)piperazin-1-yl)cyclohexyl)methyl)-4-fluoro-2-methoxy-6-methylbenzamide (**23**) as a white solid (0.13 g, 58%): mp 160−163 °C; ^{1}H NMR (300 MHz, DMSO-d_6) δ 10.65 (bs, 1H), 8.71 (bs, 0.6H), 8.15 (bs, 0.4H), 6.90−6.58 (m, 2H), 3.76 (s, 3H), 3.74−3.35 (m, 5H), 3.25−2.60 (m, 7H), 2.19 (s, 3H), 2.05−1.52 (m, 10H), 0.98 (t, J = 7.5 Hz, 3H); APCI MS m/z 506 [M + H]$^+$; HPLC > 99% (AUC) (Method B), t_R = 22.3 min.

*2-Amino-6-chloro-N-((1-(4-(methylsulfonyl)piperazin-1-yl)-cyclohexyl)methyl)benzamide Hydrochloride (**29**).* Compound **29** was prepared according to a similar procedure described for the synthesis of **10** using methylsulfonyl chloride. mp 178−181 °C; ^{1}H NMR (300 MHz, DMSO-d_6) δ 8.80 (bs, 1H), 7.08 (t, J = 8.1 Hz, 1H), 6.72−6.64 (m, 2H), 6.23 (bs, 2H), 3.84−3.27 (m, 10H), 2.91 (s, 3H), 2.17−2.01 (m, 2H), 1.80−1.44 (m, 7H), 1.25−1.02 (m, 1H); ESI MS m/z 429 [M + H]$^+$; HPLC 96.6% (AUC) (Method B), t_R = 19.6 min.

*2-Amino-6-chloro-N-((1-(4-(ethylsulfonyl)piperazin-1-yl)-cyclohexyl)methyl)benzamide Hydrochloride (**30**).* Compound **30** was prepared according to a similar procedure described for the synthesis of **10** using ethylsulfonyl chloride. mp 170−173 °C; ^{1}H NMR (300 MHz, CD_3OD) δ 7.46 (d, J = 2.0 Hz, 1H), 7.18 (s, 1H), 7.09 (s, 1H), 4.04−3.82 (m, 6H), 3.55−3.33 (m, 4H), 3.15 (q, J = 7.4 Hz, 2H), 2.18 (d, J = 11.8 Hz, 2H), 1.93−1.72 (m, 5H), 1.70−1.54 (m, 2H), 1.34 (t, J = 7.6 Hz, 3H), 1.30−1.25 (m, 1H), 1.01 (t, J = 7.5 Hz, 3H); ESI MS m/z 443 [M + H]$^+$; HPLC > 99% (AUC) (Method B), t_R = 19.8 min.

*2-Amino-6-chloro-N-((1-(4-(isobutylsulfonyl)piperazin-1-yl)-cyclohexyl)methyl)benzamide Hydrochloride (**31**).* Compound **31** was prepared according to a similar procedure described for the synthesis of **10** using isobutylsulfonyl chloride. mp 195−198 °C; ^{1}H NMR (300 MHz, DMSO-d_6) δ 8.79 (s, 1H), 7.07 (t, J = 7.8 Hz, 1H), 6.66 (q, J = 8.1 Hz, 2H), 5.78 (bs, 2H), 3.88−3.18 (m, 10H), 2.98 (d, J = 6.6 Hz, 2H), 2.25−2.06 (m, 3H), 1.98−1.39 (m, 7H), 1.23−1.08 (m, 1H), 1.03 (d, J = 6.6 Hz, 6H); APCI MS m/z 471 [M + H]$^+$; HPLC 95.1% (AUC) (Method B), t_R = 21.1 min.

*2-Amino-6-chloro-N-((1-(4-(phenylsulfonyl)piperazin-1-yl)-cyclohexyl)methyl)benzamide Hydrochloride (**32**).* Compound **32** was prepared according to a similar procedure described for the synthesis of **10** using phenylsulfonyl chloride. mp 230−232 °C; ^{1}H NMR (300 MHz, DMSO-d_6) δ 8.77 (bs, 1H), 7.80−7.66 (m, 5H), 7.12−7.06 (m, 1H), 6.73−6.65 (m, 2H), 3.88−3.28 (m, 9H), 3.30−2.76 (m, 3H), 2.16−1.91 (m, 3H), 1.86−1.37 (m, 7H), 1.15−1.00 (m, 1H); APCI MS m/z 491 [M + H]$^+$; HPLC 96.8% (AUC) (Method B), t_R = 14.4 min.

*2-Amino-N-((1-(4-(benzylsulfonyl)piperazin-1-yl)cyclohexyl)-methyl)-6-chlorobenzamide Hydrochloride (**33**).* Compound **33** was prepared according to a similar procedure described for the synthesis of **10**. mp 215−217 °C; ^{1}H NMR (300 MHz, DMSO-d_6) δ 8.81 (bs, 1H), 7.44−7.33 (m, 5H), 7.10 (t, J = 8.1 Hz, 1H), 6.77−6.68 (m, 2H), 4.50 (s, 2H), 3.72−3.51 (m, 8H), 3.35−3.16 (m, 2H), 2.14−1.85 (m, 5H), 1.78−1.43 (m, 6H), 1.24−1.01 (m, 1H); ESI MS m/z 505 [M + H]$^+$; HPLC 96.3% (AUC), (Method B), t_R = 21.4 min.

*2,4-Dichloro-N-((1-(4-(propylsulfonyl)piperazin-1-yl)cyclohexyl)-methyl)benzamide Hydrochloride (**34**). Step G.* To a 0 °C solution of (1-(4-(propylsulfonyl)piperazin-1-yl)cyclohexyl) methanamine (**28a**, 0.30 g, 0.99 mmol) and Et_3N (0.41 mL, 2.96 mmol) in CH_2Cl_2 (3 mL) was added 2,4-dichloro benzoyl chloride (0.30 g, 1.48 mmol). The mixture stirred at rt for 16 h. The mixture was diluted with CH_2Cl_2 and washed with 1 N aq NaOH (10 mL), H_2O (10 mL), and brine (10 mL). The organic layers were dried over Na_2SO_4, filtered, and concentrated under reduced pressure. The resulting residue was chromatographed over silica gel (0−50% EtOAc in hexanes) to give 2,4-dichloro-*N*-((1-(4-(propylsulfonyl)piperazin-1-yl)cyclohexyl)-methyl)benzamide (**34**) as an off-white solid (0.27 g, 57%); ^{1}H NMR (300 MHz, $CDCl_3$) δ (d, J = 8.4 Hz, 1H), 7.41 (d, J = 2.0 Hz, 1H), 7.33 (dd, J = 2.0 Hz, 8.4 Hz, 1H), 6.89 (bs, 1H), 3.60−3.52 (d, J = 5.1 Hz, 2H), 3.28−3.20 (m, 4H), 2.90−2.80 (m, 2), 2.79−2.69 (m, 4H), 1.90−1.78 (m, 2H), 1.72−1.40 (m, 10H), 1.08−1.03 (t, J = 7.4 Hz, 3H); ESI MS m/z 476 [M + H]$^+$.

Step H. To a 0 °C solution of 2,4-dichloro-*N*-((1-(4-(propylsulfonyl)piperazin-1-yl)cyclohexyl)methyl)benzamide (0.27 g, 0.56 mmol) in CH_3CN (1 mL) was added 10% HCl in H_2O (0.5 mL). The mixture stirred at rt for 30 min and was then lyophilized to give 2,4-dichloro-*N*-((1-(4-(propylsulfonyl)piperazin-1-yl)cyclohexyl) methyl)benzamide hydrochloride (**34**) as a white solid (0.28 g, quantitative): mp 202−208 °C; ^{1}H NMR (500 MHz, DMSO-d_6) δ 10.83 (bs, 1H), 8.91 (bs, 1H), 7.72 (s, 1H), 7.53 (m, 2H), 3.75−3.59 (m, 8H), 3.28 (m, 2H), 3.11 (m, 2H), 2.08 (m, 2H), 1.93 (m, 2H), 1.69−1.50 (m, 7H), 1.16 (m, 1H), 1.02 (t, J = 7.4 Hz, 3H); ESI MS m/z 476 [M + H]$^+$; HPLC 98.7% (AUC) (Method A), t_R = 22.3 min.

*2,4-Dichloro-N-((1-(4-((cyclopropylmethyl)sulfonyl)piperazin-1-yl)cyclohexyl)methyl)benzamide Hydrochloride (**35**).* Compound **35** was prepared according to a similar procedure described for the synthesis of **34**. mp 217−219 °C; ^{1}H NMR (300 MHz, DMSO-d_6) δ 11.01 (bs, 1H), 8.92 (t, J = 6.0 Hz, 1H), 7.72 (d, J = 1.2 Hz, 1H), 7.57−7.50 (m, 2H), 3.83−3.40 (m, 10H), 3.11 (d, J = 6.9 Hz, 2H), 2.12−1.85 (m, 4H), 1.77−1.46 (m, 5H), 1.22−0.95 (m, 2H), 0.62−0.55 (m, 2H), 0.42−0.35 (m, 2H); ESI MS m/z 488 [M + H]$^+$; HPLC > 99% (AUC) (Method B), t_R = 20.5 min.

Cyclobutanesulfonyl Chloride. Step A. To a suspension of magnesium turnings (0.79 g, 32.0 mmol) in Et_2O (20 mL) was added a solution of cyclobutyl bromide (1.8 mL, 19.1 mmol) in Et_2O (20 mL) portion-wise. After the initial exothermic reaction had ceased, the mixture was heated at reflux for 1 h. The suspension was allowed to cool to rt, and the supernatant was collected and added portion-wise to a 0 °C solution of sulfuryl chloride (4.6 mL, 57.1 mmol) in CH_2Cl_2 (30 mL). The mixture stirred at rt for 1 h and was concentrated under reduced pressure. The residue was taken up in hexanes (150 mL), and the resulting precipitate was filtered. The filtrate was concentrated under reduced pressure to give cyclobutylsulfonyl chloride 2 (3.1 g, crude, >99%) as a pale brown oil, which was carried into the next step without purification.

*2,4-Dichloro-N-((1-(4-(cyclobutylsulfonyl)piperazin-1-yl)-cyclohexyl)methyl)benzamide Hydrochloride (**36**).* Compound **36** was prepared according to a similar procedure described for the synthesis of **34** using cyclobutylsulfonyl chloride. mp 249−252 °C; ^{1}H NMR (300 MHz, DMSO-d_6) δ 10.57 (bs, 1H), 8.87 (t, J = 5.7 Hz, 1H), 7.73 (s, 1H), 7.53 (d, J = 0.6 Hz, 2H), 4.10 (quintet, J = 8.4 Hz, 1H), 3.80−3.51 (m, 8H), 3.30−3.05 (m, 2H), 2.40−2.18 (m, 4H), 2.12−1.45 (m, 12H); ESI MS m/z 488 [M + H]$^+$; HPLC > 99% (AUC) (Method B), t_R = 21.5 min.

*2,4-Dichloro-N-((1-(4-((1-methyl-1H-pyrazol-4-yl)sulfonyl)-piperazin-1-yl)cyclohexyl)methyl)benzamide Hydrochloride (**37**).* Compound **37** was prepared according to a similar procedure described for the synthesis of **34** using 1-methyl-1*H*-pyrazole-4-sulfonyl chloride. mp 164−165 °C; ^{1}H NMR (400 MHz, DMSO-d_6) δ 9.40 (bs, 1H), 8.82 (bs, 1H), 8.44 (s, 1H), 7.86 (s, 1H), 7.74 (s, 1H), 7.53 (s, 2H), 3.92 (s, 3H), 3.79−3.59 (m, 6H), 2.84−2.63 (m, 4H), 2.10−1.99 (m, 2H), 1.74−1.45 (m, 7H), 1.21−0.97 (m, 1H); APCI MS m/z 514 [M + H]$^+$; HPLC 98.2% (AUC) (Method B), t_R = 18.9 min.

*2,4-Dichloro-N-((1-(4-((1-methyl-1H-imidazol-4-yl)sulfonyl)-piperazin-1-yl)cyclohexyl)methyl)benzamide Hydrochloride (**38**).*

DOI: 10.1021/acs.jmedchem.6b00914
J. Med. Chem. XXXX, XXX, XXX−XXX

Compound **38** was prepared according to a similar procedure described for the synthesis of **34** using 1-methyl-1*H*-imidazole-4-sulfonyl chloride. mp 172−173 °C; ^{1}H NMR (300 MHz, DMSO-d_6): δ 10.14 (bs, 1H), 8.86 (s, 1H), 7.89 (d, J = 8.4 Hz, 2H), 7.73 (s, 1H), 7.52 (s, 2H), 3.79−3.58 (m, 9H), 3.42−3.07 (m, 4H), 2.11−1.94 (m, 2H), 1.87−1.41 (m, 7H), 1.21−0.99 (m, 1H); ESI MS m/z 514 $[M + H]^+$; HPLC 97.5% (AUC) (Method B), t_R = 20.5 min.

1-Methyl-1H-1,2,3-triazole-4-sulfonyl Chloride. Step A. To a 10 °C solution of sodium 1*H*-1,2,3-triazole-4-thiolate (115 g, 0.93 mol) in EtOH (1.1 L) was added benzyl bromide (111 mL, 0.93 mol) dropwise over a period of 20 min. The mixture stirred at rt for 20 min and was then diluted with EtOAc (3 L). The organic layer was washed with H_2O (2 × 500 mL) and brine (500 mL), dried over Na_2SO_4, filtered, and concentrated to afford crude 4-(benzylthio)-1*H*-1,2,3-triazole as off white solid (165 g, 92%); ^{1}H NMR (300 MHz, $CDCl_3$) δ 13.37 (bs, 1H), 7.48 (s, 1H), 7.21 (m, 5H), 4.09 (s, 2H); ESI MS m/z 192 $[M + H]^+$.

Step B. To a solution of 4-(benzylthio)-1*H*-1,2,3-triazole (140 g, 0.73 mol) in DMF (1.4 L) was added K_2CO_3 (202 g, 1.46 mol), and the resulting mixture stirred at rt for 30 min. The reaction mixture was then cooled to 0 °C, and dimethyl sulfate (104.5 mL, 1.09 mol) was added dropwise over a period of 15 min. The mixture stirred at rt for 16 h and was then diluted with H_2O (3 L). The aqueous mixture was extracted with EtOAc (5 × 500 mL), and the combined organic extracts were dried over Na_2SO_4, filtered, and concentrated under reduced pressure. The resulting residue was chromatographed over silica gel (0−50% EtOAc in hexanes) to give 4-(benzylthio)-1-methyl-1*H*-1,2,3-triazole as off-white solid (34.1 g, 23%); ^{1}H NMR (400 MHz, CD_3OD) δ 7.65 (s, 1H), 7.24−7.16 (m, 5H), 4.04 (s, 2H), 4.0 (s, 3H); ESI MS m/z 206 $[M + H]^+$. The regioisomer was confirmed via a ^{1}H NMR NOESY experiment, which exhibited a positive NOE enhancement between the methyl group hydrogens and the triazole hydrogen. Furthermore, ^{1}H NMR NOESY experiments for the corresponding regioisomers 4-(benzylsulfonyl)-2-methyl-2*H*-1,2,3-triazole (34.1 g isolated, 23%) and 5-(benzylsulfonyl)-1-methyl-1*H*-1,2,3-triazole (34.1 g isolated, 23%) did not exhibit an NOE enhancement between the methyl group hydrogens and the triazole hydrogen.

Step C. To a solution of 4-(benzylthio)-1-methyl-1*H*-1,2,3-triazole (12.0 g, 58.5 mmol) in CH_3CN (600 mL) was added HOAc (20 mL) and H_2O (15 mL). The mixture was cooled to 5 °C, and 1,3-dichloro-5,5-dimethylimidazolidine-2,4-dione (23.0 g, 117.0 mmol) was added over a period of 20 min. The mixture continued to stir at 5 °C for an additional 2 h. The mixture was cooled to 0 °C and diluted with CH_2Cl_2 (500 mL). To this was added a solution of 5% aqueous $NaHCO_3$ (300 mL), and the mixture stirred for 10 min. The separated organic layer was washed with brine (300 mL), dried over Na_2SO_4, filtered, and concentrated to afford crude 1-methyl-1*H*-1,2,3-triazole-4-sulfonyl chloride (14.7 g), which was used as is in the next step.

*2,4-Dichloro-N-((1-(4-((1-methyl-1H-1,2,3-triazol-4-yl)sulfonyl)-piperazin-1-yl)cyclohexyl)methyl)benzamide Hydrochloride (**39**).* Compound **39** was prepared according to a similar procedure described for the synthesis of **34** using 1-methyl-1*H*-1,2,3-triazole-4-sulfonyl chloride. ^{1}H NMR (500 MHz, $CDCl_3$) δ 7.95 (s, 1H), 7.71 (d, J = 8.5 Hz, 1H), 7.41 (d, J = 2.0 Hz, 1H), 7.33 (dd, J = 8.5, 2.0 Hz, 1H), 6.79 (bs, 1H), 4.19 (s, 3H), 3.57 (d, J = 5.0 Hz, 2H), 3.29−3.22 (m, 4H), 2.79−2.73 (m, 4H), 1.68−1.55 (m, 4H), 1.50−1.40 (m, 5H), 1.28−1.21 (m, 1H); ESI MS m/z 515 $[M + H]^+$; HPLC 96.6% (AUC) (Method D), t_R = 5.3 min.

*N-((4,4-Difluoro-1-(4-((1-methyl-1H-imidazol-4-yl)sulfonyl)-piperazin-1-yl)cyclohexyl)methyl)-2,6-difluorobenzamide Hydrochloride (**44**). Step A.* To a 0 °C solution of *tert*-butyl piperazine-1-carboxylate (**12**, 10.0 g, 53.7 mmol) in CH_2Cl_2 (50 mL) was added Et_3N (22.6 mL, 161 mmol) and a solution of 1-methyl-1*H*-imidazole-4-sulfonyl chloride (11.6 g, 64.5 mmol) in CH_2Cl_2 (50 mL) dropwise over 30 min while maintaining the temperature of the reaction mixture below 5 °C. The reaction mixture was stirred at rt for an additional 5 h and was then quenched with a saturated aqueous solution of $NaHCO_3$ (50 mL). The aqueous mixture was extracted with CH_2Cl_2 (3 × 100 mL), and the combined organic extracts were washed with brine (1 × 50 mL), dried over Na_2SO_4, filtered, and concentrated under reduced pressure to give a crude solid. The solids were suspended in Et_2O and stirred for 30 min at rt then filtered, washed with cold Et_2O, and dried under vacuum to afford *tert*-butyl 4-(1-methyl-1*H*-imidazol-4-ylsulfonyl)piperazine-1-carboxylate (**40**) as an off-white solid (16.8 g, 95%): ^{1}H NMR (300 MHz, $CDCl_3$) δ (dd, J = 1.5 Hz, 14.5 Hz, 2H), 3.76 (s, 3H), 3.55−3.45 (m, 4H), 3.20−3.10 (m, 4H), 1.43 (s, 9H); ESI MS m/z 331 $[M + H]^+$.

Step B. To a 0 °C solution of *tert*-butyl 4-(1-methyl-1*H*-imidazol-4-ylsulfonyl)piperazine-1-carboxylate (**40**, 6.0 g, 18.1 mmol) in 1,4-dioxane (30 mL) was slowly added 12 N aq HCl (30 mL) dropwise over a period of 30 min. The reaction mixture stirred at rt for 2 h and was concentrated under reduced pressure. The residue was azeotroped with toluene (3 × 100 mL), and the resultant solids were dissolved in H_2O (100 mL). The aqueous mixture was washed with CH_2Cl_2 (2 × 100 mL) then carefully neutralized with solid K_2CO_3 (15 g). The aqueous mixture was then extracted with CH_2Cl_2 (4 × 100 mL), and the combined organic extracts were washed with brine (50 mL), dried over Na_2SO_4, filtered, and concentrated under reduced pressure to afford 1-(1-methyl-1*H*-imidazol-4-ylsulfonyl)piperazine (**41**) as off-white foam (3.8 g, 90%): ^{1}H NMR (400 MHz, $CDCl_3$) δ (dd, J = 1.1 Hz, 16.8 Hz, 2H), 3.80−3.75 (m, 5H), 3.74−3.65 (m, 2H), 3.37−3.1 (m, 2H), 3.0−3.25 (m, 2H); ESI MS m/z 231 $[M + H]^+$.

Step C. To a 0 °C solution of 4,4-difluorocyclohexanone (3.0 g, 22.3 mmol) in toluene (20 mL) was added TMSCN (3.3 mL, 24.8 mmol) dropwise, followed by ZnI_2 (0.360 g, 1.13 mmol). The mixture was stirred at rt for 15 min followed by the addition of a solution of 1-(1-methyl-1*H*-imidazol-4-ylsulfonyl)piperazine (**41**, 5.12 g, 22.2 mmol) in CH_3OH (90 mL). The mixture was then heated at reflux for 4 h followed by stirring at rt for an additional 16 h. The mixture was concentrated under reduced pressure, and the resulting residue was dissolved in CH_2Cl_2 (100 mL), washed with H_2O (2 × 50 mL), dried over Na_2SO_4, filtered, and concentrated under reduced pressure to give 4,4- difluoro-1-(4-(1-methyl-1*H*-imidazol-4-ylsulfonyl)piperazin-1-yl)cyclohexanecarbonitrile (**42**) as an off-white solid (3.10 g, 37%): ^{1}H NMR (300 MHz, $CDCl_3$) δ 7.52 (d, J = 1.2 Hz, 1H), 7.45 (d, J = 1.2 Hz, 1H), 3.77 (s, 3H), 3.31 (m, 4H), 2.71 (m, 4H), 2.2−1.85 (m, 8H); APCI MS m/z 374 $[M + H]^+$.

Step D. To a 0 °C solution of 4,4-difluoro-1-(4-(1-methyl-1*H*-imidazol-4-ylsulfonyl)piperazin-1-yl)cyclohexanecarbonitrile (**42**) (3.79 g, 10.2 mmol) in THF (80 mL) was added $LiAlH_4$ (1.32 g, 34.8 mmol) portion-wise over a period of 15 min. The mixture stirred at rt for 5 h and was then cooled to 0 °C and carefully quenched with H_2O (5 mL) and 4 N aq NaOH (1.4 mL). The resulting mixture was stirred at rt for 15 min, followed by addition of Na_2SO_4 (5 g). The mixture was filtered, and the filtrate was concentrated under reduced pressure. The resulting residue was triturated with hexanes, and the solids were filtered and dried under reduced pressure to give (4,4-difluoro-1-(4-((1-methyl-1*H*-imidazol-4-yl)sulfonyl)piperazin-1-yl)cyclohexyl)methanamine (**43**) (3.36 g, 87%): ^{1}H NMR (300 MHz, $CDCl_3$) δ 7.52 (d, J = 1.2 Hz, 1H), 7.45 (d, J = 1.2 Hz, 1H), 3.77 (s, 3H), 3.18 (m, 4H), 2.71 (m, 4H), 2.2−1.85 (m, 10H); APCI MS m/z 378 $[M + H]^+$.

Step E. To a 0 °C solution of (4,4-difluoro-1-(4-((1-methyl-1*H*-imidazol-4-yl)sulfonyl)piperazin-1-yl)cyclohexyl)methanamine (**43**, 0.50 g, 1.32 mmol) in CH_2Cl_2 (10 mL) was added Et_3N (0.54 mL, 3.97 mmol) and 2,6-difluorobenzoyl chloride (0.233 g, 1.32 mmol). The resulting mixture was stirred at rt for 4 h, diluted with CH_2Cl_2, and then washed with saturated aqueous $NaHCO_3$ solution (10 mL). The organic layer was dried over Na_2SO_4, filtered, and concentrated under reduced pressure. The resulting residue was chromatographed over silica gel (0−50% EtOAc in hexanes) to give *N*-((4,4-difluoro-1-(4-((1-methyl-1*H*-imidazol-4-yl)sulfonyl)piperazin-1-yl)cyclohexyl)-methyl)-2,6-difluorobenzamide as a white solid (0.409 g, 60%): ESI MS m/z 518 $[M + H]^+$.

Step F. To a 0 °C solution of *N*-((4,4-difluoro-1-(4-((1-methyl-1*H*-imidazol-4-yl)sulfonyl)piperazin-1-yl)cyclohexyl)methyl)-2,6-difluorobenzamide (0.100 g, 0.19 mmol) in CH_3CN (1 mL) was slowly added a 1.0 M solution of HCl in H_2O (1.5 mL). The mixture was lyophilized to give *N*-((4,4-difluoro-1-(4-((1-methyl-1*H*-imidazol-4-yl)sulfonyl)

DOI: 10.1021/acs.jmedchem.6b00914
J. Med. Chem. XXXX, XXX, XXX−XXX

piperazin-1-yl)cyclohexyl)methyl)-2,6-difluorobenzamide hydrochloride (**44**) as an amorphous white solid (0.067 g, quantitative): mp 198−199 °C; ^{1}H NMR (300 MHz, DMSO-d_6) δ 10.68 (bs, 1H), 9.25 (bs, 1H), 7.88 (m, 2H), 7.52 (m, 1H), 7.22 (m, 2H), 4.00−3.12 (m, 11H), 2.35−2.03 (m, 10H); APCI MS m/z 519 [M + H]$^+$; HPLC > 99% (AUC) (Method B), t_R = 20.6 min.

*2,6-Dichloro-N-((4,4-difluoro-1-(4-((1-methyl-1H-imidazol-4-yl)-sulfonyl)piperazin-1-yl)cyclohexyl)methyl)benzamide Hydrochloride (**45**).* Compound **45** was prepared according to a similar procedure described for the synthesis of **44** using 2,6-dichlorobenzoyl chloride. mp 174−175 °C; ^{1}H NMR (300 MHz, DMSO-d_6) δ 10.56 (s, 1H), 9.16 (s, 1H), 7.89 (m, 2H), 7.58−7.46 (m, 3H), 3.73 (s, 3H), 3.62 (m, 2H), 3.41 (m, 4H), 3.25 (m, 4H), 2.40−2.00 (m, 8H); APCI MS m/z 551 [M + H]$^+$; HPLC > 99% (AUC) (Method B), t_R = 19.0 min.

*2-Chloro-N-((4,4-difluoro-1-(4-((1-methyl-1H-imidazol-4-yl)-sulfonyl)piperazin-1-yl)cyclohexyl)methyl)-6-(trifluoromethoxy)-benzamide Hydrochloride (**46**). Step A.* A mixture of (4,4-difluoro -1-(4-((1-methyl-1*H*-imidazol-4-yl)sulfonyl)piperazin-1-yl)cyclohexyl)-methanamine (**43**, 0.150 g, 0.39 mmol), 2-chloro-6-(trifluoromethoxy)-benzoic acid (0.09 g, 0.39 mmol), EDCI·HCl (0.07 g, 0.39 mmol), HOBt (0.05 g, 0.39 mmol), and Et_3N (0.3 mL, 1.91 mmol) in DMF (10 mL) stirred at rt for 16 h. The mixture was diluted with H_2O (20 mL) and extracted with EtOAc (3 × 20 mL). The combined organic extracts were washed with H_2O (3 × 20 mL) and brine (20 mL). The organic layers were then dried over Na_2SO_4, filtered, and concentrated under reduced pressure. The resulting residue was chromatographed over silica gel (0−50% EtOAc in hexanes) to give 2-chloro-*N*-((4,4-difluoro-1-(4-((1-methyl-1*H*-imidazol-4-yl)sulfonyl)-piperazin-1-yl)cyclohexyl)methyl)-6-(trifluoromethoxy)benzamide as a white solid (0.057 g, 25%): ESI MS m/z 601 [M + H]$^+$.

Step B. To a 0 °C solution of 2-chloro-*N*-((4,4-difluoro-1-(4-((1-methyl-1*H*-imidazol-4-yl)sulfonyl)piperazin-1-yl)cyclohexyl)methyl)-6-(trifluoromethoxy)benzamide (0.050 g, 0.08 mmol) in CH_3CN (5 mL) was added a 1.0 M solution of HCl in H_2O (1.0 mL, 1.0 mmol). The mixture stirred at rt for 30 min and was lyophilized to give 2-chloro-*N*-((4,4-difluoro-1-(4-((1-methyl-1*H*-imidazol-4-yl)sulfonyl)-piperazin-1-yl)cyclohexyl)methyl)-6-(trifluoromethoxy)benzamide hydrochloride (**46**) as a white solid (0.021 g, 50%): mp 185−188 °C; ^{1}H NMR (300 MHz, DMSO-d_6) δ 10.09 (s, 1H), 9.14 (s, 1H), 7.89 (m, 2H), 7.55 (m, 3H), 3.73 (s, 3H), 3.62 (m, 2H), 3.41 (m, 4H), 3.25 (m, 4H), 2.40−2.00 (m, 8H); ESI MS m/z 600 [M + H]$^+$; HPLC > 99% (AUC) (Method B), t_R = 22.8 min.

*2,4-Dichloro-N-((4,4-difluoro-1-(4-((1-methyl-1H-imidazol-4-yl)-sulfonyl)piperazin-1-yl)cyclohexyl)methyl)benzamide Hydrochloride (**47**).* Compound **47** was prepared according to a similar procedure described for the synthesis of **44** using 2,4-dichlorobenzoyl chloride. mp 235 °C; ^{1}H NMR (300 MHz, DMSO-d_6) δ 10.27 (s, 1H), 8.97 (s, 1H), 7.89 (m, 2H), 7.74 (m, 1H), 7.55 (m, 2H), 7.58−7.46 (m, 3H), 3.73 (s, 3H), 3.62 (m, 3H), 3.41 (m, 2H), 3.25 (m, 2H), 2.40−2.00 (m, 8H); ESI MS m/z 550 [M + H]$^+$; HPLC 97.8% (AUC) (Method B), t_R = 19.5 min.

*2-Chloro-N-((4,4-difluoro-1-(4-((1-methyl-1H-imidazol-4-yl)-sulfonyl)piperazin-1-yl)cyclohexyl)methyl)-4-fluorobenzamide Hydrochloride (**48**).* Compound **48** was prepared according to a similar procedure described for the synthesis of **46** using 2-chloro-4-fluorobenzoic acid. mp 232 °C; ^{1}H NMR (300 MHz, DMSO-d_6) δ 10.15 (s, 1H), 8.91 (s, 1H), 7.86 (m, 2H), 7.80−7.34 (m, 3H), 3.73 (s, 3H), 3.62 (m, 2H), 3.41 (m, 4H), 3.25 (m, 4H), 2.40−2.00 (m, 8H); ESI MS m/z 534 [M + H]$^+$; HPLC 97.1% (AUC) (Method B), t_R = 19.6 min.

*2-Chloro-N-((4,4-difluoro-1-(4-((1-methyl-1H-imidazol-4-yl)-sulfonyl)piperazin-1-yl)cyclohexyl)methyl)-4-(trifluoromethyl)-benzamide Hydrochloride (**49**).* Compound **49** was prepared according to a similar procedure described for the synthesis of **46** using 2-chloro-4-(trifluoromethyl)benzoic acid. mp 181−183 °C; ^{1}H NMR (300 MHz, DMSO-d_6) δ 10.78 (s, 1H), 9.07 (s, 1H), 7.89 (m, 4H), 7.71 (m, 1H), 3.73 (s, 3H), 3.62 (m, 2H), 3.41 (m, 4H), 3.25 (m, 4H), 2.40−2.00 (m, 8H); APCI MS m/z 585 [M + H]$^+$; HPLC 98.8% (AUC) (Method B), t_R = 20.3 min.

*N-((4,4-Difluoro-1-(4-((1-methyl-1H-1,2,3-triazol-4-yl)sulfonyl)-piperazin-1-yl)cyclohexyl)methyl)-2,6-difluorobenzamide Hydrochloride (**54**). Step A.* To a 0 °C solution of *tert*-butyl piperazine-1-carboxylate (**12**, 10.0 g, 53.7 mmol) and Et_3N (22.6 mL, 161.2 mmol) in CH_2Cl_2 (50 mL) was added a solution of 1-methyl-1*H*-1,2,3-triazole-4-sulfonyl chloride (11.7 g, 64.5 mmol) in CH_2Cl_2 (50 mL) dropwise over a period of 30 min. The reaction mixture stirred at rt for 5 h and was then washed with a saturated solution of $NaHCO_3$ (50 mL) and brine (50 mL). The organic layer was dried over Na_2SO_4, filtered, and concentrated under reduced pressure to give *tert*-butyl 4-((1-methyl-1*H*-1,2,3-triazol-4-yl)sulfonyl)piperazine-1-carboxylate (**50**) as a crude solid, which was used as-is in the next step.

Step B. *tert*-Butyl 4-((1-methyl-1*H*-1,2,3-triazol-4-yl)sulfonyl)-piperazine-1-carboxylate (**50**) was dissolved in CH_2Cl_2 (50 mL). This solution was cooled to 0 °C and TFA (30.6 g, 268.5 mmol) was added. The mixture stirred at rt for 16 h and was then neutralized with a saturated aqueous solution of $NaHCO_3$. The separated organic layer was washed with brine (50 mL), dried over Na_2SO_4, filtered, and concentrated under reduced pressure to give 1-((1-methyl-1*H*-1,2,3-triazol-4-yl)sulfonyl)piperazine (**51**) as crude solid, which was used as-is in the next step (8.4 g, 68%): ESI MS m/z 232 [M + H]$^+$.

Step C. To a 0 °C solution of 4,4-difluorocyclohexanone (2.0 g, 14.9 mmol) in toluene (20 mL) was added TMSCN (2.18 mL, 16.3 mmol) dropwise, followed by ZnI_2 (0.236 g, 0.74 mmol). The mixture stirred at rt for 15 min followed by addition of a solution of 1-((1-methyl-1*H*-1,2,3-triazol-4-yl)sulfonyl)piperazine (**51**, 3.43 g, 14.8 mmol) in CH_3OH (90 mL). The mixture was heated at reflux for 4 h, then at rt for 16 h. The mixture was concentrated under reduced pressure. The resulting residue was dissolved in CH_2Cl_2 (100 mL), washed with H_2O (2 × 50 mL), dried over Na_2SO_4, filtered, and concentrated under reduced pressure to give 4, 4-difluoro-1-(4-((1-methyl-1*H*-1,2,3-triazol-4-yl)sulfonyl)piperazin-1-yl)cyclohexanecarbonitrile (**52**) as an off-white solid (1.89 g, 34%): ESI MS m/z 375 [M + H]$^+$.

Step D. To a 0 °C solution of 4,4-difluoro-1-(4-((1-methyl-1*H*-1,2,3-triazol-4-yl)sulfonyl)piperazin-1-yl)cyclohexanecarbonitrile (**52**, 2.0 g, 5.34 mmol) in THF (80 mL) was added $LiAlH_4$ (0.691 g, 18.2 mmol) portion-wise over 15 min. The mixture was stirred at rt for 5 h then cooled to 0 °C and carefully quenched by with H_2O (5 mL) and 4 N aq NaOH (1.4 mL). The resulting mixture was stirred at rt 15 min followed by addition of Na_2SO_4 (5 g). The mixture was stirred for an additional 30 min and was filtered. The filtrate was concentrated under reduced pressure and the resulting residue was triturated with hexanes to give a white solid, which was filtered and dried under reduced pressure to give (4,4-difluoro-1-(4-((1-methyl-1*H*-1,2,3-triazol-4-yl)sulfonyl)piperazin-1-yl)cyclohexyl)methanamine (**53**) as a white foam (1.75 g, 87%): ^{1}H NMR (300 MHz, $CDCl_3$) δ 7.94 (s, 1H), 4.19 (s, 3H), 3.22 (s, 4H), 2.79−2.80 (m, 4H), 2.71 (s, 2H), 1.75−1.95 (m, 6H), 1.55−1.65 (m, 2H); ESI MS m/z 379 [M + H]$^+$.

Step E. To a 0 °C solution of (4,4-difluoro-1-(4-((1-methyl-1*H*-1,2,3-triazol-4-yl)sulfonyl)piperazin-1-yl)cyclohexyl)methanamine (**53**, 0.500 g, 1.32 mmol) in CH_2Cl_2 (10 mL) was added Et_3N (0.54 mL, 3.97 mmol) and 2,6-difluorobenzoyl chloride (0.233 g, 1.32 mmol). The resulting mixture was stirred at rt for 4 h, diluted with CH_2Cl_2, and then washed with saturated aqueous $NaHCO_3$ solution (10 mL). The organic layer was dried over Na_2SO_4, filtered, and concentrated under reduced pressure. The resulting residue was chromatographed over silica gel (0−50% EtOAc in hexanes) to give *N*-((4,4-difluoro -1-(4-((1-methyl-1*H*-1,2,3-triazol-4-yl)sulfonyl)piperazin-1-yl)cyclohexyl)-methyl)-2,6-difluorobenzamide as a white solid (0.465 g, 68%): ^{1}H NMR (300 MHz, DMSO-d_6) δ 7.96 (s, 1H), 7.39 (m, 1H), 6.96 (m, 2H), 6.08 (m, 1H), 4.19 (s, 3H), 3.55 (d, J = 6.2 Hz, 2H), 3.28 (m, 4H), 2.79 (m, 4H), 1.93 (m, 6H), 1.67 (m, 2H), 1.26 (m, 4H); ESI MS m/z 518 [M + H]$^+$.

Step F. To a 0 °C solution of *N*-((4,4-difluoro-1-(4-(1-methyl-1*H*-1,2,3-triazol-4-ylsulfonyl)piperazin-1-yl)cyclohexyl)methyl)-2,6-difluorobenzamide (0.153 g, 0.295 mmol) in CH_3CN (1 mL) was added a 1.0 M solution of HCl in H_2O (5 mL). The mixture stirred at rt for 30 min and was lyophilized to give *N*-((4,4-difluoro-1-(4-(1-methyl-1*H*-1,2,3-triazol-4-ylsulfonyl)piperazin-1-yl)cyclohexyl)methyl)-2,6-difluorobenzamide hydrochloride (**54**) as a white solid (0.163 g, quantitative): mp 202−205 °C; ^{1}H NMR (300 MHz, DMSO-d_6) δ

DOI: 10.1021/acs.jmedchem.6b00914
J. Med. Chem. XXXX, XXX, XXX−XXX

9.24 (m, 1H), 8.71 (m, 2H), 7.53 (m, 1H), 7.20 (m, 2H), 4.14 (s, 3H), 3.86 (m, 2H), 3.39 (m, 2H), 3.12 (m, 3H), 2.73 (m, 2H), 2.11 (m, 2H), 1.91 (m, 2H), 1.78 (m, 2H), 1.53 (m, 2H); APCI MS m/z 519 $[M + H]^+$; HPLC > 99% (AUC) (Method C), t_R = 18.0 min.

*2,6-Dichloro-N-((4,4-difluoro-1-(4-((1-methyl-1H-1,2,3-triazol-4-yl)sulfonyl)piperazin-1-yl)cyclohexyl)methyl)benzamide Hydrochloride (**55**).* Compound **55** was prepared according to a similar procedure described for the synthesis of **54** using 2,6-dichlorobenzoyl chloride. mp 265−270 °C; ^{1}H NMR (300 MHz, DMSO-d_6) δ 10.13 (bs, 1H), 8.70 (bs, 1H), 8.95−8.55 (m, 1H), 7.67−7.37 (m, 3H), 4.13 (s, 3H), 3.80−3.75 (m, 2H), 3.73−3.33 (m, 2H), 3.33−2.89 (m, 4H), 2.78 (m, 2H), 2.44−1.51 (m, 8H); ESI MS m/z 551 $[M + H]^+$; HPLC 97.8% (AUC) (Method C), t_R = 18.5 min.

*2-Chloro-N-((4,4-difluoro-1-(4-((1-methyl-1H-1,2,3-triazol-4-yl)sulfonyl)piperazin-1-yl)cyclohexyl)methyl)-6-(trifluoromethoxy)benzamide Hydrochloride (**56**). Step A.* A mixture of (4,4-difluoro-1-(4-(1-methyl-1*H*-1,2,3-triazol-4-ylsulfonyl)piperazin-1-yl)cyclohexyl)-methanamine (**53**, 0.150 g, 0.39 mmol), 2-chloro-6-(trifluoromethoxy)benzoic acid (0.09 g, 0.39 mmol), EDCI·HCl (0.07 g, 0.39 mmol), HOBt (0.050 g, 0.39 mmol), and Et_3N (0.37 mL, 1.93 mmol) in DMF (10 mL) was stirred at rt for 16 h. The mixture was diluted with H_2O (20 mL) and extracted with EtOAc (3 × 20 mL). The combined organic extracts were washed with H_2O (3 × 20 mL) and brine (20 mL). The organic layers were then dried over Na_2SO_4, filtered, and concentrated under reduced pressure. The resulting residue was chromatographed over silica gel (0−50% EtOAc in hexanes) to give 2-chloro-*N*-((4,4-difluoro-1-(4-(1-methyl-1*H*-1,2,3-triazol-4-ylsulfonyl)piperazin-1-yl)cyclohexyl)methyl)-6-(trifluoromethoxy)benzamide as a white solid (0.051 g, 20%): ^{1}H NMR (300 MHz, $CDCl_3$) δ 8.12 (s, 1H), 7.95 (s, 1H), 7.36−7.39 (m, 2H), 5.82−5.89 (m, 1H), 4.19 (s, 3H), 3.56 (d, J = 6.2 Hz, 2H), 3.25−3.33 (m, 4H), 2.74−2.82 (m, 4H), 1.81−1.99 (m, 6H), 1.72−1.80 (m, 2H); ESI MS m/z 601 $[M + H]^+$.

Step B. To a 0 °C solution of 2-chloro-*N*-((4,4-difluoro-1-(4-(1-methyl-1*H*-1,2,3-triazol-4-ylsulfonyl)piperazin-1-yl)cyclohexyl)-methyl)-6-(trifluoromethoxy)benzamide (0.051 g, 0.08 mmol) in CH_3CN was added a 1.0 M solution of HCl in H_2O (1.0 mL, 1.0 mmol). The mixture was stirred at rt for 30 min and was lyophilized to give 2-chloro-*N*-((4,4-difluoro-1-(4-(1-methyl-1*H*-1,2,3-triazol-4-ylsulfonyl)piperazin-1-yl)cyclohexyl)methyl)-6-(trifluoromethoxy)-benzamide hydrochloride (**56**) as a white solid (0.021 g, 50%): mp 260−265 °C; ^{1}H NMR (300 MHz, DMSO-d_6) δ 10.30 (bs, 1H), 9.15 (bs, 1H), 8.95−8.55 (m, 1H), 7.77−7.32 (m, 3H), 4.13 (s, 3H), 3.80−3.75 (m, 2H), 3.73−3.33 (m, 2H), 3.32−2.89 (m, 4H), 2.87−2.74 (m, 2H), 2.44−1.51 (m, 8H); ESI MS m/z 601 $[M + H]^+$; HPLC 98.3% (AUC) (Method C), t_R = 20.1 min.

*2,4-Dichloro-N-((4,4-difluoro-1-(4-((1-methyl-1H-1,2,3-triazol-4-yl)sulfonyl)piperazin-1-yl)cyclohexyl)methyl)benzamide Hydrochloride (**57**).* Compound **57** was prepared according to a similar procedure described for the synthesis of **55** using 2,4-dichlorobenzoyl chloride. mp 175−180 °C; ^{1}H NMR (300 MHz, DMSO-d_6) δ 10.31 (bs, 1H), 8.70−8.92 (m, 1H), 8.33−8.45 (m, 1H), 7.62−7.71 (m, 1H), 7.32−7.57 (m, 2H), 4.13 (s, 3H), 3.75−3.80 (m, 2H), 3.33−3.73 (m, 2H), 2.89−3.33 (m, 4H), 2.78−2.89 (m, 2H), 1.51−2.44 (m, 8H); ESI MS m/z 551 $[M + H]^+$; HPLC 97.4% purity (Method A).

*2-Chloro-N-((4,4-difluoro-1-(4-((1-methyl-1H-1,2,3-triazol-4-yl)sulfonyl)piperazin-1-yl)cyclohexyl)methyl)-4-fluorobenzamide Hydrochloride (**58**).* Compound **58** was prepared according to a similar procedure described for the synthesis of **56** using 2-chloro-4-fluorobenzoic acid. mp 230−232 °C; ^{1}H NMR (300 MHz, DMSO-d_6) δ 10.13 (bs, 0.4H), 8.91 (bs, 0.6H), 9.95 (bs, 1H), 8.35−8.51 (m, 1H), 7.21−7.67 (m, 3H), 4.13 (s, 3H), 3.75−3.80 (m, 2H), 3.33−3.73 (m, 3H), 2.89−3.33 (m, 4H), 2.78−2.89 (m, 2H), 1.51−2.44 (m, 8H); ESI MS m/z 535 $[M + H]^+$; HPLC 98.7% (AUC) (Method C), t_R = 18.4 min.

*2-Chloro-N-((4,4-difluoro-1-(4-((1-methyl-1H-1,2,3-triazol-4-yl)sulfonyl)piperazin-1-yl)cyclohexyl)methyl)-4-(trifluoromethyl)-benzamide Hydrochloride (**59**).* Compound **59** was prepared according to a similar procedure described for the synthesis of **56** using 2-chloro-4-(trifluoromethyl)benzoic acid. mp 190−192 °C; ^{1}H NMR (300 MHz, DMSO-d_6) δ 10.31 (bs, 1H), 9.15 (bs, 1H), 8.55−8.95 (m, 1H), 7.52−8.05 (m, 3H), 4.13 (s, 3H), 3.75−3.80 (m, 2H), 3.33−3.73 (m, 2H), 2.89−3.33 (m, 4H), 2.78−2.89 (m, 2H), 1.51−2.44 (m, 8H); ESI MS m/z 585 $[M + H]^+$. %CHNCl for $C_{22}H_{26}ClF_5N_6O_3S$·HCl: calcd %C = 42.52, %H = 4.38, %N = 13.52, %Cl = 11.41; found %C = 42.38, %H = 4.31, %N = 13.37, %Cl = 11.24; HPLC 98.0% (AUC) (Method C), t_R = 20.2 min.

*N-((4,4-Difluoro-1-(4-((1-methyl-1H-1,2,3-triazol-4-yl)sulfonyl)-piperazin-1-yl)cyclohexyl)methyl)-2,4-bis(trifluoromethyl)-benzamide Hydrochloride (**60**).* Compound **60** was prepared according to a similar procedure described for the synthesis of **56** using 2,4-bis(trifluoromethyl)benzoic acid. mp 180−182 °C; ^{1}H NMR (300 MHz, DMSO-d_6) δ 8.75 (s, 1H), 8.62 (s, 1H), 8.18−8.12 (m, 2H), 7.74−7.71 (m, 1H), 4.15 (s, 3H), 3.31−3.30 (m, 2H), 3.10−2.90 (m, 4H), 2.85−2.70 (m, 4H), 2.00−1.40 (m, 8H); ESI MS m/z 619 $[M + H]^+$; HPLC > 99% (AUC) (Method C), t_R = 20.9 min.

*2-Chloro-N-(1-(4,4-difluoro-1-(4-((1-methyl-1H-1,2,3-triazol-4-yl)sulfonyl)piperazin-1-yl)cyclohexyl)ethyl)-4-(trifluoromethyl)-benzamide Hydrochloride ((−)-**66** and (+)-**67**). Step A.* ZnI_2 (2.53 g, 7.95 mmol) was added to a solution of 1-benzylpiperazine (**24**, 14.0 g, 79.5 mmol) and 4,4-difluorocyclohexanone (10.6 g, 79.5 mmol) in a 1:1 mixture of toluene and CH_3OH (160 mL), and the resulting mixture stirred at rt for 1 h. The reaction mixture was cooled to 0 °C and TMSCN (11.0 mL, 87.4 mmol) was added dropwise over a period of 15 min. The reaction mixture stirred at rt for 4 h then at reflux for 12 h. The reaction mixture was allowed to cool to rt and was concentrated under reduced pressure. The resulting residue was dissolved in EtOAc (300 mL), and the organic layer was washed with H_2O (2 × 200 mL) and brine (1 × 100 mL). The organic layer was dried over Na_2SO_4, filtered, and concentrated under reduced pressure, and the resulting residue was chromatographed over silica gel (0−10% EtOAc in hexanes) to give 1-(4-benzylpiperazin-1-yl)-4,4-difluorocyclohexanecarbonitrile (**61**) as white amorphous solid (24.6 g, 97%): ^{1}H NMR (300 MHz, $CDCl_3$) δ 7.37−7.27 (m, 5H), 3.50 (s, 2H), 2.72 (m, 4H), 2.53 (m, 4H), 2.21−1.93 (m, 8H).

Step B. To a 0 °C solution of 1-(4-benzylpiperazin-1-yl)-4,4-difluorocyclohexanecarbonitrile (**61**, 16.0 g, 50.14 mmol) in anhydrous Et_2O (160 mL) was added a 3.0 M solution of CH_3Li in DME (25 mL, 75.2 mmol) dropwise. The mixture was then heated at reflux for 6 h and then cooled to 0 °C. To this mixture was added $NaBH_4$ (5.68 g, 15.0 mmol) followed by dropwise addition of CH_3OH (160 mL). The mixture stirred at rt for 2 h, followed by dropwise addition H_2O (25 mL). The mixture was concentrated under reduced pressure, and the resulting residue was dissolved in EtOAc (300 mL). The organic layer was washed with H_2O (100 mL) and brine (100 mL), dried over Na_2SO_4, filtered, and concentrated to afford 1-(1-(4-benzylpiperazin-1-yl)-4,4-difluorocyclohexyl)ethanamine as an oil (17.8 g, crude, >99%). To a 0 °C solution of 1-(1-(4-benzylpiperazin-1-yl)-4,4-difluorocyclohexyl)ethanamine (17.8 g, crude, 52.9 mmol) and Et_3N (14.8 mL, 105 mmol) in CH_2Cl_2 (100 mL) was added a solution of di-*tert*-butyl dicarbonate (12.71 g, 58.2 mmol) in CH_2Cl_2 (80 mL) dropwise over a period of 15 min. The mixture stirred at rt for 5 h and was washed with H_2O (2 × 150 mL) and brine (150 mL). The organic layer was dried over Na_2SO_4, filtered, and concentrated under reduced pressure. The resulting residue was chromatographed over silica gel (0−30% EtOAc in hexanes) to afford (±)-*tert*-butyl (1-(1-(4-benzylpiperazin-1-yl)-4,4-difluorocyclohexyl)ethyl)carbamate ((±)-**62**) as white solid (18.4 g, 80%): ^{1}H NMR (300 MHz, $CDCl_3$) δ 7.35−7.28 (m, 5H), 4.35 (m, 1H), 3.87 (m, 1H), 3.48 (s, 2H), 2.78 (m, 4H), 2.41 (m, 4H), 1.77 (m, 5H), 1.42 (m, 10 H), 1.05 (d, J = 4.2 Hz, 3H).

Step C. A mixture of (±)-*tert*-butyl (1-(1-(4-benzylpiperazin-1-yl)-4,4-difluorocyclohexyl)ethyl)carbamate ((±)-**62**, 11.3 g, 25.8 mmol), 10% Pd/C (10 wt %/wt loading, 2.26 g) and ammonium formate (16.2 g, 258 mmol) in CH_3OH (180 mL) was heated at reflux for 4 h. The mixture was allowed to cool to rt and was filtered through a pad of Celite. The filtrate was concentrated under reduced pressure to afford (±)-*tert*-butyl (1-(4,4-difluoro-1-(piperazin-1-yl)cyclohexyl)ethyl)-carbamate ((±)-**63**) (8.0 g, crude) as colorless foam, which was used as-is in the next step.

Step D. Crude (±)-*tert*-butyl (1-(4,4-difluoro-1-(piperazin-1-yl)-cyclohexyl)ethyl)carbamate ((±)-**63**, 8.0 g, 23.0 mmol) was dissolved

DOI: 10.1021/acs.jmedchem.6b00914
J. Med. Chem. XXXX, XXX, XXX−XXX

in CH_2Cl_2 (50 mL) and cooled to 0 °C. To this solution was added Et_3N (16.2 mL, 115.2 mmol) followed by dropwise addition of a solution of 1-methyl-1*H*-1,2,3-triazole-4-sulfonyl chloride (6.25 g, 34.5 mmol) in CH_2Cl_2 (50 mL). The mixture was stirred at rt for 2 h and was diluted with CH_2Cl_2 (250 mL) and washed with saturated aqueous $NaHCO_3$ (100 mL). The organic layer was washed with brine (100 mL), dried over Na_2SO_4, filtered, and concentrated under reduced pressure to afford (±)-*tert*-butyl (1-(4,4-difluoro-1-(4-((1-methyl-1*H*-1,2,3-triazol-4-yl)sulfonyl)piperazin-1-yl)cyclohexyl)ethyl)-carbamate ((±)-**64**) as off-white solid (8.1 g, over two steps 71%): ^{1}H NMR (300 MHz, $CDCl_3$) δ 8.00 (s, 1H), 4.41 (m, 1H), 3.89 (m, 1H), 3.21 (m, 3H), 2.85 (m, 4H), 1.90−1.71 (m, 6H), 1.42 (m, 10 H), 1.05 (d, J = 4.2 Hz, 3H).

Step E. To a to 0 °C solution of (±)-*tert*-butyl (1-(4,4-difluoro-1-(4-((1-methyl-1*H*-1,2,3-triazol-4-yl)sulfonyl)piperazin-1-yl)cyclohexyl)-ethyl)carbamate ((±)-**64**, 8.0 g, 16.2 mmol) in CH_3OH (40 mL) was slowly added 12 N aq HCl (40 mL) over a period of 30 min. The mixture stirred at rt for 5 h and was concentrated under reduced pressure. The resulting residue was dissolved in H_2O (50 mL) and neutralized with solid $NaHCO_3$. The aqueous mixture was extracted with EtOAc (2 × 100 mL), and the combined organic extracts were washed with brine (100 mL), dried over Na_2SO_4, filtered, and concentrated under reduced pressure to afford (±)-1-(4,4-difluoro-1-(4-((1-methyl-1*H*-1,2,3-triazol-4-yl)sulfonyl)piperazin-1-yl)cyclohexyl)ethanamine as white solid ((±)-**64**, 6.2 g, 97%): ESI MS m/z 393 $[M + H]^+$.

To a solution of (±)-1-(4,4-difluoro-1-(4-((1-methyl-1*H*-1,2,3-triazol-4-yl)sulfonyl)piperazin-1-yl)cyclohexyl)ethanamine ((±)-**64**, 4.7 g, 11.9 mmol) in DMF (50 mL) was added 2-chloro-4-(trifluoromethyl)benzoic acid (2.95 g, 13.1 mmol), HOBt (2.42 g, 17.9 mmol), EDCI·HCl (3.43 g, 17.9 mmol), and Et_3N (5.0 mL, 35.9 mmol). The resulting mixture stirred a rt for 16 h and was diluted with H_2O (300 mL). The aqueous mixture was extracted with EtOAc (2 × 100 mL), and the combined organic extracts were washed with H_2O (3 × 100 mL) and brine (150 mL). The organic layer was dried over Na_2SO_4, filtered, and concentrated under reduced pressure. The resulting residue was chromatographed over silica gel (0−10% EtOAc in hexanes) to give (±)-2-chloro-*N*-(1-(4,4-difluoro-1-(4-((1-methyl-1*H*-1,2,3-triazol-4-yl)sulfonyl)piperazin-1-yl)cyclohexyl)ethyl)-4-(trifluoromethyl)benzamide as an off-white solid ((±)-65, 5.0 g, 69%); ^{1}H NMR (300 MHz, DMSO-d_6) δ 8.79 (s, 1H), 8.48 (m, 1H), 7.95 (s, 1H), 7.80 (m, 1H), 7.55 (m, 1H), 4.26 (m, 1H), 4.13 (s, 3H), 3.20−2.30 (m, 7H), 2.00−1.51 (m, 9H), 1.10 (m, 3H); APCI MS m/z 599 $[M + H]^+$.

Step F. (±)-2-Chloro-*N*-(1-(4,4-difluoro-1-(4-((1-methyl-1*H*-1,2,3-triazol-4-yl)sulfonyl)piperazin-1-yl)cyclohexyl)ethyl)-4-(trifluoromethyl)-benzamide ((±)-**65**, 0.289 g) was resolved by preparative chiral HPLC to give (−)-**66** (after treatment with 1.0 M solution of HCl in H_2O in CH_3CN to give the corresponding HCl salt) as a white solid (0.121 g, 41%) and (+)-**67** (after treatment with 1.0 M solution of HCl in H_2O in CH_3CN to give the corresponding HCl salt) as a white solid (0.112 g, 38%).

Spectral data for (−)-**66**: mp 134−136 °C; ^{1}H NMR (300 MHz, DMSO-d_6) δ 8.79 (s, 1H), 8.48 (m, 1H), 7.95 (s, 1H), 7.80 (m, 1H), 7.55 (m, 1H), 4.26 (m, 1H), 4.13 (s, 3H), 3.20−2.30 (m, 7H), 2.00−1.51 (m, 9H), 1.10 (m, 3H); APCI MS m/z 599 $[M + H]^+$; HPLC > 99% (AUC) (Method B), t_R = 26.0 min; $[\alpha]^{20}_D$ = −9.78° (c = 0.47, CH_3OH); chiral HPLC > 99% (AUC) (Method E), t_R = 7.45 min.

Spectral data for (+)-**67**: mp 134−136 °C; ^{1}H NMR (300 MHz, DMSO-d_6) δ 8.79 (s, 1H), 8.48 (m, 1H), 7.95 (s, 1H), 7.80 (m, 1H), 7.55 (m, 1H), 4.26 (m, 1H), 4.13 (s, 3H), 3.20−2.30 (m, 7H), 2.00−1.51 (m, 9H), 1.10 (m, 3H); APCI MS m/z 599 $[M + H]^+$; %CHNCl for $C_{23}H_{28}ClF_5N_6O_3S$·HCl·0.75H_2O: calcd %C = 42.57, %H = 4.74, %N = 12.95, %Cl = 10.93; found %C = 42.48, %H = 5.07, %N = 12.51, %Cl = 11.03; HPLC > 99% (AUC) (Method B), t_R = 26.0 min; $[\alpha]^{20}_D$ = +8.0° (c = 0.87, CH_3OH); chiral HPLC > 99% (AUC) (Method E), t_R = 16.2 min.

■ ASSOCIATED CONTENT

Supporting Information

The Supporting Information is available free of charge on the ACS Publications website at DOI: 10.1021/acs.jmedchem.6b00914.

In vivo protocols (PDF)

IC_{50} data (CSV)

■ AUTHOR INFORMATION

Corresponding Authors

*Tel: 518-283-6451. E-mail: christopher.cioffi@acphs.edu.

*Tel: 518-878-6470. E-mail: shuang@consynance.com.

Present Addresses

⊥Albany College of Pharmacy and Health Sciences, 106 New Scotland Ave, Albany, New York 12208, United States.

#ConSynance Therapeutics, Inc., Schenectady, New York 12303, United States.

▽Pharma Inventor, Inc., University of British Columbia Campus, 3800 Wesbrook Mall, Suite #215, Vancouver, British Columbia, V6S 2L9, Canada.

○Hummingbird Bioscience, PTE, Ltd., 28 Seah Street, #03-01, 188384, Singapore.

◆Brains Online, Inc., 7000 Shoreline Court, South San Francisco, California 94080, United States.

¶Fred Hutchinson Cancer Research Center, 1100 Fairview Ave N, Seattle, Washington 98109, United States.

Notes

The authors declare the following competing financial interest(s): ConSynance Therapeutics, Inc. has executed an exclusive license with AMRI that covers the intellectual property for all of the GlyT-1 inhibitors disclosed within.

■ ACKNOWLEDGMENTS

The authors acknowledge the following for conducting the various *in vivo* studies described within: 1) Pharmaron Beijing, Co. Ltd. for conducting rat PK studies; 2) Covance Laboratories Inc. for conducting rat *in vivo* CSF glycine studies; 3) Maccine Pte Ltd. for conducting the in-life portion of PK and CSF glycine studies with cynomolgus monkeys, and 4) Brains On-Line LLC., for conducting rat microdialysis experiments.

■ ABBREVIATIONS USED

NMDA receptor, *N*-methyl-D-aspartate receptor; GlyT-1, glycine transporter-1; GlyT-2, glycine transporter-2; iGluRs, ionotropic glutamate receptors; LTP, long-term potentiation; LTD, long-term depression; GlyR, glycine receptor; CSF, cerebral spinal fluid; SAR, structure−activity relationship; SPR, structure−property relationship; ADME, absorption, distribution, metabolism, elimination; PPB, plasma protein binding; OCD, obsessive compulsive disorder; SPA, scintillation proximity assay; HLM, human liver microsomes; RLM, rat liver microsomes; mPFC, medial prefrontal cortex; *n*-BuLi, *n*-butyl lithium; THF, tetrahydrofuran; DMF, *N*,*N*-dimethylformamide; DME, dimethoxyethane; CH_2Cl_2, dichloromethane; CH_3CN, acetonitrile; Et_2AlCN, diethylaluminum cyanide; Ti(*i*-PrO)$_4$, titanium isopropoxide; $LiAlH_4$, lithium aluminum hydride; PTSA, *para*-toluene sulfonic acid; Et_2O, diethyl ether; Boc_2O, di-*tert*-butyl dicarbonate; TFA, trifluoroacetic acid; TMS, tetramethylsilane; LiHMDS, lithium bis(trimethylsilyl)amide; NH_4HCO_2, ammonium formate; *i*-Pr_2NEt, *N*,*N*-diisopropylethylamine; KCN, potassium cyanide;

DOI: 10.1021/acs.jmedchem.6b00914
J. Med. Chem. XXXX, XXX, XXX−XXX

Et_3N, triethylamine; HBTU, *O*-(benzotriazol-1-yl)-*N*,*N*,*N*′,*N*′-tetramethyluronium hexafluorophosphate; EDCI·HCl, 1-ethyl-3-(3-(dimethylamino)propyl)carbodiimide hydrochloride; HOBt, hydroxybenzotriazole; Gly, glycine; CYP, cytochrome P450; CYP2C9, cytochrome P450 2C9; CYP2C19, cytochrome P450 2C19; CYP2D6, cytochrome P450 2D6; CYP3A4, cytochrome P450 3A4; hERG, human ether-à-go-go-related gene; PK, pharmacokinetics; PD, pharmacodynamics; IV, intravenous; PO, oral; QD, once daily; CL_{int}, intrinsic clearance; Cl, clearance; Vss, volume of distribution at steady state; AUC, area under the curve; %F, % bioavailability

REFERENCES

(1) Aprison, M. H. The discovery of the neurotransmitter role of glycine. In *Glycine Neurotransmission*; Ottersen, O. P., Storm Mathisen, J., Eds.; John Wiley and Sons: Chichester, United Kingdom, 1990; pp 1−23.

(2) Betz, H. Ligand-gated ion channels in the brain: the amino acid receptor superfamily. *Neuron* **1990**, *5*, 383−392.

(3) Betz, H.; Harvey, R. J.; Schloss, P. Structures, diversity and pharmacology of glycine receptors and transporters. In : *Pharmacology of GABA and Glycine Neurotransmission*; Möhler, H., Ed.; Springer-Verlag; New York, 2000; pp 375−401.

(4) (a) Wojciech, D.; Parsons, C. G. Glycine and *N*-methyl-D-aspartate receptors: physiological significance and possible therapeutic applications. *Pharmacol. Rev.* **1998**, *50*, 597−664. (b) Wolosker, H. NMDA receptor regulation by D-serine: new findings and perspectives. *Mol. Neurobiol.* **2007**, *36*, 152−164.

(5) (a) Bliss, T. V.; Collingridge, G. L. A synaptic model of memory: long-term potentiation in the hippocampus. *Nature* **1993**, *361*, 31−39. (b) Bliss, T. V.; Collingridge, G. L. Memories of NMDA receptors and LTP. *Trends Neurosci.* **1995**, *18*, 54−56. (c) Traynelis, S. F.; Wollmuth, L. P.; McBain, C. J.; Menniti, F. S.; Vance, K. M.; Ogden, K. K.; Hansen, K. B.; Yuan, H.; Myers, S. J.; Dingledine, R.; Danysz, W. Glutamate receptor ion channels: structure, regulation, and function. *Pharmacol. Rev.* **2010**, *62*, 405−496.

(6) Eulenburg, V.; Armsen, W.; Betz, H.; Gomeza, J. Glycine transporters: essential regulators of neurotransmission. *Trends Biochem. Sci.* **2005**, *30*, 325−333.

(7) (a) Zafra, F.; Aragón, C.; Olivares, L.; Danbolt, N. C.; Giménez, C.; Strom-Mathisenm, J. Glycine transporters are differentially expressed among CNS cells. *J. Neurosci.* **1995**, *15*, 3952−3969. (b) Zafra, F.; Gomeza, C.; Olivares, L.; Aragón, C.; Giménez, C. Regional distribution and developmental variation of the glycine transporters GLYT1 and GLYT2 in the rat CNS. *Eur. J. Neurosci.* **1995**, *7*, 1342−1352. (c) Guastella, J.; Brecha, N.; Weigmann, C.; Lester, H. A.; Davidson, N. Cloning, expression, and localization of a rat brain high-affinity glycine transporter. *Proc. Natl. Acad. Sci. U. S. A.* **1992**, *89*, 7189−7193. (d) Liu, Q. R.; Nelson, H.; Mandiyan, S.; Lopez-Corcuera, B.; Nelson, H. Cloning and expression of a glycine transporter from mouse brain. *FEBS Lett.* **1992**, *305*, 110−114. (e) Mallorga, P. J.; Williams, J. B.; Jacobson, M.; Marques, R.; Chauhary, A.; Conn, P. J.; Pettibone, D. J.; Sur, C. Pharmacology and expression analysis of glycine transporter GlyT1 with [^{3}H]-(*N*-[3-(4′-fluorophenyl)-3-(4′-phenylphenoxy)propyl])sarcosine. *Neuropharmacology* **2003**, *45*, 585−593. (f) Zeng, Z.; O'Brien, J. A.; Lemaire, W.; O'Malley, S. S.; Miller, P. J.; Zhao, Z.; Wallace, M. A.; Raab, C.; Lindsley, C. W.; Sur, C.; Williams, D. L. A novel radioligand for glycine transporter 1: characterization and use in autoradiographic and in vivo brain occupancy studies. *Nucl. Med. Biol.* **2008**, *35*, 315−325. (g) Hamill, T. G.; Eng, W.; Jennings, A.; Lewis, R.; Thomas, S.; Wood, S.; Street, L.; Wisnoski, D.; Wolkenberg, S.; Lindsley, C.; Sanabria-Bohorquez, S. M.; Patel, S.; Riffel, K.; Ryan, C.; Cook, J.; Sur, C.; Burns, H. D.; Hargreaves, R. The synthesis and preclinical evaluation in rhesus monkey of [^{18}F]MK-6577 and [^{11}C]CMPyPB glycine transporter 1 positron emission tomography radiotracers. *Synapse* **2011**, *65*, 261−270. (h) Joshi, A. D.; Sanabria-Bohorquez, S. M.; Bormans, G.; Koole, M.; De Hoon, J.; Van Hecken, A.; Depre, M.; De Lepeleire, I.; Van Laere, K.; Sur, C.; Hamill, T. G. Characterization of the novel GlyT1 PET tracer [^{18}F]MK-6577 in humans. *Synapse* **2015**, *69*, 33−40. (i) Borroni, E.; Zhou, Y.; Ostrowitzki, S.; Alberti, D.; Kumar, A.; Hainzl, D.; Hartung, T.; Hilton, J.; Dannals, R. F.; Wong, D. F. Pre-clinical characterization of [^{11}C]RO5013853 as a novel radiotracer for imaging of the glycine transporter type 1 by positron emission tomography. *NeuroImage* **2013**, *75*, 291−300.

(8) (a) Pow, D. V.; Hendrickson, A. Distribution of the glycine transporter in mammalian and non-mammalian retinae. *Vis. Neurosci.* **1999**, *16*, 231−239. (b) Lee, S.; Zhong, Y.; Yang, X. Expression of glycine receptor and transporter on bullfrog retinal Muller cells. *Neurosci. Lett.* **2005**, *387*, 75−79.

(9) Gomeza, J.; Hülsmann, S.; Ohno, K.; Eulenburg, V.; Szöke, K.; Richter, D. W.; Betz, H. Inactivation of the glycine transporter 1 gene discloses a vital role of glial glycine uptake in glycinergic inhibition. *Neuron* **2003**, *40*, 785−796.

(10) (a) Cubelos, B.; Gimenez, C.; Zafra, F. Localization of the GLYT1 glycine transporter at glutamatergic synapses in the rat brain. *Cereb. Cortex* **2005**, *15*, 448−459. (b) Raiteri, L.; Raiteri, M. Functional 'glial' GLYT1 glycine transporters expressed in neurons. *J. Neurochem.* **2010**, *114*, 647−653.

(11) (a) Johnson, J. W.; Ascher, P. Glycine potentiates the NMDA response in cultured mouse brain neurons. *Nature* **1987**, *325*, 529−531. (b) Bergeron, R.; Meyer, T. M.; Coyle, J. Y.; Greene, R. W. Modulation of *N*-methyl-D-aspartate receptor function by glycine transport. *Proc. Natl. Acad. Sci. U. S. A.* **1998**, *95*, 15730−15374.

(12) Hitchcock, S.; Amagadzie, A.; Qian, W.; Xia, X.; Harried, S. S. Piperazineacetic acid derivatives as glycine transporter-1 inhibitors and their preparation, pharmaceutical compositions and use in the treatment of schizophrenia. WO 2008002583 A1, June 26, 2007.

(13) Atkinson, B. N.; Bell, S. C.; De Vivo, M.; Kowalski, L. R.; Lechner, S. M.; Ognyanov, V. I.; Tham, C.-S.; Tsai, C.; Jia, J.; Ashton, D.; Klitenick, M. A. ALX 5407: a potent, selective inhibitor of the hGlyT1 glycine transporter. *Mol. Pharmacol.* **2001**, *60*, 1414−1420.

(14) Molander, A.; Soderpalm, B. Glycine reuptake inhibitors for treatment of drug dependence. WO 2006075011 A2, January 11, 2006.

(15) Jolidon, S.; Narquizian, R.; Nettekoven, M. H.; Norcross, R. D.; Pinard, E.; Stalder, H. Preparation of alkoxybenzoylpiperazines as inhibitors of glycine transporter 1 (GlyT-1). WO 2005014563 A1, August 2, 2004.

(16) Michardy, S. F.; Lowe, J. A., III. Preparation of bicyclic [3.1.0] heteroaryl amides as type 1 glycine transport inhibitors. WO 2006106425 A1, March 27, 2006.

(17) Dargazanli, G.; Estenne Bouhtou, G.; Magat, P.; Marabout, B.; Medaisko, F.; Roger, P.; Sevrin, M.; Veronique, C. Preparation of *N*-[phenyl(piperidin-2-yl)methyl]benzamides as specific inhibitors of glycine transporters glyt1 and/or glyt2. FR 2838739 A1, April 19, 2002.

(18) Blackaby, W. P.; Castro, P.; Jose, L.; Lewis, R. T.; Naylor, E. M.; Street, L. J. Preparation of cyclohexanesulfonyl derivatives as GlyT1 inhibitors to treat schizophrenia. US 20060276655 A1, June 5, 2006.

(19) Bradley, D. M.; Branch, C. L.; Chan, W. N.; Coulton, S.; Gilpin, M. L.; Harris, A. J.; Jaxa-Chamiec, A. A.; Lai, J. Y. Q.; Marshall, H. R.; Macritchie, J. A.; Nash, D. J.; Porter, R. A.; Spada, S.; Thewlis, K. M.; Ward, S. E. Preparation of N-(phenylmethyl) benzamides as glycine transport inhibitors. WO 2006067423 A1, December 21, 2005.

(20) (a) Lewis, D. A.; Moghaddam, B. Cognitive dysfunction in schizophrenia: convergence of gamma-aminobutyric acid and glutamate alterations. *Arch. Neurol.* **2006**, *63*, 1372−1376. (b) Homayoun, H.; Moghaddam, B. NMDA receptor hypofunction produces opposite effects on prefrontal cortex interneurons and pyramidal neurons. *J. Neurosci.* **2007**, *27*, 11496−11500. (c) Lewis, D. A.; Curley, A. A.; Glausier, J. R.; Volk, D. W. Cortical parvalbumin interneurons and cognitive dysfunction in schizophrenia. *Trends Neurosci.* **2012**, *35*, 57−67. (d) Lahti, A. C.; Koffel, B.; LaPorte, D.; Tamminga, C. A. Subanesthetic doses of ketamine stimulate psychosis in schizophrenia. *Neuropsychopharmacology* **1995**, *13*, 9−19. (e) Umbricht, D.; Schmid, L.; Koller, R.; Vollenweider, F. X.; Hell, D.; Javitt, D. C. Ketamine-induced deficits in auditory and visual context-dependent processing in

DOI: 10.1021/acs.jmedchem.6b00914
J. Med. Chem. XXXX, XXX, XXX−XXX

healthy volunteers: implications for models of cognitive deficits in schizophrenia. *Arch. Gen. Psychiatry* **2000**, *57*, 1139−1147. (f) Javitt, D. C.; Zukin, S. R. Recent advances in the phencyclidine model of schizophrenia. *Am. J. Psychiatry* **1991**, *148*, 1301−1308. (g) Kirov, G.; O'Donovan, M. C.; Owen, M. J. Finding schizophrenia genes. *J. Clin. Invest.* **2005**, *115*, 1440−1448. (h) Allen, N. C.; Bagade, S.; McQueen, M. B.; Ioannidis, J. P.; Kavvoura, F. K.; Khoury, M. J.; Tanzi, R. E.; Bertram, L. Systematic meta-analyses and field synopsis of genetic association studies in schizophrenia: The SzGene database. *Nat. Genet.* **2008**, *40*, 827−834. (i) Deutsch, S. I.; Mastropaolo, J.; Schwartz, B. L.; Rosse, R. B.; Morisha, J. M. A "glutamate hypothesis" of schizophrenia. *Clin. Neuropharmacol.* **1989**, *12*, 1−13. (j) Olney, J. W.; Farber, N. B. Glutamate receptor dysfunction and schizophrenia. *Arch. Gen. Psychiatry* **1995**, *52*, 998−1007. (k) Tamminga, C. A. Schizophrenia and glutamatergic transmission. *Crit. Rev. Neurobiol.* **1998**, *12*, 21−36. (l) Moghaddam, B. Bringing order to the glutamate chaos in schizophrenia. *Neuron* **2003**, *40*, 881−884. (m) Javitt, D. C. Glutamatergic theories of schizophrenia. *Isr. J. Psychiatry Relat. Sci.* **2010**, *47*, 4−16.

(21) (a) Cioffi, C. L.; Guzzo, P. R. Inhibitors of glycine transporter-1: potential therapeutics for the treatment of CNS disorders. *Curr. Top. Med. Chem.* DOI: 10.2174/1568026616666160405113340. (b) Porter, R. A.; Dawson, L. A. GlyT-1 inhibitors: from hits to clinical candidates. *Top. Med. Chem.* **2014**, *13*, 51−100. (c) Harsing, L. G. An overview on GlyT-1 inhibitors under evaluation for the treatment of schizophrenia. *Drugs Future* **2013**, *38*, 545−558. (d) Hashimoto, K. Glycine transporter inhibitors for the treatment of schizophrenia. *Open Med. Chem. J.* **2010**, *4*, 10−19. (e) Thomsen, C. Glycine transporter inhibitors as novel antipsychotics. *Drug Discovery Today: Ther. Strategies* **2006**, *3*, 539−545. (f) Harsing, L. G.; Juranyi, Z.; Gacsalyi, I.; Tapolcsanyi, P.; Czompa, A.; Matyus, P. Glycine transporter type-1 and its inhibitors. *Curr. Med. Chem.* **2006**, *13*, 1017−1044. (g) Hashimoto, K. Glycine transporter inhibitors as therapeutic agents for schizophrenia. *Recent Pat. CNS Drug Discovery* **2006**, *1*, 43−53. (h) Kinney, G. G.; Sur, C. Glycine site modulators and glycine transporter-1 inhibitors as novel therapeutic targets for the treatment of schizophrenia. *Curr. Neuropharmacol.* **2005**, *3*, 35−43. (i) Cioffi, C. L.; Liu, S.; Wolf, M. A. *Recent Developments in Glycine Transporter-1 Inhibitors*; Annual Reports in Medicinal Chemistry; Academic Press: Cambridge, MA, 2010; Vol. *45*, Chapter 2, pp 19−35.

(22) (a) Javitt, D. C.; Zylberman, I.; Zukin, S. R.; Heresco-Levy, U.; Lindenmayer, J. P. Amelioration of negative symptoms in schizophrenia by glycine. *Am. J. Psychiatry* **1994**, *151*, 1234−1236. (b) Heresco-Levy, U.; Javitt, D. C.; Ermilov, M.; Mordel, C.; Silipo, G.; Lichtenstein, M. Efficacy of high-dose glycine in the treatment of enduring negative symptoms of schizophrenia. *Arch. Gen. Psychiatry* **1999**, *56*, 29−36. (c) Heresco-Levy, U.; Ermilov, M.; Lichtenberg, P.; Bar, G.; Javitt, D. C. High-dose glycine added to olanzapine and risperidone for the treatment of schizophrenia. *Biol. Psychiatry* **2004**, *55*, 165−171. (d) Heresco-Levy, U.; Javitt, D. C.; Ermilov, M.; Mordel, C.; Horowitz, A.; Kelly, D. Double-blind, placebo-controlled, crossover trial of glycine adjuvant therapy for treatment-resistant schizophrenia. *Br. J. Psychiatry* **1996**, *169*, 610−617. (e) Tsai, G.; Lane, H.; Young, P. J.; Lane, N.; Chong, M. Glycine transporter 1 inhibitor, N-methylglycine (sarcosine) added to antipsychotics for the treatment of schizophrenia. *Biol. Psychiatry* **2004**, *55*, 452−456. (f) Lane, H.; Huang, C.; Wu, P.; Liu, Y.; Lin, P.; Chen, P.; Tsai, G. Glycine transporter 1 inhibitor, N-methylglycine (sarcosine), added to clozapine for the treatment of schizophrenia. *Biol. Psychiatry* **2006**, *60*, 645−649. (g) Umbricht, D.; Alberati, D.; Martin-Facklam, M.; Borroni, E.; Youssef, E. A.; Ostland, M.; Wallace, T. L.; Knoflach, F.; Dorflinger, E.; Wettstein, J. G.; Bausch, A.; Garibaldi, G.; Santarelli, L. Effect of bitopertin, a glycine reuptake inhibitor, on negative symptoms of schizophrenia. A randomized, double-blind, proof-of-concept study. *JAMA Psychiatry* **2014**, *71*, 637−646.

(23) Bitopertin disappoints as schizophrenia treatment. http://www.medscape.com/viewarticle/826805 (accessed June 15, 2016).

(24) (a) Huang, C.-C.; Wei, I.-H.; Huang, C.-L.; Chen, K.-T.; Tsai, M.-H.; Tsai, P.; Tun, R.; Huang, K.-H.; Chang, Y.-C.; Lane, H.-Y.; Tsai, G. E. Inhibition of glycine transporter-1 as a novel mechanism for the treatment of depression. *Biol. Psychiatry* **2013**, *74*, 734−741. (b) Mathew, S. J. Glycine transporter-1 inhibitors: a new class of antidepressant? *Biol. Psychiatry* **2013**, *74*, 710−711. (c) Huang, C.-C.; Wei, I.-H.; Huang, C.-L.; Chen, K.-T.; Tsai, M.-H.; Tsai, P.; Tun, R.; Huang, K.-H.; Chang, Y.-C.; Lane, H.-Y.; Tsai, G. E. Inhibition of glycine tranporter-1 as a novel mechanism for the treatment of depression. *Biol. Psychiatry* **2013**, *74*, 734−741. (d) Depoortère, R.; Dargazanli, G.; Estenne-Bouhtou, G.; Coste, A.; Lanneau, C.; Desvignes, C.; Poncelet, M.; Heaulme, M.; Santucci, V.; Decobert, M.; Cudennec, A.; Voltz, C.; Bouley, D.; Terranova, J. P.; Stemmelin, J.; Roger, P.; Marabout, B.; Sevrin, M.; Vigé, X.; Biton, B.; Steinberg, R.; Francon, D.; Alonso, R.; Avenet, P.; Oury-Donat, F.; Perrault, G.; Griebel, G.; George, P.; Soubrié, P.; Scatton, B. Neurochemical, electrophysiological and pharmacological profiles of the selective inhibitor of the glycine transporter-1 SSR504734, a potential new type of antipsychotic. *Neuropsychopharmacology* **2005**, *30*, 1963−1985. (e) Bouley, D.; Pichat, P.; Dargazanli, G.; Estenne-Bouhtou, G.; Terranova, J. P.; Rogacki, N.; Stemmelin, J.; Coste, A.; Lanneau, C.; Desvignes, C.; Cohen, C.; Alonso, R.; Vigé, X.; Biton, B.; Steinberg, R.; Sevrin, M.; Oury-Donat, F.; George, P.; Bergis, O.; Griebel, G.; Avenet, P.; Scatton, B. Characterization of SSR103800, a selective inhibitor of the glycine transporter-1 in models predictive of therapeutic activity in schizophrenia. *Pharmacol., Biochem. Behav.* **2008**, *91*, 47−58.

(25) A Study of Bitopertin (RO4917838) in Combination With Selective Serotonin Reuptake Inhibitors in Patients With Obsessive-Compulsive Disorder. https://www.clinicaltrials.gov/ct2/show/NCT01674361 (Accessed June 8, 2016).

(26) Harvey, R. J.; Yee, B. K. Glycine transporters as novel therapeutic targets in schizophrenia, alcohol dependence and pain. *Nat. Rev. Drug Discovery* **2013**, *12*, 866−885.

(27) (a) Molander, A.; Lido, H. H.; Lof, E.; Ericson, M.; Soderpalm, B. The glycine reuptake inhibitor Org 25935 decreases ethanol intake and preference in male Wistar rats. *Alcohol Alcohol.* **2007**, *42*, 11−18. (b) Vengeliene, V.; Leonardi-Essman, F.; Sommer, W. H.; Marstone, H. M.; Spanagel, R. Glycine transporter-1 blockade leads to persistently reduced relapse-like alcohol drinking in rats. *Biol. Psychiatry* **2010**, *68*, 704−711. (c) Lido, H. H.; Marston, H.; Ericson, M.; Soderpalm, B. The glycine reuptake inhibitor Org24598 and acamprosate reduce ethanol intake in the rat; tolerance development to acamprosate but not to Org24598. *Addict. Biol.* **2012**, *17*, 897−907. (d) Lido, H. H.; Ericson, M.; Marston, H.; Soderpalm, B. A role for accumbal glycine receptors in modulation of dopamine release by the glycine transporter-1 inhibitor Org25935. *Front. Psychiatry* **2011**, *2*, 1−9. (e) de Bejczy, A.; Nations, K. R.; Szegedi, A.; Schoemaker, J.; Ruwe, F.; Soderpalm, B. Efficacy and safety of the glycine transporter-1 inhibitor Org 25935 for the prevention of relapse in alcohol-dependent patients: a randomized, double-blind, placebo-controlled trial. *Alcohol.: Clin. Exp. Res.* **2014**, *38*, 2427−2435. (f) Uslaner, J. M.; Drott, J. T.; Sharik, S. S.; Theberge, C. R.; Sur, C.; Zeng, Z.; Williams, D. L.; Hutson, P. H. Inhibition of glycine transporter 1 attenuates nicotine-but not food-induced cue-potentiated reinstatement for a response previously paired with sucrose. *Behav. Brain Res.* **2010**, *207*, 37−43. (g) Cervo, L.; Di Clemente, A.; Orru, A.; Moro, F.; Cassina, C.; Pich, E. M.; Corsi, M.; Gozzi, A.; Bifone, A. Inhibition of glycine transporter-1 reduces cue-induced nicotine-seeking, but does not promote extinction of conditioned nicotine cue responding in the rat. *Addict. Biol.* **2013**, *18*, 800−811. (h) Nic Dhonnchadha, B. A.; Pinard, E.; Alberti, D.; Wettstein, J. G.; Spealman, R. D.; Kantak, K. M. Inhibiting glycine transporter-1 facilitates cocaine-cue extinction and attenuates reacquisition of cocaine-seeking behavior. *Drug Alcohol Depend.* **2012**, *122*, 119−126.

(28) (a) Barthel, F.; Urban, A.; Sclosser, L.; Eulenburg, V.; Wederhausen, R.; Brandenburger, T.; Aragon, C.; Bauer, I.; Hermanns, H. Long-term application of glycine transporter inhibitors acts antineuropathic and modulates spinal *N*-methyl-D-aspartate receptor subunit NR-1 expression in rats. *Anesthesiology* **2014**, *121*,

DOI: 10.1021/acs.jmedchem.6b00914
J. Med. Chem. XXXX, XXX, XXX−XXX

160−169. (b) Morita, K.; Motoyama, N.; Kitayama, T.; Morioka, N.; Kifune, K.; Dohi, T. Spinal Antiallodynia action of glycine transporter inhibitors in neuropathic pain models in mice. *J. Pharmacol. Exp. Ther.* **2008**, *326*, 633−645. (c) Gilron, I.; Dickenson, A. H. Emerging drugs for neuropathic pain. *Expert Opin. Emerging Drugs* **2014**, *19*, 329−341. (d) Vandenberg, R. J.; Ryan, R. M.; Carland, J. E.; Imlach, W. L.; Christie, M. J. Glycine transport inhibitors for the treatment of pain. *Trends Pharmacol. Sci.* **2014**, *35*, 423−430. (e) Centeno, M. V.; Mutso, A.; Millecamps, M.; Apkarian, A. V. Prefrontal cortex and spinal cord mediated anti-neuropathy and analgesia induces by sarcosine, a glycine-T1 transporter inhibitor. *Pain* **2009**, *145*, 176−183. (f) Dohi, T.; Morita, K.; Kitayama, T.; Motoyama, N.; Morioka, N. Glycine transporter inhibitors as a novel drug discovery strategy for neuropathic pain. *Pharmacol. Ther.* **2009**, *123*, 54−79. (g) Tanabe, M.; Takasu, K.; Yamaguchi, S.; Kodama, D.; Ono, H. Glycine transporter inhibitors as a potential therapeutic strategy for chronic pain with memory impairment. *Anesthesiology* **2008**, *108*, 929−937.

(29) Komatsu, H.; Furuya, Y.; Sawada, K.; Asada, T. Involvement of the strychnine-sensitive glycine receptor in the anxiolytic effects of GlyT-1 inhibitors on maternal separation-induced ultrasonic vocalization in rat pups. *Eur. J. Pharmacol.* **2015**, *746*, 252−257.

(30) (a) Shen, H.-Y.; van Vliet, E. A.; Bright, K.-A.; Hanthorn, M.; Lyte, N. K.; Gorter, J.; Aronica, E.; Boison, D. Glycine transporter 1 is a target for the treatment of epilepsy. *Neuropharmacology* **2015**, *99*, 554−565. (b) Socala, K.; Nieoczym, D.; Runfeldt, C.; Wlaz, P. Effects of sarcosine, a glycine transport type 1 inhibitor, in two mouse seizure models. *Pharmacol. Rep.* **2010**, *62*, 392−397. (c) Kalinichev, M.; Starr, K. R.; Teague, S.; Bradford, A. M.; Porter, R. A.; Herdon, H. J. Glycine transporter 1 (GlyT1) inhibitors exhibit anticonvulsant properties in the rat maximal electroshock threshold (MEST) test. *Brain Res.* **2010**, *1331*, 105−113. (d) Shen, H.-Y.; van Vliet, E. A.; Bright, K.-A.; Hanthorn, M.; Lytle, N. K.; Gorter, J.; Aronica, E.; Boison, D. Glycine transporter 1 is a target for the treatment of epilepsy. *Neuropharmacology* **2015**, *99*, 554−565.

(31) Pinto, M. C. X.; de Assis Lima, I. V.; da Costa, F. L. P.; Rosa, D. V.; Mendes-Goulart, V. A.; Resende, R. R.; Romano-Silva, M. A.; de Olverira, A. C. P.; Gomez, M. V.; Gomez, R. S. Glycine transporters type 1 inhibitor promotes brain preconditioning against NMDA-induced excitotoxicity. *Neuropharmacology* **2015**, *89*, 274−281.

(32) Burket, J. A.; Benson, A. D.; Green, T. L.; Rook, J. M.; Lindsley, C. W.; Conn, P. J.; Deutsch, S. I. Effects of VU0410120, a novel GlyT1 inhibitor, on measures of sociability, cognition and stereotypic behaviors in a mouse model of autism. *Prog. Neuro-Psychopharmacol. Biol. Psychiatry* **2015**, *3*, 10−17.

(33) (a) Heresco-Levy, U.; Shoham, S.; Javitt, D. C. Glycine site agonists of the N-methyl-D-aspartate receptor and Parkinson's disease: a hypothesis. *Mov. Disord.* **2013**, *28*, 419−424. (b) Tsai, C.-H.; Huang, H.-C.; Liu, B. L.; Li, C. I.; Lu, M. K.; Chen, S.; Tsai, M. C.; Yang, Y. W.; Lane, H. Y. Activation of *N*-methyl-D-aspartate receptor glycine site temporally ameliorates neuropsychiatric symptoms of Parkinson's disease with dementia. *Psychiatry Clin. Neurosci.* **2014**, *68*, 692−700. (c) Schmitz, Y.; Castagna, C.; Mrejeru, A.; Lizardi-Ortiz, J. E.; Lindsley, C. W.; Sulzer, D. Glycine transporter-1 inhibition promotes striatal axon sprouting via NMDA receptors in dopamine neurons. *J. Neurosci.* **2013**, *33*, 16778−16789.

(34) Hanuska, A.; Szenasi, G.; Albert, M.; Koles, L.; Varga, A.; Szabo, A.; Matyus, P.; Harsing, L. G., Jr. Some operational characteristics of glycine release in rat retina: the role of reverse mode operation of glycine transporter type-1 (GlyT-1) in ischemic conditions. *Neurochem. Res.* **2016**, *41*, 73−85.

(35) Alberati, D.; Koerner, A.; Pinard, E.; Winter, M. GLYT1 inhibitors for the use in the treatment of hematological disorders. WO 2015/165842 A1, November 5, 2015.

(36) Cioffi, C. L.; Wolf, M. A.; Guzzo, P. R.; Sadalapure, K.; Parthasarathy, V.; Dethe, D.; Maeng, J.-H.; Carulli, E.; Loong, D. T.; Fang, X.; Hu, M.; Gupta, P.; Chung, M.; Bai, M.; Moore, N.; Luche, M.; Khmelnitski, Y.; Love, P. L.; Watson, M. A.; Mhyre, A. J.; Liu, S. Design, synthesis, and SAR of *N*-((1-(4-(propylsulfonyl)piperazine-1-yl)cycloalkyl)methyl)benzamide inhibitors of glycine transporter-1. *Bioorg. Med. Chem. Lett.* **2013**, *23*, 1257−1261.

(37) Cioffi, C. L.; Wolf, M. A.; Guzzo, P. R.; Liu, S.; Sadalapure, K.; Parthasarathy, V.; Maeng, J.-H. Glycine transporter-1 inhibitors, methods of making them, and uses thereof. US 9045445 B2, June 5, 2015.

(38) Coulton, S.; Gilpin, M. L.; Porter, R. A. Glycine transporter inhibiting compounds and uses in medicine. PCT Int. Appl. WO 2007/147839 A1, December 27, 2007.

(39) Thomson, J. L.; Blackaby, W. P.; Jennings, A. S. R.; Goodacre, S. C.; Pike, A.; Thomas, S.; Brown, T. A.; Smith, A.; Pillai, G.; Street, L. J.; Lewis, R. T. Optimisation of a series of potent, selective and orally bioavailable GlyT1 inhibitors. *Bioorg. Med. Chem. Lett.* **2009**, *19*, 2235−2239.

(40) (a) Walter, M. W.; Hoffman, B. J.; Gordon, K.; Johnson, K.; Love, P.; Jones, M.; Man, T.; Phebus, L.; Reel, J. K.; Rudyk, H. C.; Shannon, H.; Svensson, K.; Yu, H.; Valli, M. J.; Porter, W. J. Discovery and SAR studies of novel GlyT1 inhibitors. *Bioorg. Med. Chem. Lett.* **2007**, *17*, 5233−5238. (b) Lowe, J. A.; Hou, X.; Schmidt, C.; Tingley, F. D.; McHardy, S.; Kalman, M.; DeNinno, S.; Sanner, M.; Ward, K.; Lebel, L.; Tunucci, D.; Valentine, J. the discovery of a structurally novel class of inhibitors of the type 1 glycine transporter. *Bioorg. Med. Chem. Lett.* **2009**, *19*, 2974−2976.

(41) (a) Lin, J. H. CSF as a surrogate for assessing CNS exposure: and industrial perspective. *Curr. Drug Metab.* **2008**, *9*, 45−59. (b) Schaffer, C. L. *Defining Neuropharmacokinetic Parameters in CNS Drug Discovery to Determine Cross-Species Pharmacologic Exposure-Response Relationships*; Annual Reports in Medicinal Chemistry; Academic Press: Cambridge, MA, 2010; Vol. *45*, Chapter 4, pp 55−70. (c) Rankovic, Z. CNS drug design: balancing physicochemical properties for optimal brain exposure. *J. Med. Chem.* **2015**, *58*, 2584−2608.

(42) Kopec, K.; Flood, D. G.; Gasior, M.; McKenna, B. A. W.; Zuvich, E.; Schreiber, J.; Salvino, J. M.; Durkin, J. T.; Ator, M. A.; Marino, M. J. Glycine transporter inhibitors with reduced residence time increase prepulse inhibition without inducing hyperlocomotion in DBA/2 mice. *Biochem. Pharmacol.* **2010**, *80*, 1407−1417.

(43) Mezler, M.; Hornberger, W.; Mueller, R.; Schmidt, M.; Amberg, W.; Braje, W.; Ochse, M.; Scoemaker, H.; Behl, B. Inhibitors of GlyT1 affect glycine transport via discrete binding sites. *Mol. Pharmacol.* **2008**, *74*, 1705−1715.

(44) Perry, K. W.; Falcone, J. F.; Fell, M. J.; Ryder, J. W.; Yu, H.; Love, P. L.; Katner, J.; Gordon, K. D.; Wade, M. R.; Man, T.; Nomikos, G. G.; Phebus, L. A.; Cauvin, A. J.; Johnson, K. W.; Jones, C. K.; Hoffmann, B. J.; Sandusky, G. E.; Walter, M. W.; Porter, W. J.; Yang, L.; Merchant, K. M.; Shannon, H. E.; Svensson, K. A. Neurochemical and behavioral profiling of the selective GlyT1 inhibitors ALX5407 and LY2365109 indicate a preferential action in caudal vs. cortical brain areas. *Neuropharmacology* **2008**, *55*, 743−754.

DOI: 10.1021/acs.jmedchem.6b00914
J. Med. Chem. XXXX, XXX, XXX−XXX